

Republic of Iraq
Ministry of Higher Education
and Scientific Research
University of Babylon
College of Materials Engineering
Department of Metallurgical Engineering



Investigation the Structure and Properties of Composite Biocoatings onto Ti-6Al-4V Surface using Electrophoretic Deposition Technique for Biomedical Application

A Thesis

Submitted to the Council of the College of Materials Engineering/
University of Babylon in Partial Fulfillment of the Requirements for
the Master Degree in Materials Engineering / Metallurgical

By
Sura Bahaa Mohammed

Supervised by
Prof. Dr. Abdulraheem Kadhim AbidAli

2021

1443

Dedication

To My dear parents for

their love and care

To My family for

their love and encouragement

To All My Real Friends

*To All those who support science intellectually, financially
and morally*



Sura B. Mohammed
2021

بِسْمِ اللَّهِ الرَّحْمَنِ الرَّحِيمِ

﴿ قَالَ يَا قَوْمِ أَرَأَيْتُمْ إِن كُنْتُمْ عَلَىٰ بَيِّنَةٍ مِّن رَّبِّي
وَرَزَقْتَنِي مِنْهُ رِزْقًا حَسَنًا ۖ وَمَا أُرِيدُ أَنْ أَمْلِكُمْ إِلَىٰ
مَا أَنهَاكُمْ عَنْهُ ۖ إِن أُرِيدُ إِلَّا الْإِطْلَاحَ مَا اسْتَطَعْتُ
ۖ وَمَا تَوْفِيقِي إِلَّا بِاللَّهِ ۖ عَلَيْهِ تَوَكَّلْتُ وَإِلَيْهِ

أُنِيبُ ﴿

بِسْمِ اللَّهِ الرَّحْمَنِ الرَّحِيمِ

Acknowledgements

In The Name of Allah, the Most Gracious, the Most Merciful

Writing this thesis has been fascinating and extremely rewarding. I would like to thank who have contributed to the final result in many different ways:

To commence with, I want to offer this endeavor to our **GOD**, the almighty to have bestowed me good health, courage, inspiration, zeal and the light to complete this research.

I would like to express my sincere gratitude to thank my thesis advisor: **Dr. Abdulraheem Kadhim AbidAli**, he always accommodates and have a helping hands if I had question about my research or writing. He shows support in everything I do and teach me the right direction for my thesis writing. Deep sense of gratitude and respectful regards to my husband **Dr. Mohammed Mansour Kadhun**, for the continuous support along my study. I could not have imagined having better advisors and mentors for my study.

Nobody has been more important to me in the pursuit of this project than the members of my **family**. I would like to thank my **parents**, whose love and support are with me in whatever I pursue.



**Sura Bahaa Mohammed
(2021)**

Abstract

In the present study, single layer, and composite biocoatings of hydroxyapatite / titanium dioxide (HAp/TiO₂) micro-particles coatings were fabricated by electrophoretic deposition on Ti-6Al-4V substrate. As a result of accidents, diseases and other causes, efforts and research are continued to reach results closest. The damaged that occur to some of them in the living of the organism in general and the human being in particular, This can be done throughout the existing the implantation of medical minerals, ligaments of bones, teeth and other parts that compensate. Through science, opportunities and experiments have been provided to obtain satisfactory results in terms of the biocompatibility of titanium implants and their alloys, which are classified as one of the best biocompatible materials within vivo tissues.

This study aims to increase the bioconductivity of Ti-based alloy, and improve its corrosive and antibacterial properties by coating the surface with a bioceramic (HAp/TiO₂) micro-powders. Pure TiO₂, pure HAp and composite biocoatings were made on ($\alpha+\beta$) Ti6Al4V substrate using an electrophoretic deposition (EPD) technique, charged particles suspended in ethanol at a concentration of 50 g/L, for each powder. Polyethyleneimine (PEI) 6 g/L as binder at room temperature, with ideal conditions of 20V and a deposition time of one min, and under a heat treatment of the coated samples to be carried out in an inert atmosphere of argon at 950°C for one hour to improve the adhesion.

The surface characteristics of coated substrates, such as thickness, topography, morphology phase transformations, and corrosion behavior, micro-hardness, surface roughness, wettability and antibacterial test were evaluated and compared to that of the uncoated substrates. The results showed that the EPD is a promising technique to create a composite

biocoatings on Ti6Al4V surface with outstanding structure and properties for biomedical applications.

The results demonstrated that the coated sample under coating conditions (20V, 1.0min) had a ratio of calcium to phosphate equal to 1.81, which is close to the ratio found in living bone. The results also of the wettability test showed that the contact angle of the deposited paint is 13.11 degrees, and this positive result is useful for biomedical applications and proved that the coating is hydrophilic.

List of Contents

Acknowledgements	I
Abstract	II
List of Contents	IV
List of Tables	VII
List of Figures	VIII
List of Abbreviations	X
1 INTRODUCTION	1
1.1 General Overview	1
1.2 Looking for Biomaterials	2
1.3 Biomedical Coating	5
1.4 Problems of Metallic Implants	5
1.5 Objectives of the Present Study	12
1.6 Thesis Contents	13
2 REVIEW OF LITERATURE	15
2.1 General View	15
2.2 Types of Biomaterials	16
2.2.1 Polymers.....	17
2.2.2 Ceramics	17
2.2.3 Metals and alloys	18
2.2.3 <i>Composite Materials</i>	21
2.3 Functionally Graded Materials	22
2.4 Functionally Graded Materials Applications	25
2.4.1 Aerospace Field.....	25
2.4.2 Optoelectronics Field	25
2.4.3 Defense Field	25
2.4.4 Energy Sector	26
2.4.5 Construction Field	26
2.5 Physical Metallurgy of Titanium Alloys	27
2.6 Alloy Classification.....	28
2.7 Titanium Aluminum Vanadium Ti-6Al-4V Alloy	33
2.8 Nature of the Physiological Environment.....	34

2.9 Ion Release of Ti6Al4v Alloy in Human Body.....	35
2.10 Influence of Surface Texture and Wettability on Initial Bacterial Adhesion on Metallic Implant.....	37
2.11 Biocompatible Coating	39
2.12 Electrophoretic Deposition Technique	40
2.12.1 Kinetics of EPD.....	43
2.12.2 Suspension of Particles.....	45
2.12.3 Double layer and ζ -potential	45
2.12.4 Deposition.....	46
2.12.5 Parameters	47
2.12.5.1 Suspension Parameters	47
2.12.5.2 Physical Parameters	50
2.13 Role of Binders In EPD.....	52
2.14 Previous Studies on Biomedical Coating	52
2.15 Concluding Remarks	55
3 THE EXPERIMENTAL PROGRAM	56
3.1 Introduction	56
3.2 Particle Size Analyzer	57
3.3 Materials	58
3.4 Method	59
3.5 Sintering of Deposited Coatings	62
3.6 Characterizations of Samples.....	63
3.6.1 Surface Roughness.....	63
3.6.2 Contact Angle Measurement	63
3.6.3 Micro Hardness.....	64
3.7.4 Electrochemical Test	64
3.7.5 Antimicrobial Test.....	66
3.7.6 Light Optical Microscope (LOM)	67
3.7.7 Metals Ions Release (Static Immersion Tests).....	68
3.7.8 X-Ray Diffraction Analysis.....	68
3.7.9 Scanning Electron Microscopy (SEM)	69
4 RESULTS AND DISCUSSION	70
4.1 Introduction	70
4.2 Microstructure of the Ti6Al4V Substrate	71

4.3 Scanning Electron Microscopy Analysis.....	72
4.4 X-Ray Diffraction Test Result.....	77
4.5 Micro Hardness.....	81
4.6 Surface Roughness.....	83
4.7 Wettability.....	84
4.8 Electrochemical Corrosion.....	86
4.9 Metal Ion Release.....	91
4.10 Antibacterial Study	93
5 CONCLUSIONS AND RECOMMENDATIONS	95
5.1 Key Findings	95
5.2 Recommendations for Further Research	96
REFERENCES	97
MATERIAL DATA	APPENDIX A
CALCULATION OF ION RELEASE	APPENDIX B

List of Tables

2-1	Chemical compositions of important commercial titanium alloys.	29
2-2	Properties of some titanium alloys including density (ρ), ultimate tensile strength and Young's modulus	31
2-3	Bioceramic coatings with different coating materials used for medical applications in the human body.	40
2-4	The physical properties of popular solvents	48
3-1	Chemical composition of prepared specimens.	61
3-2	Simulated body fluids used in electrochemical corrosion test.	66
4-1	Quantitative EDX Results for selective area.	77
4-2	Experimental data of the coated and uncoated samples.	82
4-3	Contact angle (θ°) of Ti6Al4V and coated samples	84
4-4	Electrochemical parameters of Ti6Al4V substrate and coated samples in different media	88
4-5	Results of atomic adsorption spectroscopy test for base (Ti6Al4V) and FGC.....	92

List of Figures

1-1	Application of biomaterials as implants in different areas of human body.....	4
1-2	Simple scheme of stress shielding.	7
1-3	Two possible toxicity routes for metal ions released into body fluids due to corrosion and wear	9
1-4	The four stages of biofilm development. (a) Initial bacterial attachment. (b) Bacteria start to produce multiple layers through cell aggregation and accumulation. (c) Biofilm development and matrix elaboration. (d) Bacteria start a new cycle of biofilm formation in different location.....	11
2-1	Variation of properties in conventional composites and FGM	24
2-2	Functionally graded coating	24
2-3	Crystal structure of (a) bcc phase (also called β phase) and (b) hcp phase (also called α phase)	28
2-4	Schematic section through a β isomorphous phase diagram. M_s is the temperature at which martensite begins to form when cooling from the β phase field to room temperature and M_f is the temperature at which reaction is complete. Adapted from	32
2-5	Phase diagram of Ti-Al-V alloy	34
2-6	Schematic diagrams of electrophoretic deposition (EPD) on metal substrates (working electrodes)	42
2-7	EPD scheme of deposited weight against deposition time.....	44
2-8	Electric double layer structure.....	46
3-1	Block diagram of the research plan	57
3-2	Geometrical configuration of research samples (dimensions and weight).....	58
3-3	Garmenting processes of FG coating samples.....	60
3-4	Sample coated time process.....	62
3-5	The adopted sintering schedule	63
3-6	Sintering furnace.....	63
3-7	The electrochemical corrosion cell.....	66
3-8	Light optical microscope.	68

4-1	As-received microstructure of Ti-6Al-4V alloy showing elongated α (blue arrow), equiaxed α (red arrow) and intergranular β (black arrow) using different magnification.....	71
4-2	Schematic of SEM cross section image for functionally graded sample.	72
4-3	SEM image for electrophoretic deposited (a- titania and b- hydroxyapatite) on Ti6Al4V alloy.	73
4-4	SEM micrograph of the surface morphology of functionally graded coating on Ti6Al4V alloy	74
4-5	Cross-sectional SEM micrographs of the deposited HAp coating after sintering.....	74
4-6	EDX analysis of functionally graded HA/TiO ₂ coatings.	76
4-7	The linear EDX analysis of functionally graded HA/TiO ₂ coatings.....	76
4-8	XRD pattern for the Ti-6Al-4V sample, indicating $\alpha+\beta$ phases.....	78
4-9	XRD pattern for the TiO ₂ coating specimen.....	79
4-10	XRD pattern for the HAp coating specimen	80
4-11	XRD pattern for the functionally graded HAp/ TiO ₂ coating specimen.....	81
4-12	Vicker's micro-hardness (HV).....	83
4-13	Surface roughness values (Ra) μm	84
4-14	Effect of surface roughness on wettability.	85
4-15	Photometric quantification of contact angle θ° bound to the different experimental coating surfaces.....	86
4-16	Potentiodynamic polarization curves of coated and uncoated samples in Ringer's solution.....	87
4-17	Potentiodynamic polarization curves of coated and uncoated samples in NaCl 0.9%.....	87
4-18	Potentiodynamic polarization curves of coated and uncoated samples in artificial saliva	88
4-19	Corrosion rate of the base (Ti6Al4V) alloy and different ceramic coatings in different medias.....	91
4-20	The effect of different immersion media on the accumulative ions release concentrations (Ug/l) from FG coated/uncoated Ti6Al4V	91

4-21	The effect of different immersion media on the accumulative ions release concentrations (Ug/l) from FG coated/uncoated Ti6Al4V.	93
4-22	Images of the antibacterial tests of HAp/TiO ₂ against E. coli,	94

Table of Abbreviations

List of Abbreviations

Abbreviation	Meaning
AC-EPD	Alternating current- Electrophoretic deposition
AFM	Atomic-force Microscopy
BCC	Body Center Cubic
CP-Ti	Commercially Pure Titanium
C_R	Corrosion Rate
CTE	Coefficient of Thermal Expansion
DC-EPD	Direct current- Electrophoretic Deposition
EDX	Energy- Dispersive X-Ray Spectroscopy
EPD	Electrophoretic deposition
EW	Equivalent Weight
FGM	Functionally graded materials
H.V.	The Vickers Micro-hardness
HAp	Hydroxyapatite
HCP	Hexagonal Close Packed
LOM	Light Optical Microscope
mV	Millivolt
OCP	Open Circuit Potential
PEI	Polyethyleneimine
pH	Acidic Number
SBF	Simulated Body Fluid
SEM	Scanning Electron Microscopy
SMA _s	Shape Memory Alloys
SS	Stainless Steel
XRD	X-Ray Diffraction

Introduction

1.1 General Introduction

Occasionally, accidents happen and crucial parts of our bodies are in required of replacement or mending. Other times, as increasingly seen on a global scale, the same parts are worn out by a lifelong service to its host. Thanks to the dedicated work of countless medical professionals, scientists and engineers. However, biocompatible materials, surgical procedures, medicines, and antibiotics have been developed to successfully mend this, significantly improving the quality of life for millions of people. Nevertheless, the complexity of our biological system and its intricate symbiotic relationship with bacteria can still cause materials, surgical procedures or treatments to fail. These challenges, along with longer life expectancies and higher demands from society, have resulted in a pressing need for improvements and the development of new advanced products and technologies [1].

Biomedical material is any substance that has been engineered to interact with biological systems for a medical purpose, which may be therapeutic (i.e., to treat, augment, repair, or replace malfunctioning tissue in the body) or diagnostic. Among the various types of biomedical materials, metallic materials are the most widely used because of their high load-supporting capacity, desirable qualities of wear and friction, and acceptable biocompatibility [2].

Titanium and titanium alloys are the most frequently used metallic materials for biomedical applications due to their high strength-to-weight ratio, high fatigue resistance, and good biocompatibility [3,4].

Regrettably, metallic implants suffer from different deficiencies, such as low/high corrosion resistance, releasing toxic ions, and low biocompatibility. Microbial infections in the biomedical implants pose a grave threat in modern medicine. A biofilm infection stays a prime reason of failure in biomaterial implants. Thus, the application of the antimicrobial agents into implant surfaces to prohibit implant-associated infection has attracted lots of surveillance. To find a solution to this matter, many surface modification methods are proposed that coating techniques are among the most paramount ones. Each of these techniques elucidates different capabilities and one has to choose a coating method based on their needs and implementations. Among these techniques, the most popular are sol-gel, high-velocity suspension spray, and electrochemical coating processes [5].

1.2 Biomaterials

Biomaterial is acquainted as "A nondrug substance proper for listing in systems which increment or replace the function of bodily tissues or organs" [6].

Biomaterials are broadly classified into three major categories according to biocompatibility are as follows: bioinert, bioactive, and bioresorbable.

- i. Bioinert: These are the materials which when placed has minimal interaction with the tissue surrounding it, thus leading to osteogenesis. Some of the examples are stainless steel, titanium, zirconium, alumina, and ultra-high-molecular-weight polyethylene.

- ii. **Bioactive:** These are the materials once placed inside the oral cavity react with the hard tissues as well as the soft tissues. Examples are synthetic hydroxyapatite, glass ceramic, and bioglass.
- iii. **Bioresorbable:** These materials on placement begin to resorb which get slowly replaced with bone. Examples are tricalcium phosphate, polylactic–polyglycolic acid copolymers, calcium oxide, calcium carbonate, and gypsum.

Thus, bioinert and bioactive materials are called as "osteoconductive" materials as they have the ability to act as "scaffolds" for bone deposition on its surfaces [7].

Biomaterials can also be classified based on chemical composition into metals, ceramics, and polymers as follows :

- i. **Metals:** titanium, titanium alloys, stainless steel, cobalt chromium alloys, gold alloys, and tantalum
- ii. **Ceramics:** alumina, hydroxyapatite, beta-tricalcium phosphate, carbon, carbon/silicon, bioglass, zirconia, and zirconia-toughened alumina
- iii. **Polymers:** polymethyl methacrylate, polytetrafluoroethylene, polyethylene, polysulfone, polyurethane, and polyether ether ketone [8].

The first and foremost requirement for the choice of the biomaterial is its acceptability by the living body. The implanted material should not cause any adverse effects like allergy, inflammation and toxicity either immediately after surgery or under post-operative conditions. Secondly, biomaterials should possess sufficient mechanical strength to sustain the forces to which they are subjected, so that they do not undergo fracture and more importantly, a bioimplant should have very high corrosion and wear resistance in highly corrosive body environment and varying loading conditions, apart from fatigue strength and fracture toughness. The success of a biomaterial or an implant is highly dependent on three major factors (i)

the properties (mechanical, chemical and tribological) of the biomaterial in question (ii) biocompatibility of the implant and (iii) the health condition of the recipient and the competency of the surgeon [9, 10].

Application of biomaterials in human body as implants is very common nowadays. In **Figure (1.1)**, the locations of implants in different areas of human body are shown. As illustrated, biomaterials can be used in many locations in human body such as shoulders, hips, joints, bones, dental implants, etc. Once these biomaterials are planted in the human body, they will be subjected to human body fluid environment. The living body fluid is corrosive for metallic biomaterials. As a result, biomaterials degradation occurs ultimately unless they are covered with appropriate coatings that could prevent corrosion [9].

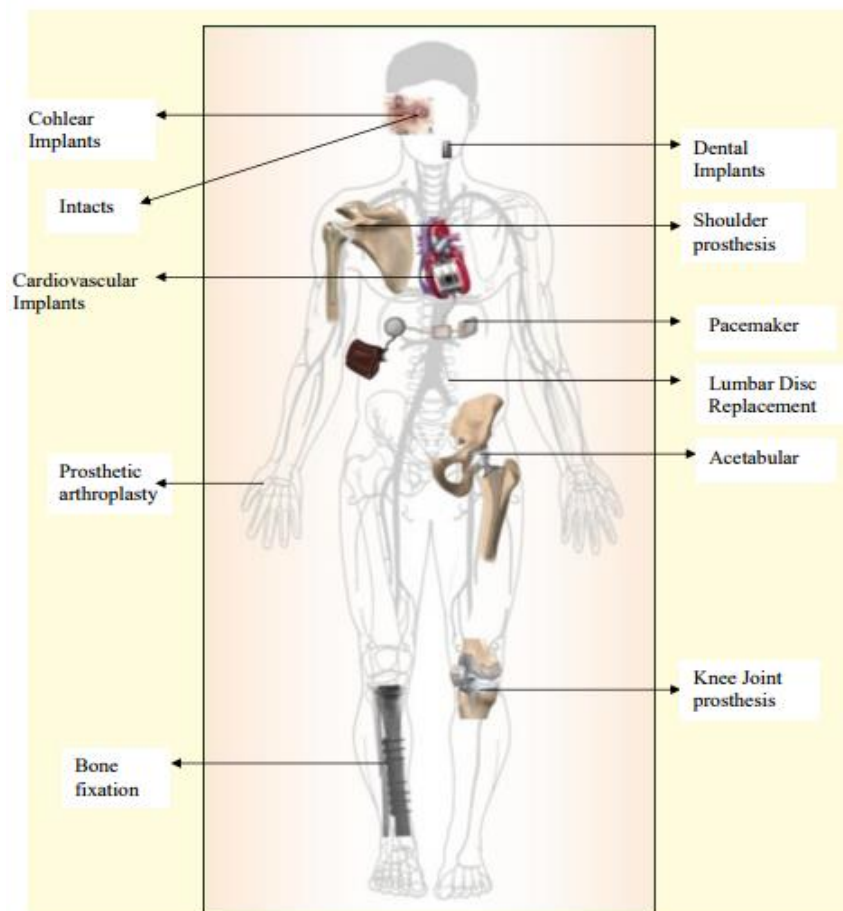


Figure (1.1): Application of biomaterials as implants in different areas of human body [9].

1.3 Biomedical Coating

The biological behavior of an implant is quite dependent on the chemical composition and morphology of the surface. Assortment of coating systems comprising biopolymers, bioceramics and their combinations have been developed to amend the surface characteristics of metallic implants, enhancing the biocompatibility and bone-to-implant connect. At the same time, coatings also act as a barrier to shield the implant from the body fluid environment and thus protect against corrosion [11, 12]. Moreover, the prepared coating can do as a local drug surrender platform, releasing biomolecules (growth factors, antibiotics, peptides, proteins, genes) which have been preloaded into the coating structure, to transform biomaterials to "living tissues" for a certain implementation. Since one of the reasons for the failure of metal implants is bacterial infection, it is necessary to find a coating that acts as an anti-adhesion and growth of bacteria on the surface of the implant[13].

1.4 Problems of Metallic Implants

There are several challenges associated with the use of implantable metals:

1. **Stress shielding (biomechanical stabilities):** It is well known that the stress transfer between an implant device and a bone is not homogeneous when Young's moduli of the implant device and the bone is different; this is defined as stress shielding. In such conditions, bone atrophy occurs and leads to the loosening of the implant and refracturing of the bone [14]. Therefore, it is desirable if the stiffness (Young's modulus) is not too high compared to that of bone. Implant devices are mainly made from metallic biomaterials such as stainless steels, Co-Cr alloys, and titanium (Ti) and its alloys. Young's moduli of these metallic biomaterials are generally much

greater than that of the bone. Young's moduli of the most widely used stainless steel for implant devices, SUS316L stainless steel and Co-Cr alloys, are around 180 GPa and 210 GPa, respectively [15]. Young's moduli of Ti (pure titanium) and its alloys are generally smaller than those of stainless steels and Co-Cr alloys. For example, Ti and its alloy, Ti-6Al-4V extra low interstitial, which are widely used for constructing implant devices, have a Young's modulus of around 110 GPa. However, this value is still higher than that of the bone, that is, 10–30 GPa [16]. When a metal implant is implanted into the femur, the physiological loading is often transferred to the implant from the surrounding bone. Therefore, the implanted femur is experiencing decreased loads when compared to it in its natural state. Bone remodeling occurs in which bone gets resorbed and loses mass, which is known as stress shielding [17]. The reduced bone stock can lead to serious complications including peri-prosthetic fracture, and clinically can present with thigh pain [18]. In addition, stress shielding can also reduce the quality of the remaining bone stock which leads to an increased risk for fracture and aseptic loosening.

Stress shielding in femur occurs when some of the loads are taken by prosthesis and shielded from going to the bone. Normally, femur carries its external load by itself where the load is transmitted from the femoral head through the femoral neck to the cortical bone of the proximal femur as shown in **Figure (1.2-a)**. When stiffer stem is introduced into the canal, it shares the load and the carrying capacity with bone. Originally, the load is carried by bone, but it is now carried by implant and bone. As a result, the bone is subjected to reduce stresses and hence stress shielded. The upper part of the femur

receives fewer loads. The stress shielded area is whiter as shown in **Figure (1.2-b) [19]**.

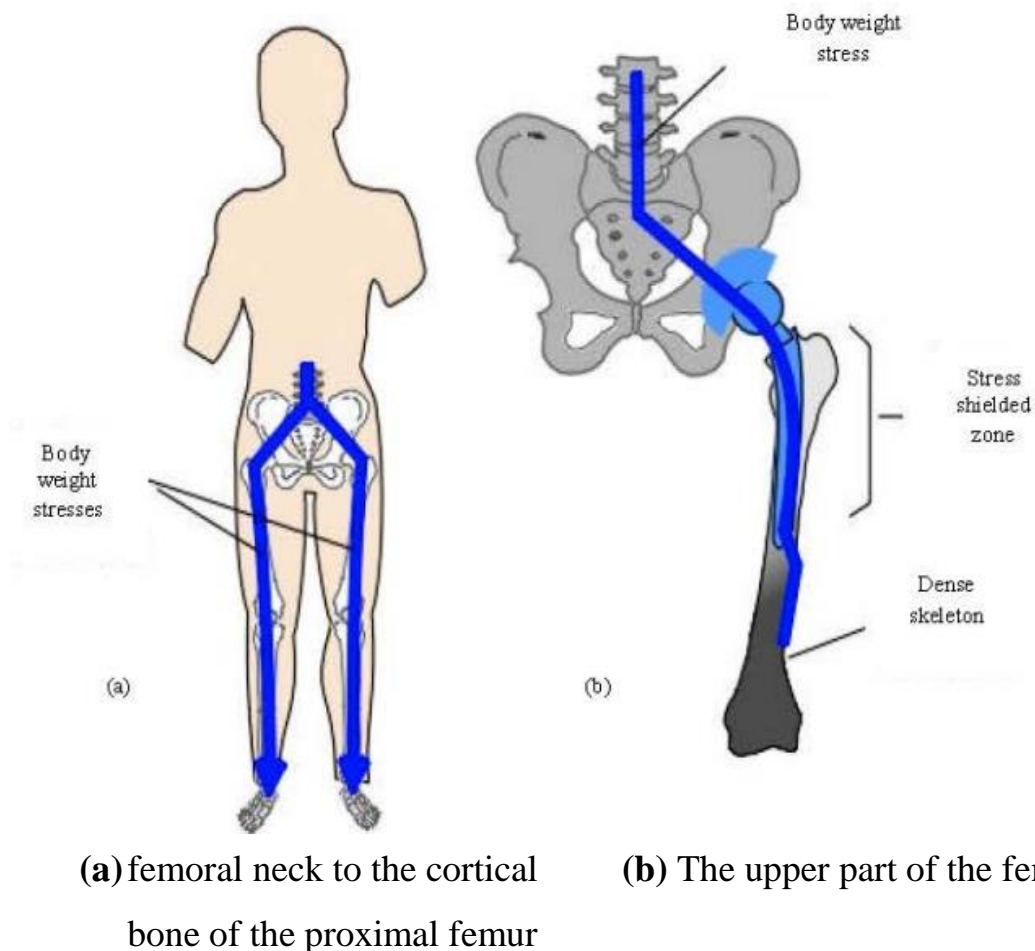


Figure (1.2): Simple scheme of stress shielding [19].

2. **Corrosion (toxicity risk):** Corrosion is an important factor in the design and selection of metals and alloys for service in vivo. In addition, various corrosion mechanisms can lead to implant loosening and failure [20, 21]. Corrosion, the gradual degradation of materials by electrochemical attack is of great concern particularly when a metallic implant is placed in the hostile electrolytic environment of the human body. The implants face severe corrosion environment which includes blood and other constituents of the body fluid which encompass several constituents like water, sodium, chlorine, proteins, plasma, amino acids along with mucin in the case

of saliva [22]. The corrosion of metallic implants can affect the surrounding tissues in three ways: (i) electrical current may affect the behaviour of cells, (ii) the corrosion process may change the chemical environment, and (iii) metal ions may affect cellular metabolism [23,24].

Corrosion occurs when a material gradually deteriorates after undergoing electrochemical reactions as a result of being placed in the body's harsh electrolytic environment. The fluid medium in the body is made up of various anions, cations, and other components.

Biological molecules, such as proteins, interfere with the equilibrium of corrosion reactions by binding themselves to the ions discharged from the metal whereas those absorbed on the surface reduce the oxygen diffusion at certain regions thus, causing corrosion [25]. In general, corrosion stems from either metal imbalance such as phase variation, grain boundaries, and impurities or from shape and environmental changes such as crevices, scratches, defects in coating, amount of oxygen, and others. For a metal (M), the general corrosion reactions that would occur in a physiological environment is represented below [26]:

Anodic reaction:



Cathode reaction:



Product formation:



Metal ions released into the human body do not always harm it; the partner for combination with them is very important, see **Figure (1.3)**. Whether anion will be active and immediately react with water molecules or inorganic, anions it, depends on the number and mass of the molecules. For example, titanium ion is very active and readily reacts with hydroxyl radicals and anions, forming oxide and salt in body fluids, thus indicating that the possibility of combination with biomolecules is low. However, this does not mean that the reaction of titanium ions with biomolecules will not occur at all. Zirconium, niobium and tantalum ions behave like titanium ions. On the other hand, inactive ions, for example, of nickel and copper, do not immediately combine with water molecules and inorganic anions and last in the ionic state for relatively long time. Therefore, these ions have higher chance of combining with biomolecules and exhibit toxicity. To conclude, the following factors must be considered when dealing with toxicity of metallic biomaterials: (i) corrosion resistance of the material, (ii) ions released by corrosion and wear, (iii) activity of the released ions, and (iv) toxicity of the ion itself [27].

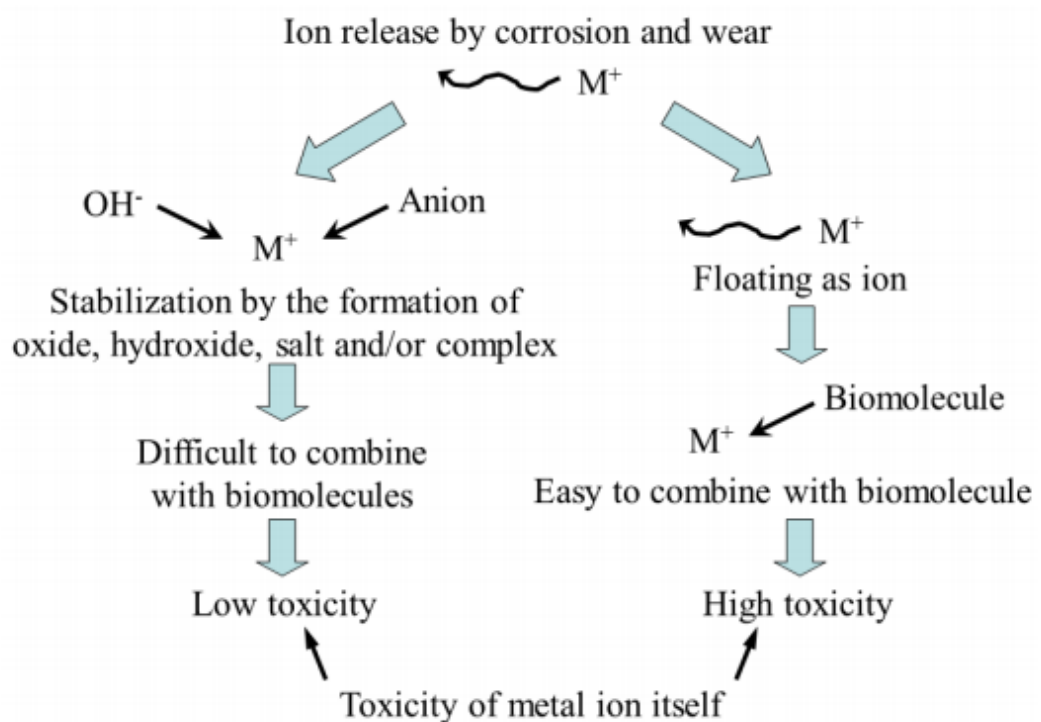


Figure (1.3): Two possible toxicity routes for metal ions released into body fluids due to corrosion and wear[27].

The types of corrosion that are pertinent to the currently used alloys are pitting, crevice, galvanic, intergranular, stress-corrosion cracking, corrosion fatigue and fretting corrosion.

3. **Osseointegration** is defined as a direct structural and functional connection between ordered, living bone and the surface of a load-carrying implant, is critical for implant stability. Osseointegration is also a measure of implant stability, which can occur at two different stages: primary and secondary. Primary stability of an implant mainly comes from mechanical engagement with compact bone. Secondary stability, on other hand, offers biological stability through bone regeneration and remodeling. The former is a requirement for secondary stability. The latter, however dictates the time of functional loading [28].
4. **Infection:** Infection is a major problem in orthopedics leading to implant failure. It is a challenging task to treat orthopedic implant infections that may lead to implant replacement and, in severe cases, may result in amputation and mortality [29]. Sources of infectious bacteria include the environment of the operating room, surgical equipment, clothing worn by medical and paramedical staff, resident bacteria on the patient's skin and bacteria already residing in the patient's body. Implant-associated infections are the result of bacteria adhesion to an implant surface and subsequent biofilm formation at the implantation site [30]. Formation of biofilm takes place in several stages, starting with rapid surface attachment, followed by multilayered bacterial cell proliferation and intercellular adhesion in an extracellular polysaccharide matrix [31]. There are four steps for

biofilm formation on implant (see **Figure 1.4**). Step one: The bacteria initially attach on the substrate. Step two: Accumulation of multiple cell layers through cell aggregation and accumulation. Step three: matrix elaboration and biofilm development. Step four: Bacterial release to start a new cycle of biofilm formation in a proximal location [32].

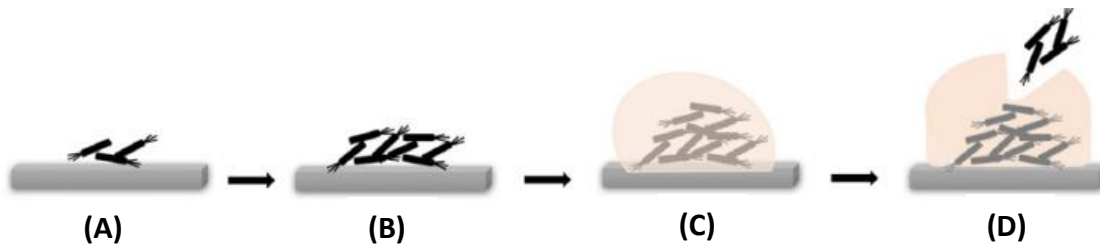


Figure (1.4): The four stages of biofilm development. (a) Initial bacterial attachment. (b) Bacteria start to produce multiple layers through cell aggregation and accumulation. (c) Biofilm development and matrix elaboration. (d) Bacteria start a new cycle of biofilm formation in different location [33].

The formation of biofilms on medical devices presents three major problems as follows.

- i. First, bacterial communities on these surfaces represent a reservoir of bacteria that can be shed into the body, leading to a chronic infection.
- ii. Second, biofilm bacteria are highly resistant to treatment with antibiotics; therefore, once these bacterial communities form, they are extremely difficult to eliminate with conventional antimicrobial therapies.
- iii. Finally, because host responses and antimicrobial therapies are often unable to eliminate bacteria growing in a biofilm, a chronic inflammatory response at the site of the biofilm may be produced[31].

Can be concluded from the mentioned above, these problems are sometimes severe in the traditional metallic implants. So in order to overcome these problems, titanium alloy (Ti6Al4V) coated by functionally graded bioactive micro titanium dioxide and hydroxyapatite (TiO₂/HAp) layer which are close as possible to practical conditions. This research is sought to cover the limited area of research about this problem.

1.5 Objectives of the Present Study

It is clear that there is a lack of experimental studies on the behavior of titanium alloy (Ti6Al4V) coated by composite biocoatings bioactive micro titanium dioxide and hydroxyapatite (TiO₂/HAp) layer. Therefore, the origin of this idea is the need to study the performance of composite biocoatings bioactive coatings in human body environments using (artificial Saliva, NaCl 0.9% and Ringer's solutions).

The overall aim of this work is to provide a strategy for preparing the biomaterial Ti6Al4V to be coated with a functionally graded bioactive material of titanium dioxide and hydroxyapatite (TiO₂/HAp) layer in different weight percentages in order to increase its biocompatibility and to prevent the growth and adhesion of bacteria and microbes on the surface of the implant and to reduce the thermal stresses. The method used is electrophoretic deposition (EPD) for this purpose. To address this knowledge gap the following research objectives are set-out as a part of this research:

1. Studying experimentally, the development of biocompatible coating on the surface of Ti6Al4V alloy using ceramic micro-particles TiO₂/HAp by EPD technique.
2. Searching the influence of suspension composition and EPD processing parameters (deposition voltage and deposition time) to reach the optimal coating conditions of samples.

3. Investigating experimentally the reduction of corrosion effect and dissolution behavior of metallic implants in artificial Saliva and Hank's solution.
4. Assessing the produced composite biocoatings materials part will be performed via scanning electron microscope (SEM), energy dispersive X-ray (EDX) and X-ray diffraction (XRD) analysis, as well as mechanical properties such as microhardness have to be evaluated for composite biocoatings materials.
5. Experimentally studying of antibacterial properties which grow on the fabricated surface.
6. Experimentally studying the influence of changes in thermal expansion behavior of coating-substrate interface after sintering by implementation of composite biocoatings material.

1.6 Thesis Contents

This thesis comprises of five chapters including the introductory chapter. The appendices are also included to provide supporting data for the present work.

Chapter one (introduction) lists the definition, applications and historical background of the biomaterials. Also, it gives a description of the research importance objectives, and the research outline.

Chapter two (Theoretical part and literature review) reviews a number of studies and scientific researches which have been published on the definition, principle and mechanism of electrophoretic deposition technology accredited scholars and researchers.

Chapter three (experimental program) includes details of the materials considered throughout this work, mix proportion, method of coating, testing procedures and experimental details.

Chapter four (results and discussion) the results obtained from the experimental work are presented and discussed in details. It explains the characterization of prepared composite biocoatings material and the obtained results of mechanical, metal ion release and corrosion tests of the prepared composite biocoatings material. In addition, it discusses the X-ray diffraction (XRD), scanning electron microscopy (SEM), and hardness tests.

Chapter five (conclusions and recommendations) includes the summary and the conclusion of the research work. This chapter also includes recommendations for future studies.

Review of Literature

2.1 General View

This chapter covers a general view about biotic titanium alloy Ti-6Al-4V and functionally gradient coating of HA/TiO₂ bio-ceramic used in metallic implants. There will be a focus on the functionally graded materials (FGMs) properties and their applications in various fields, also the difference between them and traditional composites, as well as coating techniques. This chapter will cover up the literature relevant to this study, several neoteric experimental and theoretical investigations about biomaterials on the one hand and electrophoretic deposition, on the other in general.

The world people median age is growing; so the demand for bone substitute metallic implant will increase. Property features like as relatively low elastic modulus, high fatigue strength, and the osseointegration made titanium an appropriate choice for bone implant industrialization. However, weak surface characteristics such as depressed hardness, scant wear and scratch resistance deemed as its blind spot. Therefore research and development on titanium implants was concentrated on surface engineering. The using of bioactive hydroxyapatite (HAp) as a coating the titanium implant surface, gets better the surface characteristics. As well as accelerates the induction and conduction of the osteoblast cells, which in turn reduce the implant fixation time in the host tissue.

In spite of the common utilize of HAp coating, its permanency has permanently been a challenge due to a contradiction between ceramic coating and metallic substrate characteristics, especially coefficient of thermal expansion which outcomes in residual stresses. Insufficient coating coherency and indigent adhesion to the substrate lead to the coating delamination and detachment under loading in the physiological environment and inflammatory responses arise. Therefore, the coated implant not only will have utility over non-coated ones but also has more destructive consequences, so in spite of coating procedure, permanency and durability of HAp coating deemed as a general demand [1,7].

The TiO₂ layer is a favorable option as an intermediate layer between the HAp coating and the titanium substrate, because of the high mechanical integrity of TiO₂ with HAp and its chemical similarity to both HAp and titanium [16]. Moreover, the TiO₂ coating has superior tribological properties, anti-bacterial activity, and its biocompatibility has been proven by in-vitro and in-vivo biological tests [22,23]. [17] are amongst the researchers who accomplished promising outcomes by using the TiO₂ as a middle layer.

2.2 Types of Biomaterials

A biomaterial is any material, natural or man-made, that comprises whole or part of a living structure or biomedical device which performs, augments, or replaces a natural function [24]. These biomaterials are specifically designed by utilizing the classes of materials: polymers, ceramics, metals and composite materials. Most of the biomaterials available today are developed either singly or in combination of the materials of these classes. These classes of materials have different atomic arrangement which present the diversified structural, physical, chemical, and mechanical properties and hence offer various alternative applications in the body. The classes of the materials are illustrated in the following sections [25].

2.2.1 Polymers

Polymers are the convenient materials for biomedical applications and used as cardiovascular devices for replacement and proliferation of various soft tissues. There are a large number of polymeric materials that have been used as implants. The current applications of them include cardiac valves, artificial hearts, vascular grafts, breast prosthesis, dental materials [26], contact and intraocular lenses [27], fixtures of extracorporeal oxygenators, dialysis and plasmapheresis systems, coating materials for medical products, surgical materials, tissue adhesives, etc. [28]. The composition, structure, and organization of constituent macromolecules specify the properties of polymers. Further, the versatility in diverse application requires the production of polymers that are pre-pared in different structures and compositions with appropriate physicochemical, interfacial, and biomimetic properties to meet specific purpose[29].

2.2.2 Ceramics

Ceramics are another class of materials used for designing biomaterials. The use of ceramics is motivated by their inertness in the body, their assay formability into a variety of shapes and porosities, high compressive strength, and excellent wear characteristics. Ceramics are used as parts of the musculoskeletal system, hip prostheses, artificial knees, bone grafts, dental and orthopedic implants, orbital and middle ear implants, cardiac valves, and coatings to improve the biocompatibility of metallic implants. Though ceramics are utilized for designing biomaterials, yet they have been preferred less commonly than either metals or polymers. Applications of ceramics in some cases are severely restricted due to brittleness and poor tensile strength. However, bioceramics of phosphates are widely used to manufacture ideal biomaterials due to their high biocompatibility and bone integration, as well as being the materials that are

most similar to the mineral component of the bones [30]. Some of the materials which used in this study are:

A-Hydroxyapatite (HAp)

Hydroxyapatite (HAp) has been used as a bioactive component in dental and orthopedic fields for many decades [31]. HA belongs to the calcium phosphates group possessing the following chemical formula of $\text{Ca}(\text{PO}_4)_6(\text{OH})_2$, which can be found in nature chemically synthesized. It seems to be the most suitable ceramic material for hard tissue replacement implants from the view of biocompatibility. The methodology behind the wide use of HAp is because of its similar composition to bone. Therefore, HAp ceramics don't exhibit any cytotoxic effects. Around 70% of human bone and up to 90% of human dental enamel is made up of calcium phosphate. Since HAp closely resembles the chemical structure of bone, rapid integration and bone regeneration will be obtained by using HAp [32]. To overcome the brittle character of bioceramics, HAp is usually coated on the surface of titanium implants as load-bearing prosthesis [33].

Among the ceramics, apatite's occupied a prominent role. The calcium phosphate-based biomaterials are used in a number of different applications throughout the body, covering all areas of the skeleton. A few of its applications include dental implants, transdermic devices and use in periodontal treatment, treatment of bone defects, fracture treatment, total joint replacement, orthopedics, cranio-maxillofacial reconstruction, otolaryngology, and spinal surgery. Second, hydroxyapatite has been used as filler for bone defects and as an implant in load-free anatomic sites such as nasal septal bone and middle ear. It is also used to develop bio-eye hydroxyapatite orbital implants [34] and hydroxyapatite block ceramic [35]. In addition to these applications, hydroxyapatite has been used as a coating material for stainless steels, titanium and its alloys based implants, and on metallic orthopedic and dental implants to promote their fixation in bone. In

this case, the fundamental metal surfaces to the surrounding bone strongly bonds to hydroxyapatite. However, care has to be taken to avoid delamination. Since, delamination of the ceramic layer from the metal surface causes serious problems and results in the implant failure [36].

B-Titania (TiO₂)

Three phases of oxide titanium or titania in atmosphere air are anatase, rutile and brookite. Pure Rutile is a desirable phase in clinical applications due to the high corrosion protection of metallic implants, a large single crystals can be easily obtained, high biocompatibility and usually stated to be the thermodynamically most stable form of TiO₂. Anatase phase also has bioactivity properties. Anatase gradually transforms to rutile depending on temperature that has bioactivity properties. There are only small differences in Gibbs free energy between anatase, brookite and rutile (4-20 kJ/mol) meaning that the metastable polymer phase is almost as stable as rutile at normal pressures and temperatures [37, 38].

Titanium dioxide combines excellent resistance to corrosion and superior biocompatibility with photocatalytic activity. These properties make TiO₂ an ideal biomaterial with various ubiquitous applications in pharmaceuticals, pigments and cosmetics, and it has attracted particularly wide usage in the biomedical field as an integrating agent for implant-bone tissues. These ideal properties are due to its physio-chemical properties, including inertness, thermal stability, and an ability to assume various polymorphic forms: anatase, rutile, brookite, and oxygen deficient α -Ti₃O₅ [39]. The application of TiO₂ anatase coatings on the Ti-implant surface is one of the best ways to enhance the interactions between the material and the biological environment at the interface. **Lorenzetti** [25], reported that an anatase layer significantly reduced bacterial attachment with respect to the

amorphous titania layer, without adverse effects on the cell metabolic activity [40].

2.2.3 Metals and Alloys

Metallic implant materials have gained immense clinical importance in the medical field for a long time. Many of metal and metal alloys which are used for medical requirements include stainless steel (316L), titanium and alloys (Cp-Ti, Ti6Al4V), cobalt chromium alloys (Co Cr), zirconium niobium, and tungsten heavy alloys. The rapid growth and development in biomaterial field has created scope to develop many medical products made of metal such as dental implants, craniofacial plates and screws; parts of artificial hearts, pacemakers, clips, valves, balloon catheters, medical devices and equipments; and bone fixation devices, dental materials, medical radiation shielding products, prosthetic and orthodontic devices for biomedical applications [29]. Though there are other classes of materials from which biomaterials can be prepared, engineers prefer metals as a crucial one to design the required biomaterial. The main criteria in selection of metal-based materials for biomedical applications are their excellent biocompatibility, convenient mechanical properties, good corrosion resistance, and low cost [41].

The mechanical properties of metals have a great importance while designing load-bearing dental and orthopedic implants. However, when the implant requires high wear resistance such as artificial joints, Co Cr Mo alloys are used to serve the purpose. The properties of high tensile strength and fatigue limit of the metals allow them the possibility to design the implants that can carry good mechanical loads compared with ceramics and polymeric materials. In comparison to polymers, metals have higher ultimate tensile strength and elastic modulus but lower strains at failure. However, in comparison to ceramics, metals have lower strengths and elastic modulus with higher strains to failure [42].

In the biologic medium, when the metal-based biomaterial is implanted, the surface of material can change and degrade to release some by-products. Owing to this releasing process, interactions between metallic implant surface and cell or tissues occur [29]. This factor has stimulated the present day researchers to give great importance in understanding the surface properties of metallic products in order to develop biocompatible materials [25].

2.2.4 Composite Materials

Composites are engineering materials which contain two or more physical and/or chemical distinct, properly arranged or distributed constituent materials that have different physical properties than those of individual constituent materials. Composite materials have a continuous bulk phase called matrix and one or more discontinuous dispersed phases called reinforcement, which usually has superior properties than the matrix. Separately, there is a third phase named as interphase between matrix and reinforced phases [43]. Composites have unique properties and are usually stronger than any of the single materials from which they are made, hence are applied to some difficult problems where tissue in-growth is necessary. In recent years, scientific research has been focused to develop variety of biomedical composite materials, because they are new alternative solutions for load-bearing tissue components.

The main advantage of the composite biomaterials is though the individual metals or ceramic materials suffer from disadvantages like exhibition of low biocompatibility and corrosion by metals, brittleness, and low fracture strength by ceramic materials, the composite materials provide alternative route to improve many undesirable properties of homogenous materials (metals or ceramics).

The properties of the constituent materials have significant influence on composite biomaterials. One of the factor “linear expansion” plays a crucial role in designing composite biomaterial. Often composites are made from constituents that have similar linear expansion constants. If the constituent materials possess distinct linear expansion constants, contact area (interface) between reinforcement and matrix materials can generate large voids through the contact surface, which blots the purpose of the implant. Therefore, more care is required in selection of individual constituents while processing the composite biomaterial by bone tissue engineers [25].

2.3 Functionally Graded Materials

Functionally graded materials are a special class of composite materials, whose composition and/or microstructure vary in space in a controlled manner. In traditional (not graded) composites, the distribution of the constituent phases is - on average - uniform in space, involving a compromise between their peculiar properties. Composite materials permit prominent combinations giving hard, wear resistant surface and soft core as per functional requirement of the application. Heterogeneity, anisotropy, symmetry, and hierarchy are the major properties of composite materials reaping particular interest for numerous applications. Higher resistance to fatigue, wear and corrosion, high reliability and other properties are the benefits of composites over pure or alloyed metals. Although all these advantages, composite materials are exposed to the sharp transition of properties at the interface which can outcome in component failure (by delamination) at perilous working situations (See **Figure 2.1**). Instead, graded structures integrate different materials without severe internal stresses and combine different properties in one material system; in other words, the desirable properties of the ingredient materials can be fully exploited without

creating an abrupt interface between macro-domains of heterogeneous composition [44, 45].

This damage of traditional composites reduced by improved composites forms known as FGMs. In these materials, the sharp interface is subrogated by a gradient interface and that led to the smooth transition of characteristics from one material to the other. These sophisticated materials with engineered gradients of composition, specific characteristics and structure in the preferred direction are superior to a homogeneous material composed of comparable ingredients [46].

Even if the most common idea of FGM implies that two different constituent phases change gradually from one to the other (for example, from ceramic to metal), FGMs include all those functional materials whose properties change locally according to a specific design, arbitrarily introduced to fit an intended application or to enhance a wide variety of properties, especially the mechanical ones. As a matter of fact, if appropriately designed, the presence of a functional gradient at the microscale may result in improved properties at the macroscale [47]. Therefore, the FGCs are developed version of the traditional double layered coatings, in which their chemical composition changes gradually according to a predetermined pattern [8]; presented the opportunity to combine various layers with minimum residual stresses and improved interface bonding.

The mechanical characteristics such as elastic modulus, poisson's ratio, elastic modulus for shear, the density of materials and thermal expansion coefficient are differing smoothly and continuously in favorite FGMs directions. Due to these different properties, the functionally graded materials used as a biomedical material and there are many examples of natural FGCs like bones, teeth and skin [49]. Basically, a functionally graded film is composed of a buffer layer at the substrate which gives maximum bonding whilst the outermost top coat layer provides good

bioactive properties to accelerate bone healing. In between the two there lies a transition layer with intermediate properties as shown in **Figure (2.2)** [50].

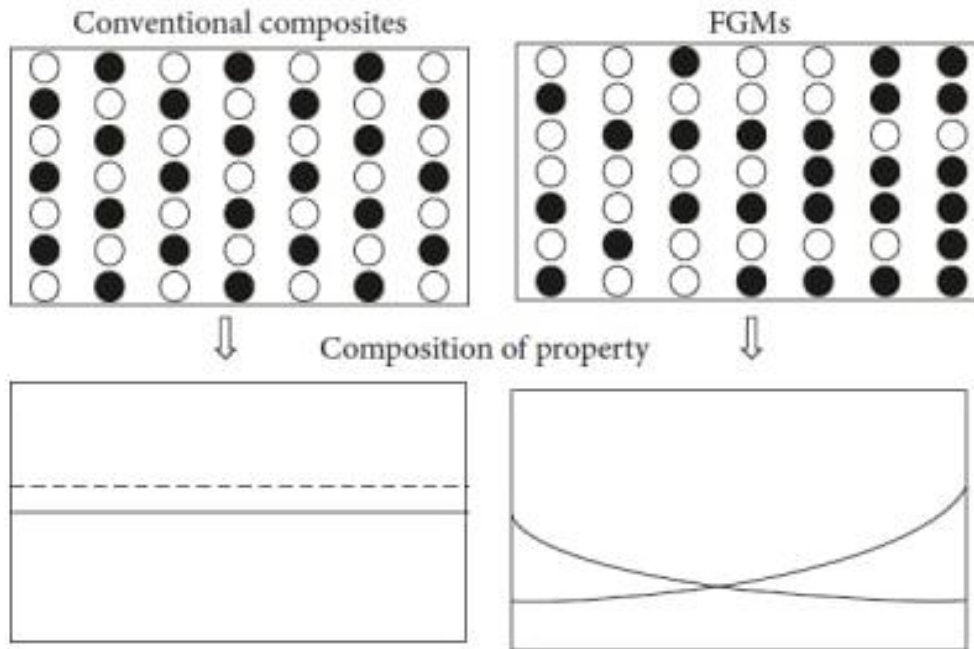


Figure (2.1): Variation of properties in conventional composites and FGM [44].

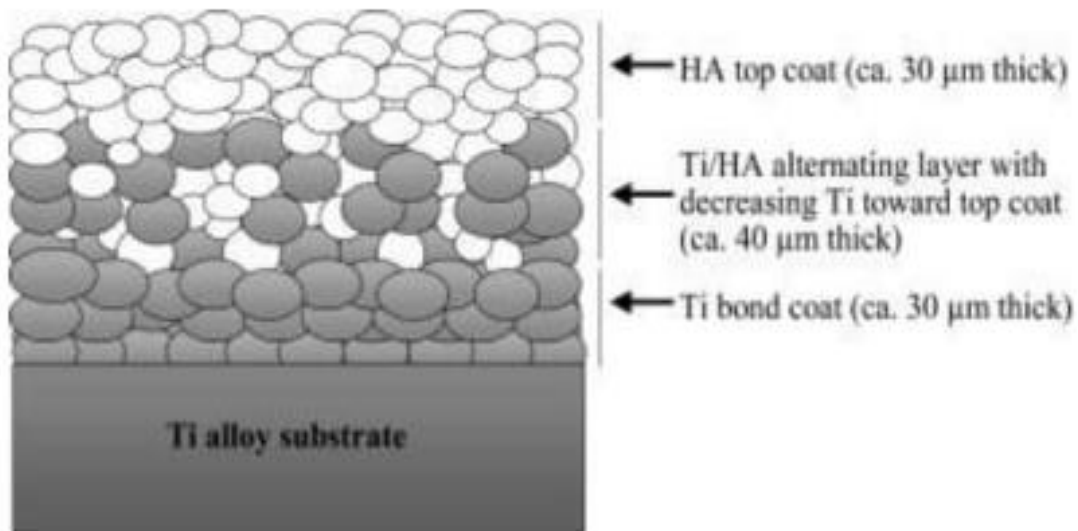


Figure (2.2): Functionally graded coating [50].

2.4 Functionally Graded Materials Applications

There are numerous implementations for (FGMs) and below several of them:

2.4.1 Aerospace Field

(FGMs) are utilized in aerospace manufacture due to the ability of these materials to impedance the high thermal gradient, the withstanding for very high thermal gradient make these materials appropriate structures in airplane body, the components of the rocket motor and numerous other implementations in the space [51].

2.4.2 Optoelectronics Field

Nowadays, graded materials are widely used for antireflective layers, fibers, GRIN lenses and other passive elements made from dielectrics, also for sensors and energy applications. For example, the modulation of refractive index could be obtained in such components through the change in material composition. Another possibility is to apply concept of gradation in semiconductor active devices. In semiconductors the material function can describe energetic band gap, refractive index, carrier concentration, carrier mobility, diffusion length, built-in electric field and another properties which strong influence the parameters of optoelectronic devices [52].

2.4.3 Defense Field

Through the characteristics of the functionally graded materials is well known these materials have an superior ability to prohibit cracks from spreading. These properties help to implement these materials in defense especially to conserve soldiers from a gun by manufacturing armour plates and bullet-proof vests [53].

2.4.3 Energy Sector

Functionally graded materials also have special properties based on heat resistance, corrosion resistance and thermal shock resistance. In particular, the development of various special function graded materials has made FGM play an important role in the energy field [54].

2.4.4 Biological Field

The gradient material is common in nature, such as the shell of layered structure, the hard and tough animal skeleton, and the layered human skin. The medical development of FGM makes medical assistance to patients more timely and effective. The functionally graded material has the characteristics of high specific strength, high specific modulus, abrasion resistance and biocompatibility. Based on this, the artificial joint developed makes the artificial prosthesis and the patient's own skeleton have strong binding force and reliable Durable, showing good biocompatibility, but also has good self-healing and repair of regenerative properties. With its superior properties, FGM has a good application prospect in the biomedical fields, such as artificial bones, teeth, and heart [54].

2.4.5 Construction Field

Construction manufacturing mug numerous challenges that related to materials performance, cost of materials and their environmental affect. As well the change of the functionality of the building structures that vary depending on the building location open the way to use FGMs in the construction field. When utilize (FGMs) the structure and the composition of materials will be changed gradually over the volume, and that leads to the different material properties [55].

2.5 Physical Metallurgy of Titanium Alloys

Titanium does not occur as a pure metal in nature, but forms compounds with other chemical elements e.g. oxygen. Common ores are rutile and ilmenite. Titanium is present in the Earth's crust at a level of approximately 0.6%, and it is the fourth most abundant structural metal after aluminum (Al), iron (Fe) and magnesium (Mg) [56]. It is a transition metal and has an atomic number of 22 and an atomic weight of 47.9. Because it has an incomplete electron shell in its electronic structure, elements which are within the range of 0.85-1.15 of the atomic radius of titanium can alloy substitutionally and have a significant solubility. Elements with an atomic radius that is substantially smaller than the radius of titanium, e.g. oxygen (O), nitrogen (N) and hydrogen (H), occupy interstitial sites in the crystal structure [57, 58]. Titanium can crystallize to form various structures, but each is only stable within a particular temperature range [59]. Pure titanium exists in two allotropic forms. The low-temperature (A), hexagonal close packed structure (hcp), is stable below 882.5 °C the transus temperature. The high-temperature (B), body centred cubic structure (bcc), is stable between 882.5 °C and the melting point of 1670 °C [60]. The crystal structure of the hcp α and bcc β phases are shown in **Figure (2.3 A,B)**. Adding certain alpha stabilizing elements, such as Al, gallium (Ga), oxygen (O) and germanium (Gr), can raise the transus temperature of titanium. Elements such as molybdenum (Mo), vanadium (V) and chromium (Cr) stabilize the β phase by lowering the temperature of transformation from the hexagonal structure to the cubic structure [61].

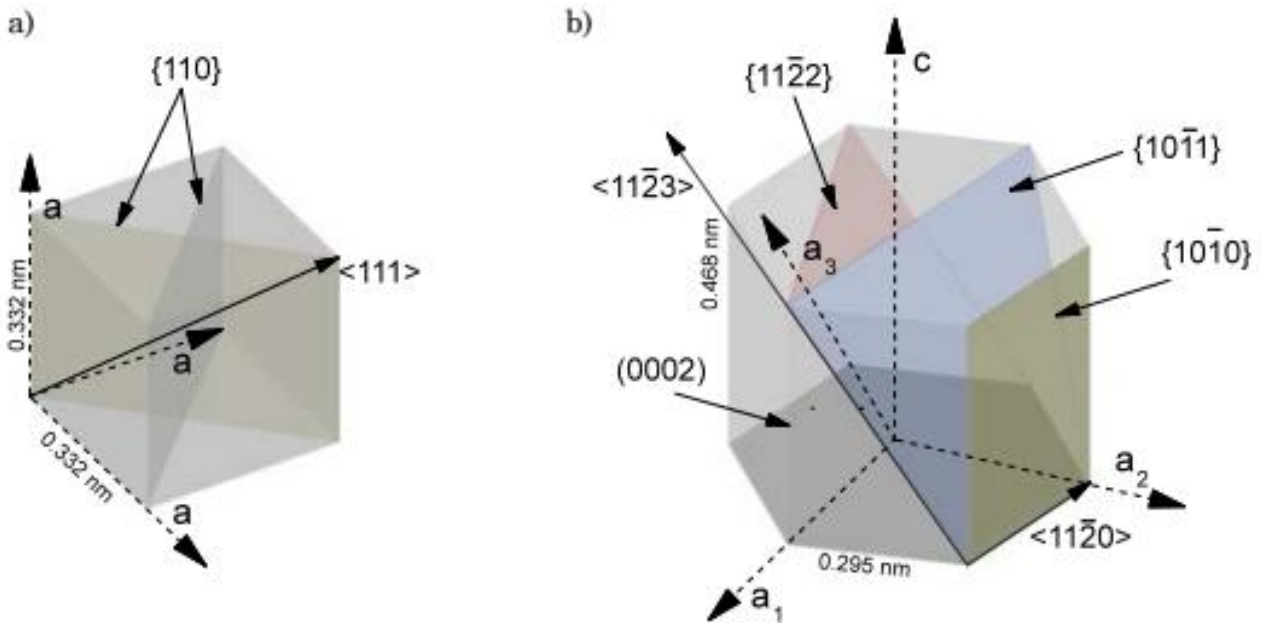


Figure (2.3): Crystal structure of (A) bcc phase (also called β phase) and (B) hcp phase (also called α phase) [61].

2.6 Alloy Classification

Depending on the alloying stabilizers and phases present in the microstructure, titanium alloys are classified as; α , β or $\alpha + \beta$. Commercially unalloyed titanium (also known as CP-Ti) and α alloys have essentially all-alpha microstructures. β alloys have largely all-beta microstructures after air cooling from the solution treatment temperature above the beta transus. $\alpha + \beta$ alloys contain a mixture of alpha and beta phases at room temperature. A list of the most important commercial alloys belonging to each of these three different groups is shown in Table (2-1) [61].

The widely used, classification by [57] suggested three main classes; α , $\alpha + \beta$, and (meta-stable and stable) β -alloys, based on their location in the pseudo-binary β -isomorphous phase diagram. T_β is the β solvus temperature. Adapted from [62].

Table (2-1): Chemical compositions of important commercial titanium alloys [61].

Alloy classification	Alloy name	Alloy composition (wt.%)	T _β [°C]
α and near-α	CP Grade 1	CP-Ti (0.2Fe, 0.18O)	890
	CP Grade 2	CP-Ti (0.3Fe, 0.25O)	915
	CP Grade 4	CP-Ti (0.5Fe, 0.40O)	950
	CP Grade 12	Ti-0.3Mo-0.8Ni 880	880
	IMI 834	Ti-5.8Al-4Sn-3.5Zr-0.7Nb-0.5Mo-0.35Si	1045
α + β	Ti-6Al-4V	Ti-6Al-4V	995
	Ti-6242	Ti-6Al-2Sn-4Zr-2Mo-0.1Si	995
	Ti-6246	Ti-6Al-2Sn-4Zr-6Mo	940
β	Ti-17	Ti-5Al-2Sn-2Zr-4Mo-4Cr	890
	Ti-5553	Ti-5Al-5Mo-5V-3Cr-0.5Fe	-
	Ti-15-3	Ti-5V-3Cr-3Al-3Sn	760
	Beta-CEZ	Ti-5Al-2Sn-2Cr-4Mo-4Zr-1Fe	890

2.6.1 α and near-α alloys

The class of α titanium consists of unalloyed titanium and α (near-α) alloys. Unalloyed titanium and α alloys have a single-phase, hexagonal close packed crystal structure. Because these alloys are single-phase, their tensile strength is relatively low [63]. Single phase α alloys are widely used in applications that are not particularly demanding in terms of strength. α alloys are attractive due to their corrosion resistance and are used in applications such as tube heat exchangers. The different grades of CP Ti differ with respect to their iron and oxygen content from 0.18% (grade 1) to 0.40% (grade 4). Oxygen is an interstitial alloying element which significantly increases strength with a reduction in ductility. Small amounts of beta

stabilizers are also sometimes added to allow greater manipulation of the microstructure during processing. Titanium alloys based on the α phase are attractive materials for structural applications due to their high strength (700-1000 MPa), good fracture toughness, relatively low density and corrosion resistance. The most widely used commercial high-temperature titanium alloys for aero-engine application belong to the near α class. Near- α alloys contain up to 2% beta stabilizing elements. As a result, these alloys contain a small amount of beta phase in the microstructure and they behave more like α alloys than $\alpha+\beta$ alloys [56, 63]. Despite all these attractive properties, the performance of Ti alloys is often hindered by the phenomenon of dwell fatigue.

2.6.2 $\alpha + \beta$ alloys

$\alpha+\beta$ titanium alloys contain both alpha and beta phases. Ti-6Al-4V is the most commonly used alloy which has a good combination of mechanical properties, wide processing window, and can be used up to a temperature of 350 °C [64]. Aluminum is added to stabilize and strengthen the alpha phase while the addition of vanadium, as a beta stabilizing element, offers a greater proportion of the ductile beta phase during hot forming operations such as rolling. Mechanical performance is controlled via ageing to control microstructural development. **Table (2-2)** summarizes the physical and mechanical properties along with the temperature capabilities of some of the commercially used Ti alloys. Ti-6Al-4V is referred to as like 'workhorse' of the titanium industry because it is the most commonly used titanium alloy. This alloy is usually subjected to heat treatment to achieve moderate increase in strength [65]. Ti-6Al-4V can be considered for any application where a combination of light weight, high specific strength, corrosion resistance, excellent high temperature properties and metallurgical stability are required. This material has been used in many applications such as, aerospace

applications, medical devices, biomedical applications, automotive parts, marine applications, and sports equipment [65,66].

$\alpha + \beta$ alloys account for approximately 60 wt.% of the titanium used in aerospace and up to 80 to 90 wt.% of that used for airframes. The understanding microstructural variances of titanium alloys and the effect on mechanical properties are important, because the failure of a component may cause serious consequences for the aircraft.

Table (2-2): Properties of some titanium alloys including density (ρ), ultimate tensile strength and Young's modulus [60].

Alloy classification	Alloy name	Density (g/cm ³)	Young's modulus (GPa)	Ultimate tensile strength (MPa)
α and near- α	IMI 834	4.55	117	1035
$\alpha + \beta$	Ti-6Al-4V	4.43	110	1035
	Ti-6242	4.54	120	1010
β	Ti-15-3	3 4.76	107	1135

2.6.3 β alloys

β titanium alloys can be further classified into three groups; stable β , metastable β , and beta-rich $\alpha + \beta$ alloys. A schematic phase diagram for isomorphous titanium alloys is shown in **Figure (2.4)**. The stability of the beta phase is determined by the cumulative wt.% of β stabilizers. Alloys containing between 10 wt.% and 15 wt.% of β stabilizing elements, resulting in the beta phase being retained at room temperature in a metastable condition. These alloys are an attractive alternative to $\alpha + \beta$ titanium alloys due to their high strength, deep hardening and wide processing window. Another advantage of these alloys is their excellent forge ability. However because of the large amount of heavy elements required to stabilize the beta phase, beta alloys are 10% heavier than $\alpha + \beta$ alloys [67]. These alloys can be found in mainly airframe applications, power plants, sporting goods,

automotive, and orthopedic implants.

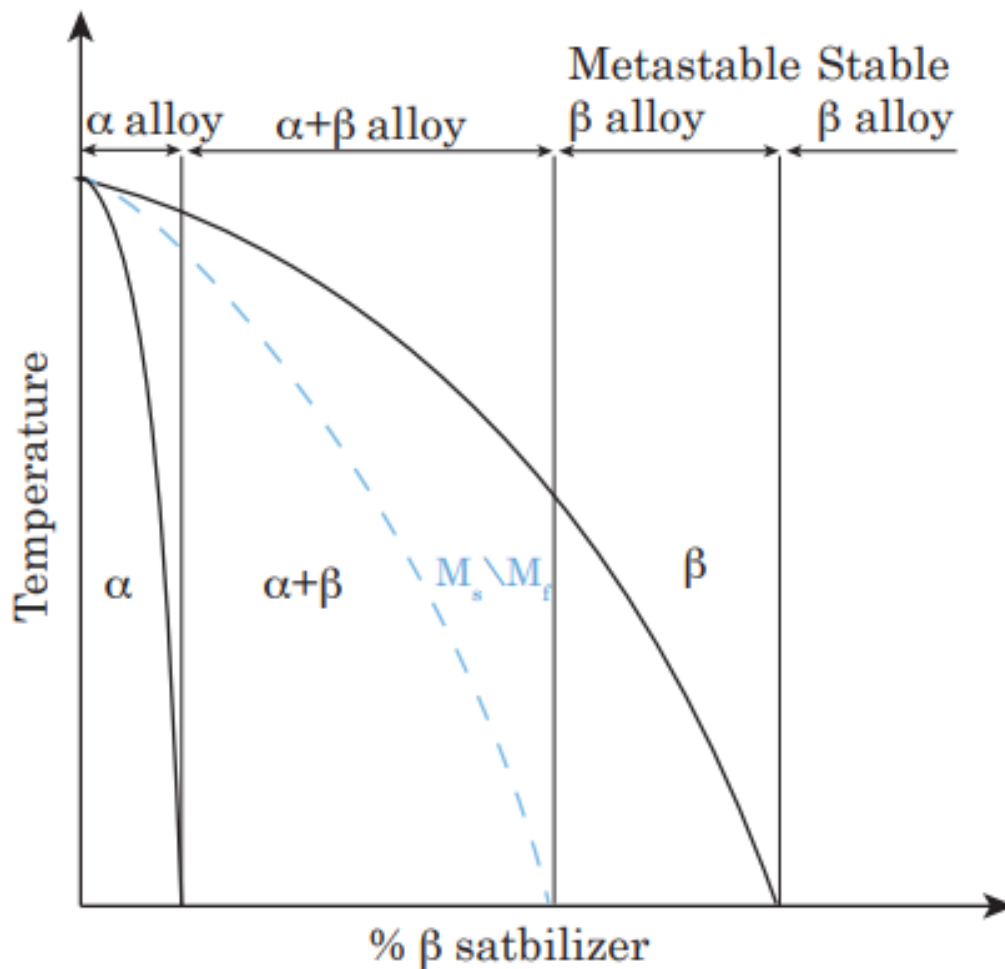


Figure (2.4): Schematic section through a β isomorphous phase diagram. M_s is the temperature at which martensite begins to form when cooling from the β phase field to room temperature and M_f is the temperature at which reaction is complete. Adapted from [63].

2.7 Titanium Aluminum Vanadium Ti-6Al-4V alloy

F 136 Ti-6Al-4V for orthopedic load-bearing implants alloying, addition of 6% aluminum with α phase and 4% vanadium with β phase to cpTi, results in any alloy having good mechanical properties yield strength is about 880MPa (increasing the yield and tensile strength, acceptable elongations) and chemical inertness. From **Figure (2.5)** it is clear that for

this aluminum level of about 6% the α / β , transformation temperature of 882°C for pure titanium is increased to about 1000°C for the two phase region $\alpha + \beta$. Since vanadium is a β -stabilizer, this means that the higher temperature β more readily transforms to α during cooling after processing, and also during any subsequent heat treatment at relatively low temperatures, annealing at 700–750°C [68].

The most popular titanium alloy, more than 50% of alloys in use today are of this composition. The passive film consists of TiO_2 as the major component and Aluminum oxide (Al_2O_3), vanadium oxide (VO_2) respectively on the metal surface. In return to VO_2 is thermodynamically unstable and performs into solution body. An inert fibrous capsule formation around the implant to prevent damage to surrounding tissues and eliminated by body within 24 hours, this is presumably why implants made of Ti-6Al-4V alloy have not shown any serious disadvantages so far [68]. In general, there is a problem in using Ti-6Al-4V alloy for implant applications belong to the large modulus mismatch between the Ti-6Al-4V alloy (~110GPa) and the bone (~10-50GPa), which could cause insufficient loading of the bone adjacent to the implant. Development of new alloy materials and modification of the surface of the currently used Ti alloys have been widely explored to overcome these problems. Either the development of Ti6Al7Nb and Ti5Al2.5Fe, where Nb and Fe were substituted for V in Ti-6Al-4V alloy as less toxic alternatives or numerous bioactive surface modifications of titanium alloys for biomedical applications are very important for achieving further developed biocompatibility [69].

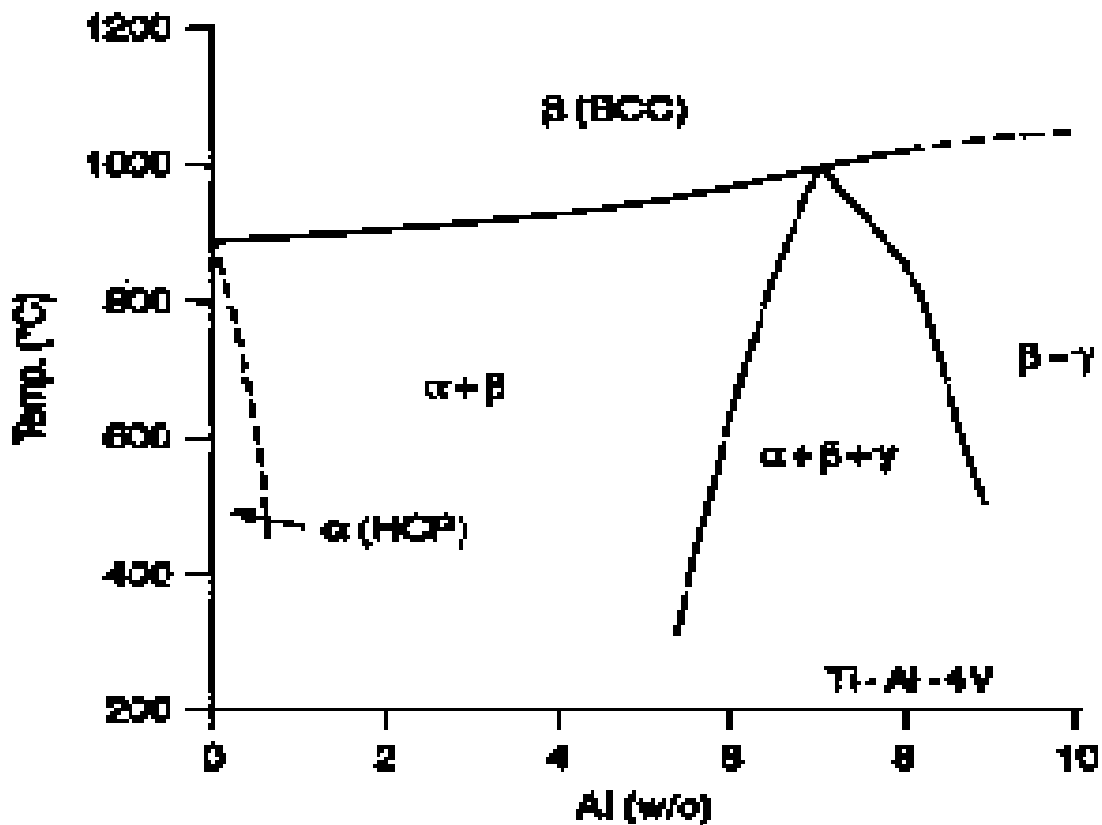


Figure (2.5): Phase diagram of Ti-Al-V alloy [68].

2.8 Nature of the Physiological Environment

The nature of physiological environment is extremely hostile to all foreign materials and hence the effect of environment on metallic implant and the effect of implant on its host tissue are of primary concern. The concentrations of chloride ions in serum and interstitial fluid are 113 and 117 mEq/L, respectively, which are about one-third the concentration of brine and a seriously corrosive environment for metallic materials [70]. The aqueous layer at the implant site naturally contain numerous hydrated ionic species (Na^+ , Ca^{2+} , etc.). The type and concentration of ions in solution are likely to change over a period of time as the cells surrounding the implant react and adapt to the presence of foreign material. Other electrolytes present

in the body fluid include Ca^{2+} , Mg^{2+} , PO_4^{3-} SO_4^{2-} and organic acid anions. Some complex compounds present in smaller amounts are phospholipids, cholesterol, natural fats, proteins, glucose and amino acids [71]. Dissolved oxygen, dissolved bicarbonate and some other constituents of body fluids (e.g., phosphates, cholesterol and phospholipids) are usually thought to either play no role in the corrosion process or exist at insignificant levels. Therefore, most *in vitro* experiments have been conducted in either saline or standard isotonic solutions such as Ringer's or Hank's, in which the presence of bicarbonate and calcium chloride is the main difference compared to saline [72]. The oral environment undergoes significant changes during the day. The mastication forces, oral pH, the presence of different chemical compounds from the food, drinking water, mouthwash products and inflammatory reactions play an important role on the degradation of the implants. Lactic acid is naturally released by bacteria in the oral cavity. This acid simulates the conditions which are reached during drinking acidic beverages, regurgitation or the presence of dentobacterial plaque. Bacteria present in the dental plaque generate a formation of mixture of acids like lactic, acetic and other metabolic acids which cause the decrease of pH up to 4 or lower. Such low pH of the saliva destroys the tooth [73, 74]. With respect to dental implants, the environment in the oral cavity is not well-defined. Several recipes exist for artificial saliva, the most popular one is that of Fusayama [75], that is, $0.400 \text{ g}\cdot\text{dm}^{-3}$ NaCl, $0.400 \text{ g}\cdot\text{dm}^{-3}$ KCl, $0.795 \text{ g}\cdot\text{dm}^{-3}$ $\text{CaCl}_2\cdot\text{H}_2\text{O}$, $0.690 \text{ g}\cdot\text{dm}^{-3}$ $\text{NaH}_2\text{PO}_4\cdot\text{H}_2\text{O}$ and $0.005 \text{ g}\cdot\text{dm}^{-3}$ $\text{Na}_2\text{S}\cdot 9\text{H}_2\text{O}$, at pH 5.5. However, the composition of human saliva actually varies considerably between individuals, especially in the sulfide content, which can cause tarnishing of both silver and gold-based amalgams [72].

The biocompatibility of titanium implant is determined by the chemical properties of the oxide layer [76]. The titanium alloys spontaneously form a passive oxide layer (mainly TiO_2) that, to some extent, can protect these alloys against corrosion because of its thermodynamic stability, chemical inertia, and low solubility in the body fluids [77]. The passive layer plays an important role for the surrounding it tissues, and the passive film cannot undergo break down if the implant is to be successful [78].

However, severe corrosion can occur when this passive oxide layer is mechanically disrupted. In such situations, aggressive Cl^- ions may attack the implant material surface. For instance, fretting wear is known to occur at the interface of modular junctions (for example, head-neck taper junction of hip implants) due to relative micro-motions. The fretting wear disrupts the passive oxide body [79-81].

2.9 Ion Release of Ti6Al4V Alloy in Human Body

Ti6Al4V alloy contains aluminum which is well-known to cause certain bone diseases and neurological disorders. Vanadium is considered to be an essential element in the body, but may become toxic at excessive levels. The toxicity of vanadium is well-known, and can be aggravated when an implant is fractured and subsequently undergoes fretting. Release of titanium ions into the tissues adjacent to the implants results in discolouration of the tissues. This may also be detrimental to the bone attachment and further bone growth on the implant [82].

It should be noted that the amounts of Al and V released from Ti-6Al-4V may be so small that the alloy is perfectly acceptable as

an implant material. It is generally regarded as one of the most biocompatible of all the available prosthetic alloys [83].

Metallic elements have a different tendency to release ions, and even trace amounts of elements in the alloy composition should not be neglected. There are data on the significant contents of some alloying elements of Ti6Al4V within the tissue around the implanted alloy. So far reports on the consequences of ion release into the body have focused on the importance of the possible impact of released ions on biomolecules and the initiation of adverse biological reactions as the titanium ions could quickly react with water molecules or inorganic anions, easily binding with body fluids [84].

The toxicity of titanium alloy components, especially vanadium, has become an issue of concern. The release of aluminum and particularly vanadium ions from this alloy can generate long-term health problems such as peripheral neuropathy, osteomalacia and Alzheimers disease [84].

2.10 Influence of Surface Texture and Wettability on Initial Bacterial Adhesion on Metallic Implant

As soon as implant surfaces are exposed to the human oral cavity, they are immediately colonized by microorganisms [85]. The initial bacterial adhesion on implants is the first and essential step in the geneses of complex peri-implant biofilms, which, in turn, may result in peri-implantitis and loss of the supporting bone [86]. The type of implant material and its specific texture and physico-chemical surface properties influence the quantity and quality of microbial colonization [87]. In modern biomaterial research, implant surfaces are mainly modified to increase osseous integration into the alveolar bone; recently however, implant surfaces are also modified

to reduce biofilm formation after exposure to the oral cavity. Innovative implant materials or surface modifications with reduced adhesion properties or even with antibacterial properties are of pertinent clinical interest [88]. Up to now, monolithic titanium has been the most frequently used base material and gold standard for the construction of implant systems. Titanium is known for its excellent biocompatibility and outstanding mechanical properties [89].

Surface roughness, texture, and wettability are regarded as the most significant surface factors influencing microbial accumulation on implants. Increased surface roughness on implant surfaces correlates with faster and firmer integration into the surrounding bone. On the other hand, however, most studies indicate a positive correlation between surface roughness and the amount of adhering bacteria [90].

wettability is quantified by the CA, which is the angle between the tangent line to a liquid drop's surface at the three phase boundary and the horizontal solid's surface. In principle, the CA can range from 0° to 180°. Surfaces with water CAs lower than 90° are designated as hydrophilic, and those with CAs very close to 0° are superhydrophilic. Surfaces with water CAs above 90° are considered hydrophobic, and those with CAs above 150° are termed superhydrophobic. Most implant surfaces currently in clinical use are hydrophobic, according to findings and those of other groups [91,92]. However, the range of CAs found on different dental implant surfaces varies widely, from superhydrophobic angles around 150 to superhydrophilic ones of 0. Moreover, it is commonly accepted that surface topography and surface roughness have a strong influence on the bacterial adhesion [93].

2.11 Biocompatible Coating

The various coatings have been applied for many years in medicine to improve the properties of the interface between implants and tissues, which determine the biocompatibility and healing time. In past years, the reviews on such functional coatings for dental implantology [94], biocompatible coatings for bone implants [95], ion substituted hydroxyapatite thin films [96], titanium implants polymeric coatings [97], ceramic coatings for osteoporotic bones [98], and pulse laser deposited animal-originated calcium coatings can be found. The coatings for biological applications, called biocoatings, may be made of metals, polymers, ceramics, and bioglasses, or can be composite coatings, co-deposited, or formed layer-by-layer (hybrid or sandwich coatings). They may be formed by various techniques such as direct electrocathodic deposition (ECD), pulse electrocathodic deposition (PED), electrophoretic deposition (EPD) [97], plasma electrochemical oxidation (PEO) called also micro-arc oxidation (MAO) in calcium[99], and phosphorus-containing phosphate solutions, chemical vapor deposition (CVD), plasma vapor deposition (PVD), magnetron sputtering, pulsed laser deposition, and many others. They may coat the solid or porous substrates. Comparing all the existent coatings, the bioceramic coatings appear to be the best choice for metallic implants. The advantages of various types of bioceramic coatings besides their applications are shown in **Table (2-3)** [99].

The research on the biocompatibility improvement by both bioactive and bioinert functionalization coatings deposited on metallic implant surfaces has become one of the hottest topics in biomaterials. The new trend in medical application is to use the implants with antibacterial properties along with good mechanical and physical-chemical properties and high bond bonding [100].

Table (2-3): Bioceramic coatings with different coating materials used for medical applications in the human body [99].

Coating material	Medical applications	Advantages
Nitrides (TiN, ZrN, NbN, TiAlN) Oxynitrides (TiON, ZrON, TiSiON)	Dental implants Fracture fixation devices Metal components of joint end prostheses	High corrosion resistance High adhesion on the metallic surfaces Good friction Coefficient
Carbon-based coatings (DLC, CN, a-C, carbides, carbonitrides)	Artificial heart valves Orthopedic fixation devices Artificial ligaments and Tendons	Low friction coefficient and wear rate High biocompatibility with blood
Calcium phosphates, bioglass	Percutaneous devices Spinal implants Maxillofacial reconstruction Skull plates	High osseointegration Capability
Oxides (TiO ₂ , Al ₂ O ₃ , ZrO ₂)	Dental implants Devices for increasing alveolar area Maxillofacial reconstruction Ophthalmic implants	High corrosion resistance Good regenerative Capability

2.12 Electrophoretic Deposition Technique

Electrophoretic Deposition (EPD), a traditional processing method in the ceramic industry, is gaining an increase interest both in academia and in the industrial sector for production of new materials. Consequently, a wide range of novel applications of EPD in the processing of advanced monolithic materials, composites and coatings is emerging. The interest in the EPD

technique is based not only on its high versatility to be used with different materials and combinations of materials, but also its a cost- effective method usually requiring simple equipment. With EPD particulate deposits can be made in seconds on suitable surfaces of planar or more complex geometry. Moreover EPD has a high potential for scaling up to large product volumes and sizes, as well as to a variety of product shapes and 3D complex structures. As well as, some advantages like being faster, less expensive, more uniform deposited coatings on complex substrate shapes, high purity of deposits and no phase transformation during coating process would be related to EPD process [101].

EPD consists of two different steps. In the first step (named electrophoresis) charged particles in suspension move towards an oppositely charged substrate under the influence of an applied electric field. In the second one (the deposition itself) the particles coagulate to create a coherent and homogeneous coating on the surface of the conductive substrate. Once the liquid solvents are evaporated, the coating is dried, different steps, e.g. sintering, can be applied to consolidate the coating. This march is required mainly for ceramic coatings, but can be avoided for organic/inorganic coatings where the organic phase acts as binder. EPD is achieved via the motion of charged particles dispersed in a suitable liquid towards an electrode under an applied electric field. Deposit formation on the electrode occurs via particle coagulation. Electrophoretic motion of charged particles during EPD results in the accumulation of particles and formation of a homogeneous and rigid deposit at the relevant electrodes [102].

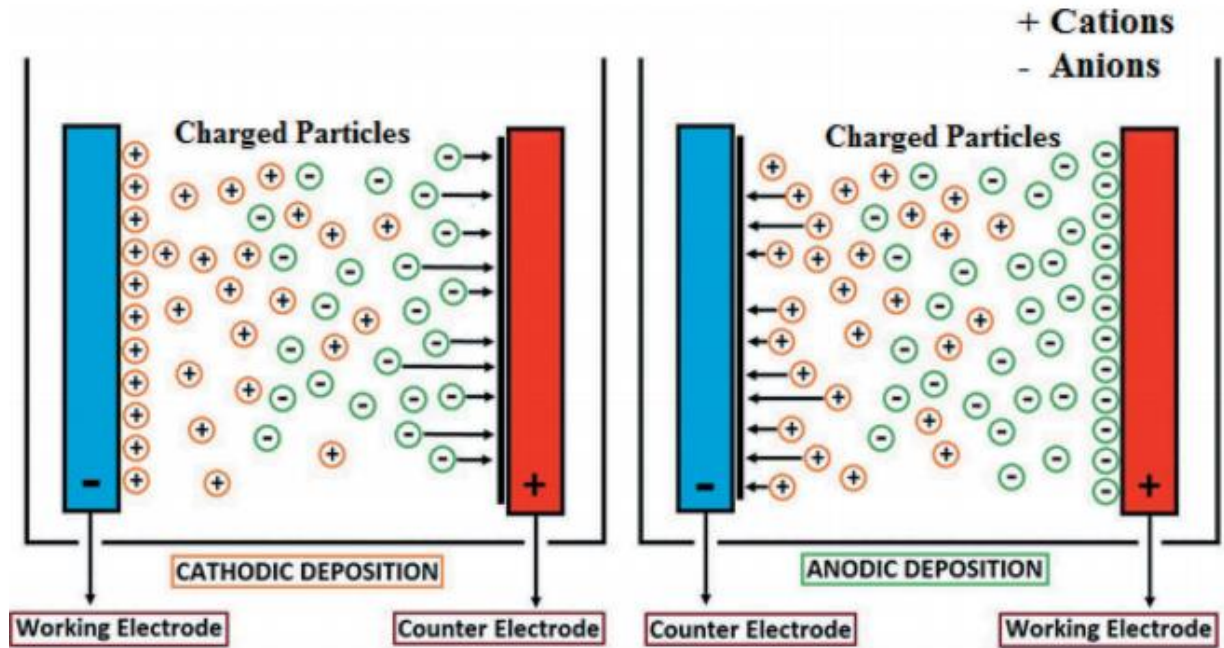


Figure (2.6): Schematic diagrams of electrophoretic deposition (EPD) on metal substrates (working electrodes) [103].

An EPD setup contains a power source, two electrodes (anode and cathode) and a EPD cell carrying the suspension with homogeneously dispersed particles or macromolecules. According to the direction of deposits, the EPD can be separated into anodic EPD, and cathodic EPD, as schematically shown in **Figure (2.6)**. Particles having a positive surface charge will be deposited on the cathode and negative charged particles be deposited on the anode under the electric field. The current supplied to electrodes can either be direct current (DC) or alternating current (AC). The nature of the suspension and processing parameters affecting electrophoretic deposition then reviewed. Suspension parameters such as the particle size, dielectric constant, conductivity and zeta potential determine the quality of the suspension, while physical parameters such as the voltage, deposition time and conductivity of the substrate determine the success of the EPD deposition. Lower surface charged particles tend to attract each other and the deposited coating is found to be porous, and particles with a

high surface charge produce a strong electrostatic repulsion force at the time of deposition, thereby producing a dense coating. Hence, a uniform particle suspension with a proper conductivity and medium dielectric constant results in better deposition [103].

2.12.1 Kinetics of EPD

One of the first approaches to understand the kinetics of EPD was made by Hamaker in 1940 [104]. He established (Eq. 2.1) that the deposition yield (w) [g] is function of the concentration of solids in suspension (C_s) [g/m³], the electrophoretic mobility (μ) [m²/(V.s)], deposition surface (A) [m²], electric field (E) [V/m] and deposition time (t) [s] [104].

$$w = C_s \cdot \mu \cdot A \cdot E \cdot t \quad \dots \dots \dots (2.1)$$

When different materials are present in suspension, the deposition rate is function of the volumetric fraction of those materials. At high volume fraction the solids deposit at equal rate, and at low volume fractions each material present an own deposition rate function of the particle mobility. Hamaker's equation does not consider the decrease of concentration in suspension as function of the time and therefore can be used only for short deposition times (like for the systems presented in this thesis).

Other attempt to describe the EPD kinetic was done by Avgustnik et al. [105], in this case the deposition for a cylindrical substrate was considered. Later Biesheuvel and Verweij [106] introduced a correction factor considering the concentration decrease in suspension (Eq. 2.2). In this approach l is the cylinder longitude, a and b are the radius of the deposition and counter electrode, respectively, ϕ_s and ϕ_d are the volumetric concentration of particles in suspension and deposit, respectively, C_d is the mass concentration of particles in the deposit [106].

$$W = \frac{2\pi \cdot \mu \cdot l \cdot E \cdot C_d}{\ln(a/b)} \cdot \frac{\phi_s}{\phi_d - \phi_s} \cdot t \quad \dots \dots \dots (2.2)$$

Sarkar and Nicholson [107] introduced an efficiency correction factor ($f \leq 1$) to Hamaker's equation based in the fact that not all the materials that reach the deposition electrode forms part of the final coating. They also considered the change of concentration in suspension and also if the deposition is conducted in potential or current constant conditions, see Figure (2.7). Just for I in this figure the deposition rate remains constant while for the rest of the systems (II to IV) an asymptotic behavior appears. It is clear that when the particle concentration in suspension decreases the deposited amount of particles is less (II and IV) than for constant concentration conditions. At constant concentration and potential conditions (III) the deposited film form an isolation layer decreasing the electrical driving force or voltage per length unit.

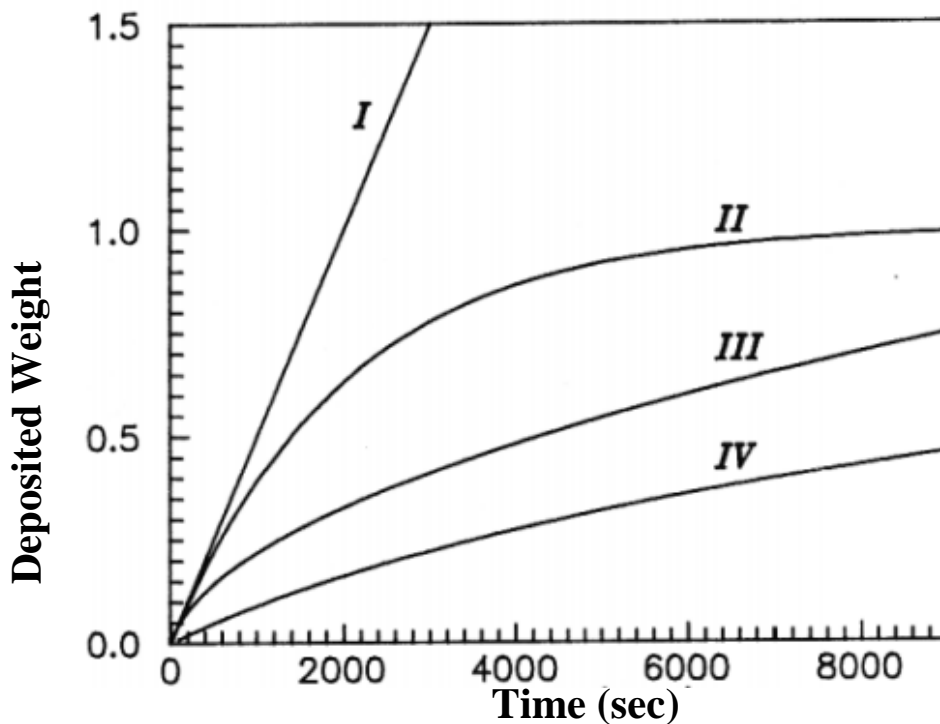


Figure (2.7): EPD scheme of deposited weight against deposition time [107].

2.12.2 Suspension of Particles

Key parameter of the electrophoretic deposition process is the slurry or suspension, it must be well stabilized, homogeneous and without agglomerated particles [108]. In presence of polar solvents, e.g. water, most substances present a surface electric charge. The development of charge on a solid particle surfaces can occur by different reasons:

- (i) dissociation or ionization of surface groups (this factor depends on the suspension pH),
- (ii) reabsorption of potential-determining ions,
- (iii) specific ions absorption on the particles surface (surfactants),
- (iv) isomorphous replacement/lattice substitution and
- (v) charged crystal surface fracturing [107].

The particles are suspended in the fluid media via the interaction of three different forces:

- (A) the van der Waals attractive force,
- (B) electrostatic repulsive force, and
- (C) steric (polymeric) force (this last one is not always present).

To have a stable suspension the electrostatic repulsive and/or the steric forces must be dominant against the van der Waals force that tries to agglomerates the particles due to the electrostatic force, same charge particles repel themselves keeping them in suspension, on the other hand they attract opposite and same charged ions that form a diffuse double layer increasing suspend ability and stability.

2.12.3 Double Layer and ζ -potential

Due to the particle surface charge a layer of opposite charged ions (counter-ions) forms around the particle, while the similar charged ions (co-ions) in the medium are repelled away from the particle. It suppose that under an electric field the particles and counter ions should move on

different directions (electrodes), but the particle/counter-ions attraction force is strong enough to keep them together, this is called the "stern layer" An external second layer is formed by the co-ions and counter-ions, this is denominated the "diffuse layer" **Figure (2.8) [109]**.

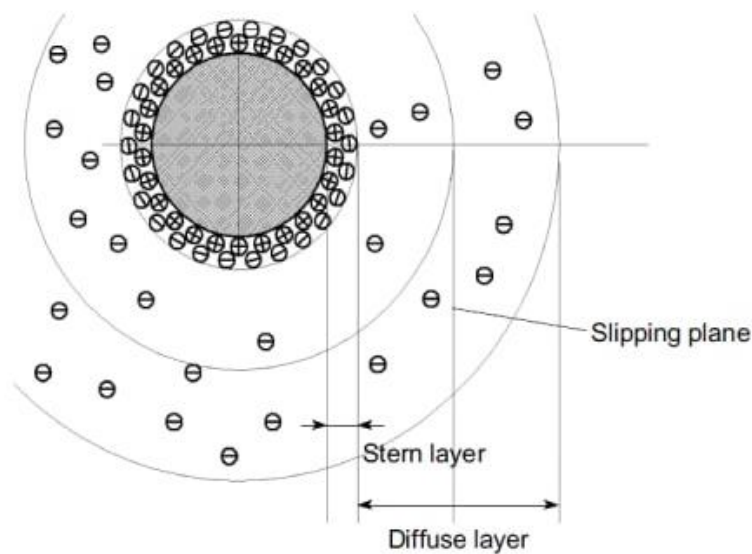


Figure (2.8): Electric Double Layer Structure [109].

2.12.4 Deposition

Electrophoresis of particles in a liquid medium near an electrode is transformed into deposition as a result of several physicochemical processes. The following deposition mechanisms have been established. flocculation of particles, electrochemical coagulation, neutralization of the particle charge at the electrode and distortion of particle EDLs under the action of external electric field [109].

2.12.5 Parameters

The thickness and microstructure of the deposited coatings can be tailored by varying the EPD parameters (physical parameters) and the composition of EPD suspensions.

2.12.5.1 Suspension Parameters

The suspension parameters include several aspects such as the physicochemical nature of both suspended particle and the liquid medium, surface properties of the powder, and the influence of type and concentration of solid in suspension.

A) Particle Size

Although there is no general rule of thumb to specify particle sizes suitable for electrophoretic deposition, good deposition for a variety of ceramic and clay systems have been reported to occur in the range of 1–20 μm . But this does not necessarily mean that deposition of particles outside this size range is not feasible. Recently, with increasing thrust on nanostructured materials, the EPD technique is being viewed with more interest for assembly of nanoparticles as well. It is important that the particles remain completely dispersed and stable for homogeneous and smooth deposition. For larger particles, the main problem is that they tend to settle due to gravity. Ideally, the mobility of particles due to electrophoresis must be higher than that due to gravity [110].

B) Dielectric constant, conductivity, and suspension viscosity

It has been stated that the liquids dielectric constant should be in the range (12–25) for the deposition occurrence. For liquids having dielectric constants lower (12), the dissociative power lack stops the deposition, whereas for liquids with dielectric constants more than (25), the electrophoresis is stopped by the decrease in the zone size of the double

layer, resulted by the high concentration of ions. The impurities are also able to vary the suspension conductivity. Furthermore, the procedure utilized for preparing the suspension also influences the conductivity vigorously. A greatly resistive suspension causes imbalance, since the electronically initiated charge composes in the particles. From the other side, the conductivity can be increased by a suitable modification of dispersant concentration and temperature. In general, a perfect suspension operation possesses a large dielectric constant, low conductivity, and low viscosity.

Organics liquids eliminates the electrodes reaction and gas evaluation so it is preferred that these reactions are occurred over the water due to electrolysis of water on application of the electric field. Another advantages are concerned with the organic solvent is that it is chemically stable and low conductivity due to low dielectric constant. The viscosity and relative dielectric constant of a few famous solvents, arranged from the best to worst are listed in **Table (2.4)** [111].

Table (2.4): The physical properties of popular solvents [111].

Solvents	Viscosity (cP) = $10^{-3}(\text{N.s.m}^{-2})$	Relative Dielectric Constant
Methanol	0.5500	32.63
Ethanol	1.0885	24.55
Water	0.8900	78.20
Acetone	0.3087	20.70
Acetyl acetone	1.0900	25.70
n-propanol	1.9365	20.33
Iso-propanol	2.0439	19.92
n-Butanol	2.5875	17.51
Toluene	0.5900	2.38

C) Zeta Potential

The zeta potential of particles in suspension is a key factor in the electrophoretic deposition process. It plays an important role in:

- i. Stabilization of the suspension by determining the intensity of repulsive interaction between particles,
- ii. Determining the direction and migration velocity of particle during EPD.
- iii. Determining the green density of the deposit.

The overall stability of a system depends on the interaction between individual particles in the suspension. A high electrostatic repulsion due to high particle charge is required to avoid particle agglomeration. When the particle charge is low, the particles would coagulate even for relative large inter-particle distances, leading to porous, sponge-like deposits. On the contrary, if the particles have a high surface charge during deposition they will repulse each other, occupying positions which will lead to a high particle packing density. The necessary condition that enables successful EPD is a stable suspension/sol, where the particles have a high zeta potential while the ionic conductivity of the suspension is kept at a low value [111].

D) Stability of Suspension

Electrophoresis is the phenomenon of motion of particles in a colloidal solution or suspension in an electric field, and generally occurs when the distance over which the double layer charge falls to zero is large compared to the particle size. In this condition, the particles will move relative to the liquid phase when the electric field is applied. Colloidal particles which are 1 μm or less in diameter, tend to remain in suspension for long periods due to Brownian motion. Particles larger than 1 μm require continuous hydrodynamic agitation to remain in suspension. The suspension stability is characterized by settling rate and tendency to undergo or avoid flocculation.

Stable suspensions show no tendency to flocculate, settle slowly and form dense and strongly adhering deposits at the bottom of the container. Flocculating suspensions settle rapidly and form low density, weakly adhering deposits. If the suspension is too stable, the repulsive forces between the particles will not be overcome by the electric field, and deposition will not occur. According to some models for electrophoretic deposition the suspension should be unstable in the vicinity of the electrodes [107].

E) PH Effect

In general, the pH value is a measurement of the ionic concentration of H^+ and OH^- ions. A low pH (<7) indicates a high concentration of H^+ compared with OH^- ions. The pH condition of a suspension is strongly related to the colloidal material and type of suspension medium used [112].

F) Concentration of Solid in Suspension

The volume fraction of solid in the suspension plays an important role, particularly for multi-component EPD. In some cases, although each of the particle species have same sign of surface charge, they could deposit at different rates depending on the volume fraction of solids in the suspension. If the volume fraction of solids is high, the powders deposit at an equal rate. If however, the volume fraction of solids is low, the particles can deposit at rates proportional to their individual electrophoretic mobility [113].

2.12.5.2 Physical Parameters

A) Electrical Field

The deposit yield is related directly to the applied electric field strength and increases with an increase in applied potential. Although powders can be deposited more quickly if greater applied fields are used, the quality of the deposit can suffer. For a higher applied field, which may cause turbulence in the suspension, the coating could be disturbed by the flows in

the surrounding medium, even during its deposition. In addition, particles can move so fast that they cannot find enough time to sit in their best positions to form a close-packed structure. Finally, high field situations restricts the lateral motion of particles on the surface of the already deposited layer, because higher applied potential exerts more pressure on particle flux and movement affecting the deposition rate and structure of the deposit [114].

B) Influence of Deposition Time

In a typical constant voltage EPD process, many researchers observed high deposition rates during the initial period of deposition, which then decreased and attained plateau at very high deposition times [115, 116]. In a constant voltage EPD, this is expected because while the potential difference between the electrodes is maintained constant, the electric field influencing electrophoresis decreases with increasing deposition time because of the formation of an insulating layer of deposited particles on the electrode surface. But during the initial period of EPD, there is generally a linear relationship between deposition mass and time [117].

C) The Conductivity of Substrate

In electrophoretic deposition, the deposited film quality is vigorously relied on the substrate conductivity. Low substrate conductivity makes the deposition slow and the deposit inhomogeneous. A combustible substrate that can be eliminated by extra heating in the sintering operation is utilized to fabricate intricate forms. But for the coatings, the worker requires to be too careful regarding the possibility of cracks formation due to drying and sintering. Such thermally formed cracks are the method impartible nature and the final surface quality relies on overcoming such problem [111].

2.13 Role of Binders In EPD

Organic binders are a necessary component for the effective processing of many commercial high performance ceramics. There are numerous organic substances that have been utilized, or groups, as potentially useful binders for ceramics.

Polyethyleneimine (PEI) is a cationic dispersant widely used in different sizes and structures. The Zeta potential gives information on the charge of the particles which can result of the adsorption of a polymer at the particle surface, or from a reaction between the surface of the particles and the solvent. This parameter can also give information on the interaction between particles [118]. The ionization pH range of low MW branched PEI is between pH=2-10 [119].

2.14 Previous Studies on Biomedical Coating

Ceramic has a vital role to better biocompatible characteristics of the implant. It can be divided into two main sorts, oxides ceramic (such as TiO_2 , ZrO_2 , Al_2O_3 , MgO ..etc.) and non-oxide ceramics (like HAp, SiC, Si_3N_4 , ZnS.. etc.).

(Khalili et al., 2013) [120] developed a bioactive and corrosion resistant by converting the bio inert surface of NiTi to bioactive and biocompatible surface by depositing TiO_2 particles on the NiTi surface using electrophoretic deposition process. TiO_2 particles were prepared using a mixture of acetone and n-butanol (0%, 30%, 60%, 80% and 100% acetone) without using any dispersant. Surface morphology of coatings showed deposition within 0% acetone causing a crack-free and dense coating with relatively coarse grains and high corrosion resistance.

(Rajan, 2012) [121] studied the improved properties of HAp of sintered (900° for 2h) and non-sintered hydroxyapatite layer coated on Ti6Al4V alloy by using electrophoretic deposition carried out at a constant

voltage of 30V for 5, 10 and 15 minute duration at different pH values of 1.5, 2.5 and 3.5 respectively. SEM images show that at constant voltage of 30V and low pH of 1.5, coated surface shows no cracks. XRD analysis showed that "before sintering, few other compounds were present in HAp powder while after sintering they were not oxidized. The more coating layers, leads to a wide different atomic intermixed between the substrate and the top-bio coating which improves the adhesion strength.

(Michal et al., 2017) [122] they studied elaborate the technology of electrophoretic deposition (EPD) of Nano hydroxyapatite (nano HAp) coatings decorated with silver nanoparticles (nano Ag) and to investigate the mechanical and chemical properties of these coatings as determined by EPD voltage and the presence of nano Ag. They tested deposition of nano HAp at two voltage values, 15 and 30 V, decoration of nano HAp coatings with nano Ag was carried out using the EPD process at a voltage value of 60 V and a deposition time of 5 min. Their experiments showed that the hardness of the undecorated nano HAp coatings obtained at 15 and 30 V of EPD voltage attained 0.2245 ± 0.036 and 0.0661 ± 0.008 GPa, respectively. They found the resistance to nano scratching was higher for thicker coatings. Also, they concluded the wettability angle was lower for coatings decorated with nano Ag.

(Kumar and Wang, 2001)[123] studied the functionally graded bioactive coatings of hydroxyapatite/titanium oxide composite system. Composite coatings were made on Ti-6Al-4V metal substrate. A functionally graded coating was obtained by coating titanium oxide (TiO₂) powders of known particle size as the first layer, which was sintered at 900 °C for a few minutes. Coating of subsequent layers of HAp-TiO₂ composites of different weight ratios (75% TiO₂ and 25% HAp, 50% TiO₂ and 50% HAp, 25% TiO₂ and 75% HAp, and 100% HAp) were performed in sequence and these layers were sintered again at 900 °C for a few minutes, so as to ensure a good

adhesion between layers. The coatings were subsequently subjected to various characterization such as X-ray diffraction (XRD), scanning electron microscopy (SEM), energy dispersive X-ray (EDX), Their experiment showed that the XRD confirms the presence of the corresponding components in HAp composites. SEM micrographs showed the surface morphology of the functionally graded layers, and the presence of elements was also identified by EDX analysis which confirmed the versatility of the coating technique performed at low temperature. They found that the nano-indentation HAp-TiO₂-Ti functionally graded coating yielded 15.1 and 0.405 GPa as the hardness and modulus values, respectively.

(Mohan et al., 2012)[124], studied the corrosion and scratch behavior of TiO₂ + 50%HAp nano ceramic coated on Ti-13Nb-13Zr orthopedic implant alloy using (EPD) sintering at 850 °C. The corrosion behavior of the coatings was evaluated using SBF-Hank's solution. The sintered coating exhibited higher density, adhesion and lower porosity compared to unsintered samples, and higher corrosion resistance compared to the substrate.

(Sorkhi et al, 2019) [125] conducted test for Electrophoretic Deposition of Hydroxyapatite-Chitosan-Titania on Stainless Steel 316 L using from alcoholic (methanol and ethanol) suspensions containing 0.5 g/L chitosan and 2 and 5 g/L HAp and 2 and 5 g/L Titania. They tested the effect of different parameters on the deposition rate, morphology, and corrosion resistance of the coatings in simulated body fluid (SBF) at 37°C. The coatings' properties were investigated using Fourier-transform infrared spectroscopy (FTIR) and scanning electron microscope (SEM). Their experiments showed that the deposition rate in ethanolic suspensions is lower than methanolic ones. Moreover, the coating surface was smoother when the ethanol was used as a solvent in suspensions in comparison to the ones where methanol was the solvent. The test results confirmed that, the

coating deposited from a suspension containing 0.5 g/L chitosan, 2 g/L HAp, and 5 g/L titania with ethanol as solvent had the highest corrosion resistance in SBF at 37 °C.

2.15 Concluding Remarks

There are indeed no researches were demonstrated in the field of biotic titanium alloy Ti-6Al-4V and functionally gradient coating of micro HA/TiO₂ bio-ceramic fabricated by EPD and used as a biocoatings materials for metallic implants. There have been a limited number of studies conducted in studying the antibacterial characteristics of fabricated parts. Therefore, this investigation provides a vulnerable information and better understanding of the Ti-6Al-4V alloy coated by functionally graded material multilayer HA-TiO₂ coatings.

Experimental Work

3.1 Introduction

In this chapter, the details of the experimental program are presented. It elaborates the research methodology adopted in achieving the objectives mentioned in chapter one. the details of the materials used, EPD processed as well as commonly used characterization techniques developed to the electrophoretically deposited coating throughout this study.

This research's experimental program consists of two parts. In the first part, the selection, coating materials preparation and assessment of the physical and chemical properties were used in this research. Subsequently, this part also conducts trail mixes to optimize the mixing weight proportions and to select the optimal conditions for EPD process and dosage of mineral and chemical additives. Then, the chosen materials were blended with the optimum mixing ratio taken. Finally, the second part, samples were examined. The block diagram shown in **Figure (3.1)** clarifies the main activities of this work.

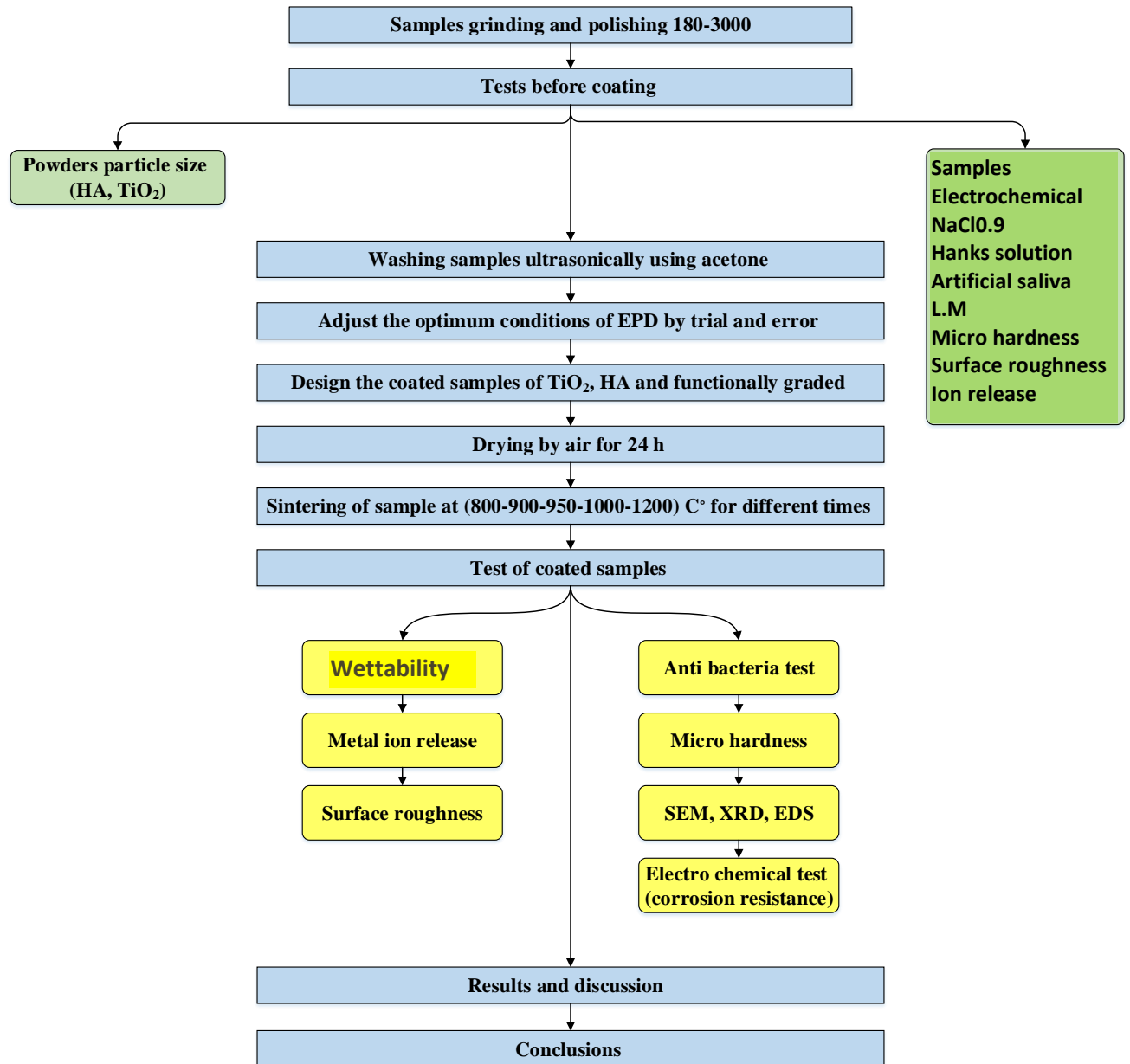


Figure (3.1): Block diagram of the research plan.

3.2 Particle Size Analyzer

Particle size analyzer type (Better size 2000 particle size analyzer), was used to determine the particle size of TiO₂ and HAp powder. Two grams of each powder were added to distilled water medium, the particles of powders were suspended in this medium. Then, they were placed in the measuring cell, which separates the particles according to the particle size. The test was

conducted at University of Babylon, College of Materials Engineering, Metallurgical Engineering Department laboratories.

3.3 Materials

Ti-6Al-4V titanium alloy rod with (20mm diameter \times 10mm thickness), was used as the cathode in the present study. 316L with (2.5mm diameter \times 10mm thickness) was the anode. Coating materials high purity (>99%) hydroxyapatite powder and titanium dioxide (anatase TiO_2) powder, with particle size respectively were used for suspension preparation in absolute ethanol 100% purity, distilled water and dilute ethanol 70% as medium of EPD process. Different types of binders were used such as; Polyethylene amine (PEI) polyethylene glycol (PEG) and polyvinylalcohol (PVA). Therefore, after many trials of mixing, PEI was kept as a binder material because, it gives better adhesion. **Figure (3.2)** depicts the materials used in this investigation.



Figure (3.2): Geometrical configuration of research samples (dimensions and weight).

3.4 Method

Ti-6Al-4V substrate as cathode, and commercially available 316L stainless steel as the counter electrode, were immersed in the suspension with a fixed distance of (15 mm). Prior to deposition, Ti-6Al-4V substrates were ground by 180 to 3000 grit SiC papers, then the specimens were polished using polish cloth and diamond paste 0.5 μ m, and then washed with distilled water and finally ultrasonic with acetone to remove oxide layer, and finally passivated by immersion in 20% HNO₃ and HF for 10 min, dried and kept in a desiccator over a silica gel pad and used for microstructure evolution and electrochemical investigation. In order for the process to be more accurate, a holder was manufactured to hold the samples and keep the distance between the electrodes constant during the coating process and to facilitate the lifting of samples when changing the suspension, as shown in the **Figure (3.3)**.

EPD process was performed in a glass beaker, magnetic stirring was employed to maintain the homogeneous dispersion of the particles during the whole EPD process. The system was equipped with a DC power supply to give potential ranging from zero to 60 volt. The voltage can be adjusted as required to achieve the best deposition. In order to determine the optimal electrophoretic parameters deposition to be performed at different voltages such as (10, 20, 30, 40, 60) V and different deposition times (1, 2, 3, 4, 5, 6, 30, 60) min from suspension containing (50 g/L)% TiO₂ and 6g/L PEI. The pH of suspension was measured by a pH meter (model PH-100 meter). After that, the coated samples were removed carefully from the EPD cell and dried in air at room temperature for 24 hrs, and then sintered in a argon furnace with at 950°C for 1 hr. The manufacturing processes of composite coating samples as shown in **Figure (3.3)**.

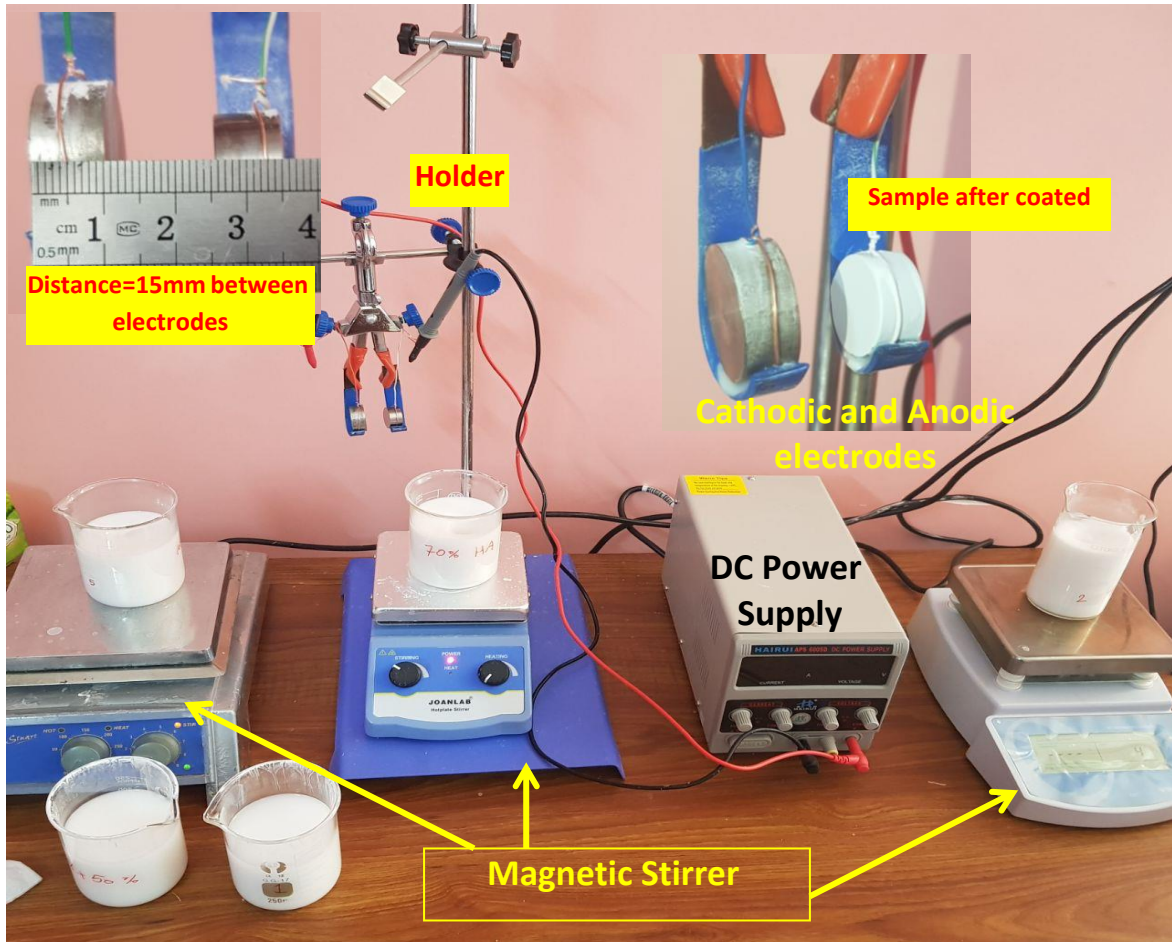


Figure (3.3): Garmenting processes of composite coating samples.

After preparing the suspensions by adding different weight ratios of powder and the binder to pure ethanol and determining the optimum conditions, voltage and time deposition were (20V, 1min). Gradient coating was done in five consecutive steps. Each step lasted 12 seconds for each layer. Total time was 1 min. The graduated coating was carried out from solution No. (1, 2, 3, 4 and 5) consecutively as shown in **Table (3-1)**, the first step TiO_2 inner layer was deposited on the Ti-6Al-4V substrate from the suspension No.1 after that three intermediate layers, TiO_2/HAp composite layers were applied from their relative stable suspensions (No. 2, 3 and 4) respectively and finally the top coating of HAp was deposited on the four previous layers from suspension No.5, the amount of HAp change gradually from 0 % wt near the substrate to 100 % wt on top coating. The monolayer

coating was carried out once from solution No. 6 (100% TiO₂) and another from solution No. 7 (100% HAp) as shown in **Table (3-1)**, for the purpose of making a comparison in the properties after a procedure sintering and then examined. The adopted method in this research, is presented in **Figure (3.4)**, based on previous researches [97, 108] and trail mixes to produce satisfactory coating.

The pH of the solution was reduced before coating with the addition of HCL acid, where no coating was obtained at a lower pH value (pH = 3.97, 4.23, 2.16), while a uniform layer was obtained at a high PH value of approximately (PH =12), in contrast to what was done in the previous researches [111, 113].

Table (3-1): Chemical composition of prepared specimens.

Suspension No.	Coating Type	Layers	TiO ₂ (g)	HAp (g)	Absolute Ethanol (ml)	PEI (g/L)
No.1	Composite Coatings	1 st	10	0	200	6
No.2		2 nd	7	3		
No.3		3 rd	5	5		
No.4		4 th	3	7		
No.5		5 th	0	10		
No.6	Monolayer coating		10	-		
No.7			-	10		

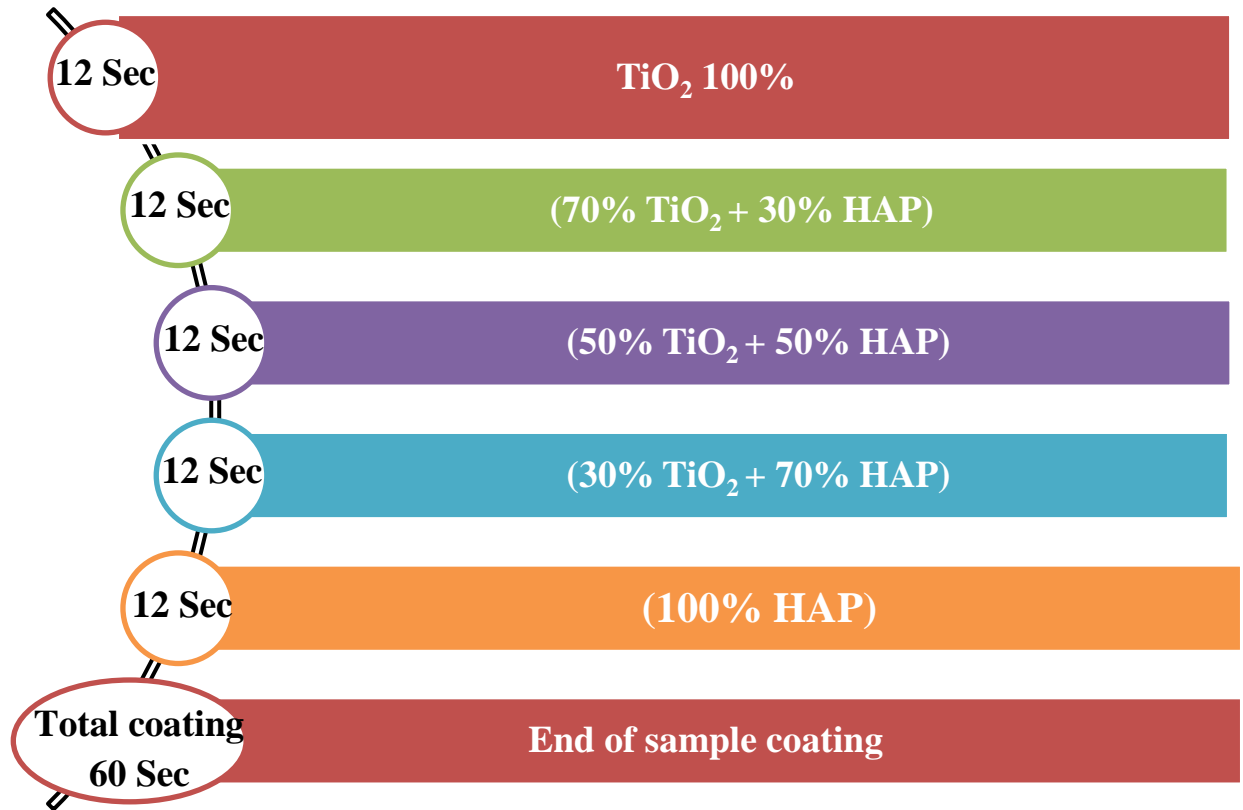


Figure (3.4): Sample coated time process.

3.5 Sintering of Deposited Coatings

After deposition, the green coatings were dried in air for 24hr at room temperature. Several attempts in this work for sintering of the coatings were carried out in an argon-purged atmosphere at (800, 900, 950 and 1200 °C). These attempts were failed by cracking of the samples except 950 °C was successful. The heating rate and cooling rate were the same (10 °C min⁻¹) and the dwell time was 1hr. After performing heat treatments under different conditions, certain variables were fixed. At first the samples were heated inside the furnace to 400 °C and kept at this temperature for one hour to get rid of the binder, and then heating to 950 °C for one hour as well. The following sintering schedule, **Figure (3.5)**, was successfully produced cracks free samples. All samples were sintered in furnace type OTF-1200X at the Kufa University / College of Engineering as shown in **Figure (3.6)**.

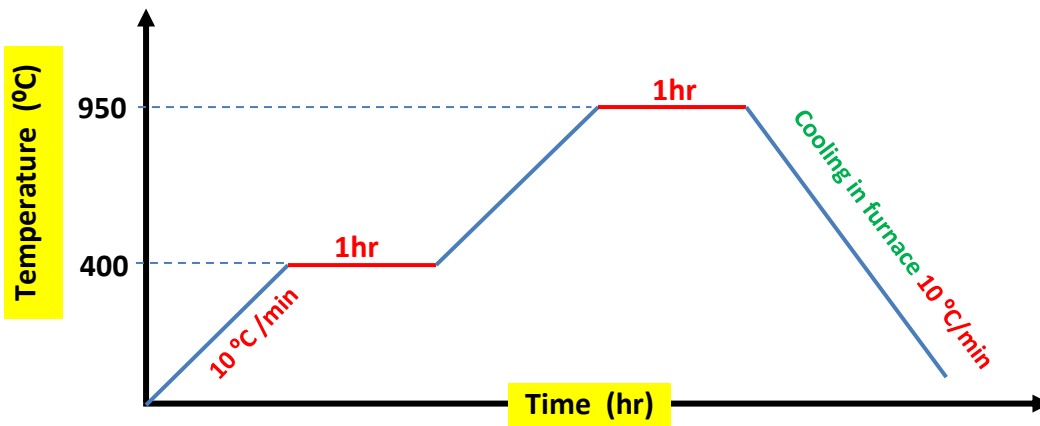


Figure (3.5): The adopted sintering schedule.



Figure (3.6): Sintering furnace uses in this study.

3.6 Characterizations of Samples

3.6.1 Surface Roughness

In this work, the surface roughness was measured before and after coating. It was measured by surface roughness tester (TR200, SaluTron, made in Germany) available at the University of Babylon- Materials Engineering College.

3.6.2 Contact Angle Measurement

The hydrophobicity or wet-ability of the coated Ti6Al4V alloy and uncoated samples were measured using the static contact angle (θ)

of droplet on solid surface, which is an important index to quantitatively evaluate the wettability of solid surface, the optical contact angle equipment type CAM 110-O4W which was attached with CCD camera was used to measure contact angle, and the contact angle measurement was taken immediately after the droplet was placed on the solid surface by a 1 μ L pipettor. In individual contact angle measurements between each test liquid and each solid surface, each contact angle was measured 5 times and 10 measurement points were selected.

3.6.3 Micro Hardness

Micro hardness Vickers tester type (Digital Micro Vickers Hardness Tester model TH-714). The utilized loads were (25, 100) g, holding time was (10) sec, and a standard 136° Vickers diamond pyramid indenter combined with optical microscopy was used to measure the diagonal length of Vickers impression as shown in previous Figure. Three readings were reordered for each sample, and the average was calculated. The Vickers micro hardness (HV) in (kg/mm^2) is specified as follows [115].

$$HV = 1.854 \times \frac{P}{d^2} \dots \dots \dots (3 - 1)$$

Where:

P= applied load kg, and d= average length of diagonal mm^2

3.6.4 Electrochemical Test

A potentiodynamic polarization and open circuit potential test was carried out in a potentiostat (EG&G 263 A) according to the ASTM G44–99 standard [112] to evaluate the corrosion resistance of a control (uncoated) and coated specimens the samples were immersed into the simulated body fluid (0.9 sodium chloride, artificial saliva and Ringer solution) electrolytes as shown in **Figure (3.7)**. A saturated silver/silver chloride electrode was used as

the reference, with a platinum counter electrode; specimens were inserted as the working electrode. The test was started by using 0.2 mV/s as the scanning rate from ± 250 mV upper and bottom the (OCP) and continued up to ± 250 mV above the (OCP), the test time was 14 min. This test was done in Corrosion Laboratory in the Laboratories of the Department of Metallurgical Engineering - University of Babylon. The chemical composition of NaCl 0.9, artificial Saliva and Ringer solution is illustrated in **Table (3.2)**. The pH of artificial saliva, NaCl 0.9 and Ringer solution were 6.4, 5.0 and 7.0 respectively. The electrochemical Test was conducted at temperature $37 \pm 2^\circ\text{C}$ on the all specimens.

For the purpose of testing the corrosion resistance of the coated and uncoated samples and obtaining more accurate results, a holder was manufactured to match the dimensions of the sample so that the sample parts being isolated except for one face as shown in the **Figure (3.7)**. These values were calculated by using the following formula:

$$CR = K \frac{i_{cor}}{\rho} EW \quad \dots \dots \dots (4 - 1)$$

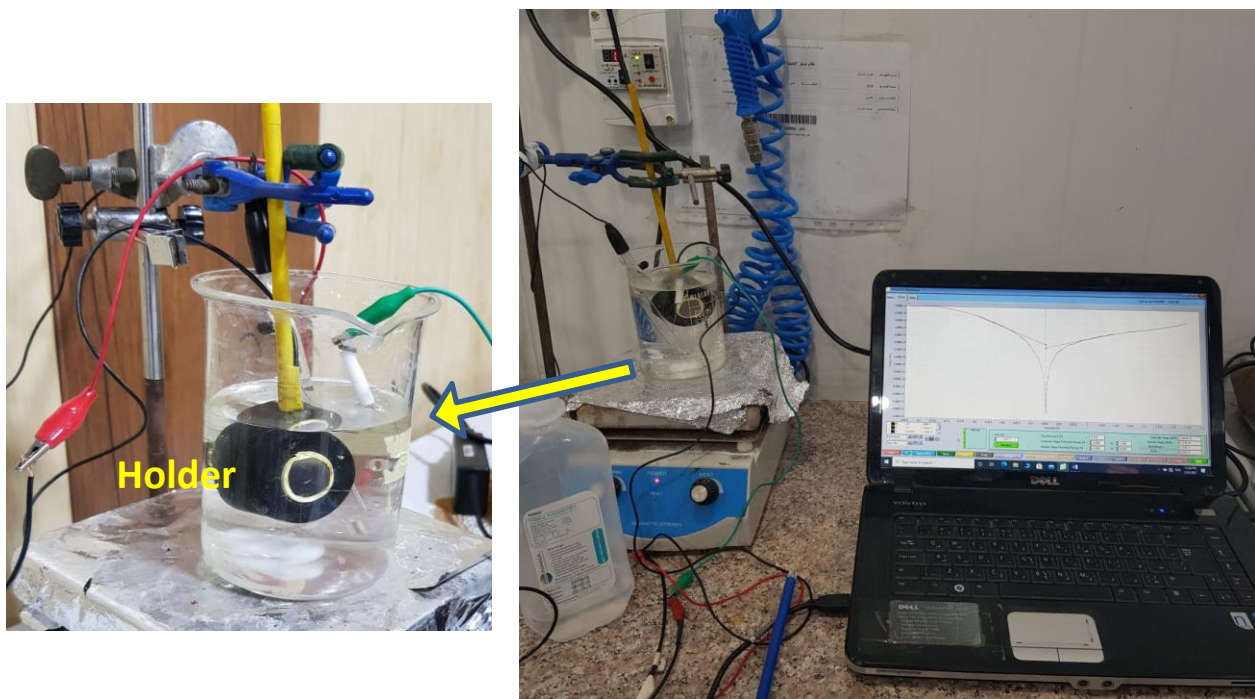
$$i_{cor} = \frac{0.026}{R_p} \quad \dots \dots \dots (4 - 2)$$

Where:

CR- corrosion rate in mm.yr^{-1} , $K = 3.27 \times 10^{-3} \text{ mm.g.}\mu\text{A}^{-1}.\text{cm}^{-1}.\text{yr}^{-1}$, i_{cor} - corrosion current density in $\mu\text{A.cm}^{-2}$, ρ - density in g.cm^{-3} , and EW- equivalent weight.

Table (3.2): Simulated body fluids used in electrochemical corrosion test.

Simulated body fluid	Components	Concentration (g/L)	PH
Artificial saliva	Potassium chloride (KCl)	0.4	6.4
	Sodium chloride (NaCl)	0.4	
	Calcium chloride dehydrate ($\text{CaCl}_2 \cdot 2\text{H}_2\text{O}$)	0.906	
	Monosodium phosphate dehydrate ($\text{NaH}_2\text{PO}_4 \cdot 2\text{H}_2\text{O}$)	0.69	
	Sodium Sulfide nonahydrate ($\text{Na}_2\text{S} \cdot 9\text{H}_2\text{O}$)	0.005	
	Urea	1.0	
Ringer's solution	Sodium chloride (NaCl)	8.6	5
	Potassium chloride (KCl)	0.3	
	Calcium chloride dehydrate ($\text{CaCl}_2 \cdot 2\text{H}_2\text{O}$)	0.33	
NaCl 0.9 %	Sodium chloride (NaCl)	9	7

**Figure (3.7):** The electrochemical corrosion cell.

3.6.5 Antimicrobial Test

The surface of biomaterial was exposed to the risk of initial microbial colonization and bacterial attack. The antibacterial activity of the HAp alone and HAp/TiO₂ micrograded suspensions was

investigated to evaluate whether the coated layer is antibacterial or not. The antibacterial activity was studied by using the inhibition zone method. An antibacterial kinetic test with bacterial strains of E.coli HB101, (E.coli, American type culture ATCC 25922, gram negative bacteria) was prepared at the University of Babylon-College of Medicine-Department of Microbiology. The E.coli could spread hematogenously from a urinary tract infection and reach to the bone and cause osteomyelitis in an adult [119, 126]. For the bacteria preparation, the E.coli grown on a nutrient agar (N. agar) and placed in the incubator for 24 h at 37 °C. Then the bacteria spread on a petri dish where the suspensions were placed in four different regions on it and incubated. After that the inhibition zones were observed.

3.6.6 Light Optical Microscope (LOM)

The microscopic structure was studied using optical microscopy in order to identify the existing phases and to see the shape and size of the grains, after grinding, polishing and etching. This test was done at specimens preparation laboratory, the microscope is type (BEL PHOTONICS) as shown in **Figure (3.8)**, Located in the Laboratory of thermal transactions in the Laboratories of the Department of Metallurgical - University of Babylon.

In the present work the materials used were (10 ml HF, 25 ml HNO₃, 20 ml Water) for etching the surface of Ti6Al4V for optical observation with time of exposure of 5 second.



Figure (3.8): Light optical microscope.

3.6.7 Metals Ions Release (Static Immersion Tests)

The investigated of the release metals of both uncoated and coated specimens with (TiO_2/HA) in vitro by immersing in artificial Saliva and Ranger's solutions are illustrated in Appendix (A). The test of static immersions is recognized in agreement with the currently specified JIS T-0304 standards for metallic biomaterial [118]. Specimens were immersed in plastic containers with 50 mL of each solution for 21 days in the incubator (Specimens were immersed in small containers, where these containers immersed in controlled water temperature to keep temperature at $37\text{ }^\circ\text{C}(\pm 2)$).

3.6.8 X-Ray Diffraction Analysis

X-ray diffraction (XRD) was carried out to define the presence of phases crystallographic properties in the Ti6Al4V substrate, HAp and TiO_2 coatings as well as the composite biocoatings layer. This test was performed in the University of Babylon - Materials Engineering College by using XRD (LabX 6000, Shimadzu, Japan origin) with nickel filter and copper generator

of $K\alpha$ radiation ($\lambda=0.154056$ nm) at 40kV and 30 mA with a speed of $2^\circ/\text{min}$. was used, and a range of $2\theta = 10$ to 90 .

3.6.9 Scanning Electron Microscopy (SEM)

For the purpose of obtaining surface composition and its morphology, a scanning electron microscope (SEM) was used. The sample is imaged through a high-pack of electrons. An Energy Dispersive X-ray Spectrometry (EDX) detector combined with SEM was employed to detect the elemental distribution of the selected points/area in the SEM image. The samples were coated with a gold layer of around 15 nm (model Q150T, QUORUM) before the observation to avoid sample charging during imaging. This test was done in University of Babylon- Pharmacy College by using SEM type (TESCAN S8000).

Results and Discussion

4.1 Introduction

The main objective of this study is to fabricate experimentally the composite biocoatings of hydroxyapatite (HAp) and titanium dioxide (TiO₂) layers on Ti6Al4V substrate to enhance biocompatibility and corrosion resistance against aggressive body fluids of artificial implants. In addition to overcome the problem of mismatch between coefficient of thermal expansion between HAp and titanium substrate which cause the cracks during sintering leads to poor adhesion of coating.

After conducting many experiments in different conditions to coating the samples until reaching the ideal conditions, then selecting and fixing it for all samples. Subsequently single-layer coating and multi-layer gradient coating were performed. Uniform and smooth coatings are formed at 20 and 1min. When the voltage increases up to 30V, the coating is nonhomogeneous. However, the formed coating starts to irregular precipitation due to the high voltage, the particles do not reach the surface of the sample at the same time. Thus, the optimal conditions for EPD process is 20V for 1 min. In this chapter presented, the practical tests conducted on samples with and without coating for the purpose of conclusion. The comparison and discussion of the test results obtained and proving the effectiveness of gradient coating in improving the biological properties that must be available in prosthetic implants. These tests

include XRD, SEM, EDS, hardness, roughness, wetting angle, corrosion resistance, anti-bacterial and metal released ions.

4.2 Microstructure of the Ti6Al4V Substrate

Figure (4.1) illustrates the microstructure of the cast Ti6Al4V where the microstructure consisted of equiaxed alpha grains, elongated alpha grains and a network of intergranular beta phase. It is observed that the samples have been etched to reveal the grain boundaries in the microstructure. Pores of different size are irregular but have been rounded. The most common types of features in the microstructure in metallic materials are the boundaries between crystalline grains and /or the boundaries between different solid phases in multiphase alloys. This observation confirms the results obtained by other investigators [54, 121].

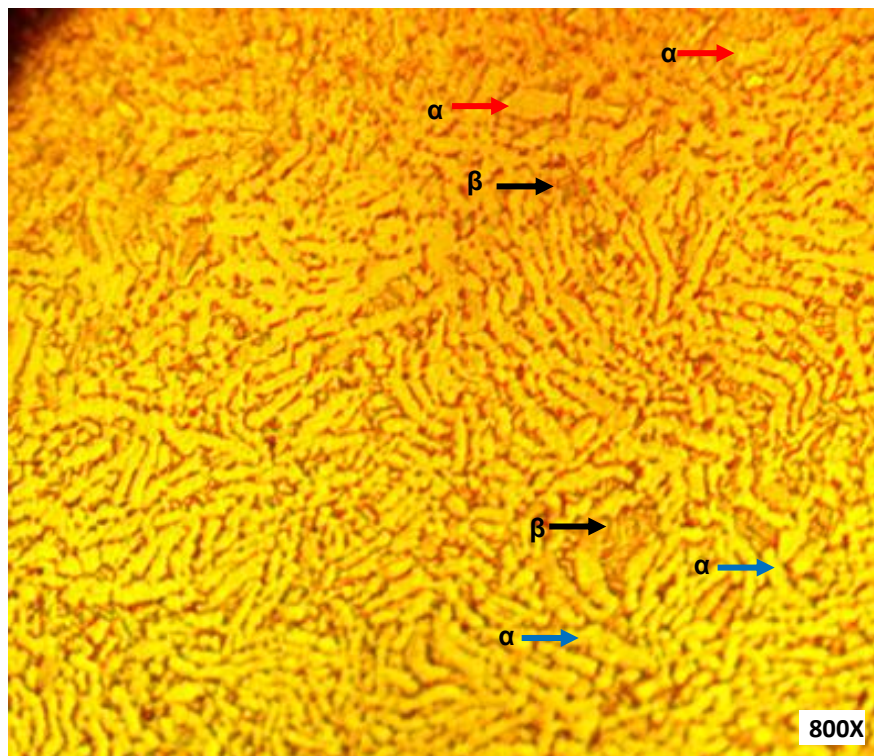


Figure (4.1): As-received microstructure of Ti-6Al-4V alloy showing elongated α (blue arrow), equiaxed α (red arrow) and intergranular β (black arrow) using different magnification.

4.3 Scanning Electron Microscopy Analysis

The cross section of the HAp/TiO₂ composite biocoatings **Figure (4.2)** reveals that it includes five layers as TiO₂ inter layer near the substrate, HAp top layer and three intermediate HAp\TiO₂ graded layers.

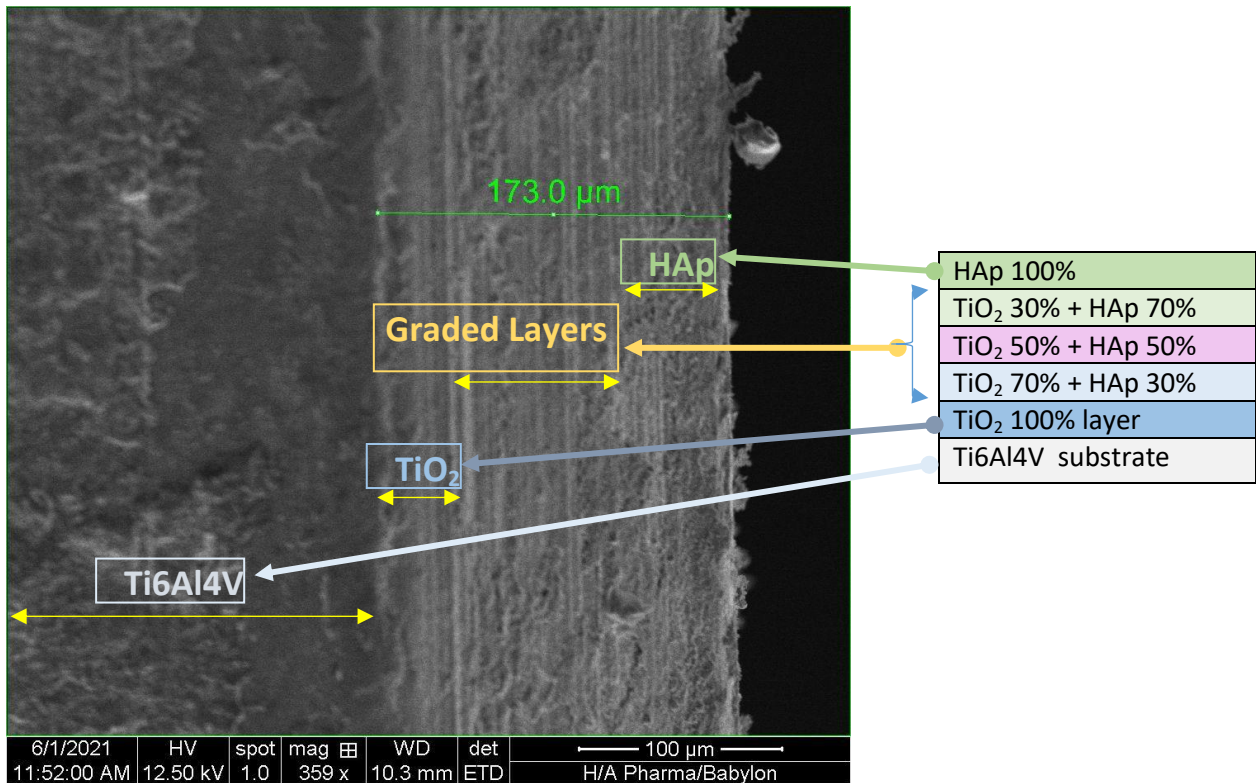


Figure (4.2): Schematic of SEM cross section image for composite biocoatings sample.

As can be seen above, introducing the TiO₂ intermediate layer and grading the composition improves the adhesion and cohesion of the coating. The total thickness of the composite biocoatings HAp/TiO₂ is measured about 173.0μm. The TiO₂ layer portion of the total coating thickness. Since the main function of the TiO₂ layer is to improve the adhesion of the HAp. Biocoating with single-layer TiO₂ and HAp coatings is displayed in **Figure (4.3a-b)**. Both of HAp and TiO₂ coatings have good interconnection between particles

after sintering. But the HAp layer is easily brittle and many cracks on surface. Because the nature of the ceramics haven't good crack toughness during the sintering process, the cracks in the layer are occurred. It is also due to the large difference in thermal expansion between the coating and the substrate.

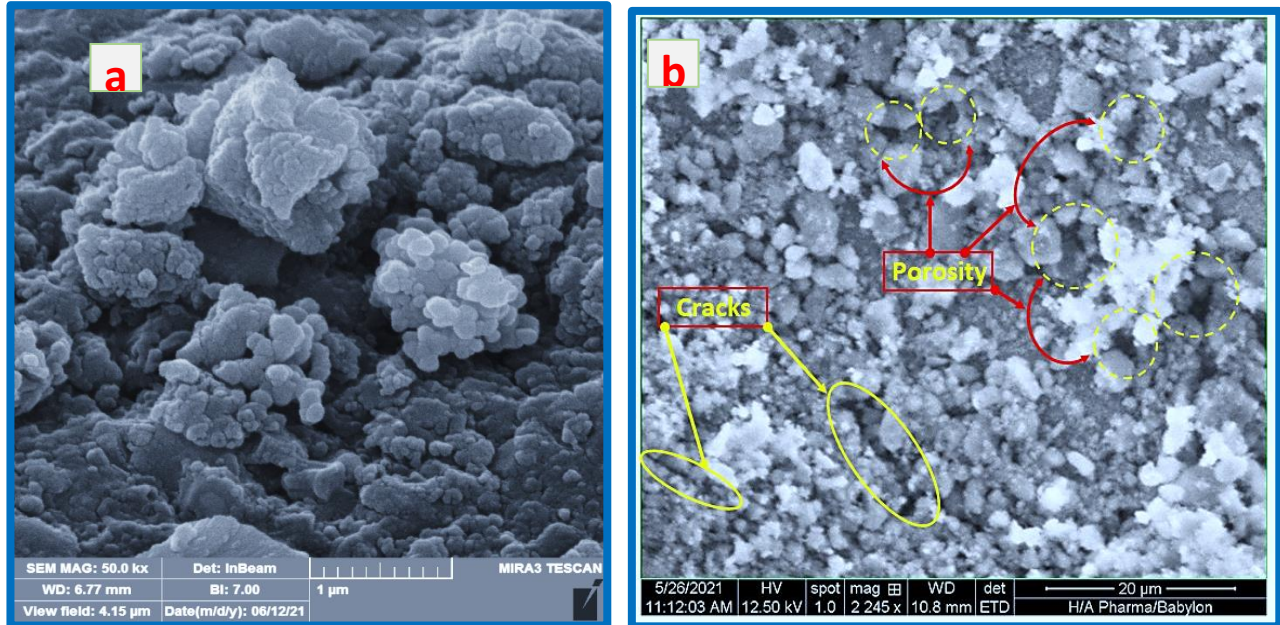


Figure (4.3): SEM image for electrophoretic deposited (a- titania and b- hydroxyapatite) on Ti6Al4V alloy.

Figure(4.4) shows that the morphology of composite biocoating, including different layers of HAp layer, TiO₂ layer, HAp/TiO₂ intermediate graded layers that are deposited at the deposition 20V for 1 min represented a smooth, dense (more close packed microstructures), good homogeneity surface with less porous structure, crack- free and uniform coating were achieved.

The rough and porous morphology of the coating surface facilitates the accumulation of nucleations and osseointegration of bone in the formation of bone-producing cells.

The SEM cross sectional micro graph of HAp single layer porous coating (see **Figure 4.5**) demonstrates that a uniform with

thickness of approximately $256.4\mu\text{m}$ is formed, obtaining the best morphological results at a voltage of 20 volts and a time of 1 min.

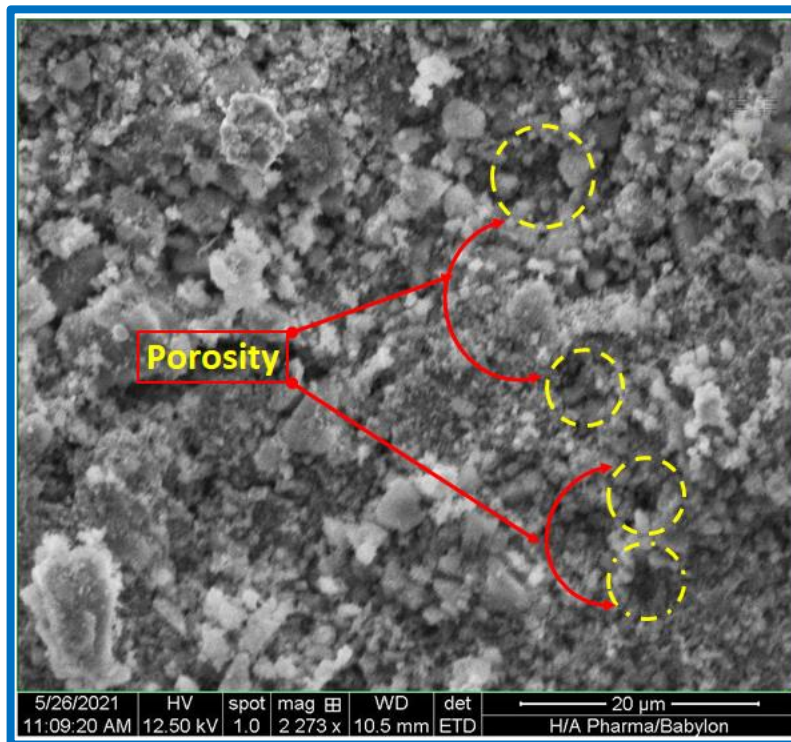


Figure (4.4): SEM micrograph of the surface morphology of composite biocoatings on Ti6Al4V alloy.

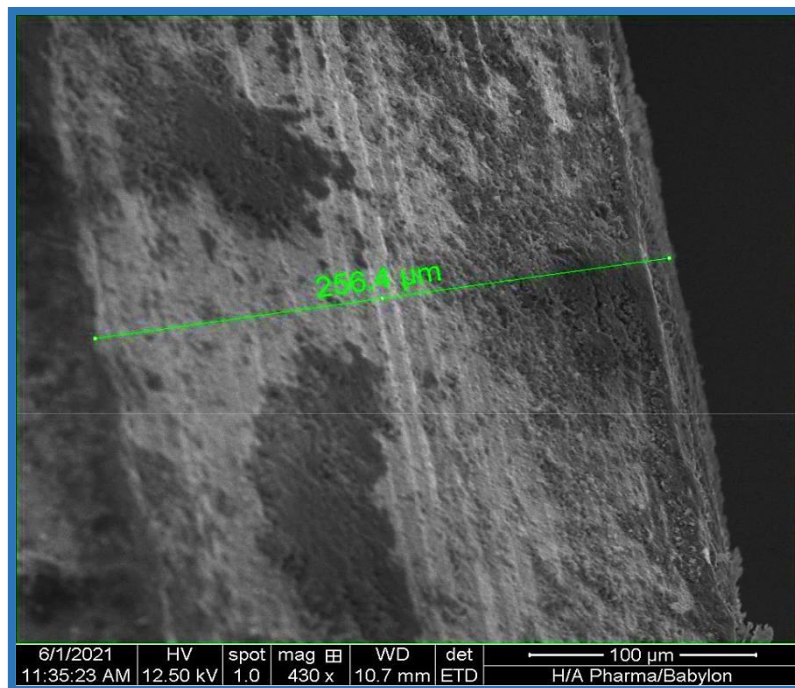


Figure (4.5): Cross-sectional SEM micrographs of the deposited HAp coating after sintering.

Supporting the XRD results, EDX analysis also revealed the presence of prominent elements in the coatings. The elemental composition of the HAp, TiO₂ and composite biocoatings HAp/TiO₂ coating deposited on the Ti6Al4V substrate are illustrated in **Figure (4.6)**. It can be observed that the main elements of Ca, P, O and Ti are presented in the coatings. The existence of these elements affirm the formation of successful coating on the substrate. Moreover, there is no other Peaks different from HAp and TiO₂ and this assure the coating purity.

It is most important to know the Ca/P ratio (1.81), which is consider a necessary parameter that defines the properties of the deposited calcium phosphate percentage in the composite biocoating that would be utilize in the biomedical applications. Also, it can be seen from this Figure, the Ti value decreases gradually from substrate to coating top surface while the Ca and P value increase from the substrate to the coating surface. This observation confirms the results obtained by other investigators [**128, 129**].

Table (4.1) illustrate these ratios for composite biocoatings sample. **Figure (4.7)** shows the linear EDX analysis of composite biocoatings HA/TiO₂ coatings. Variation of Ti, Ca, and P content from Ti-6Al-4V substrate to coating top surface is observed obviously.

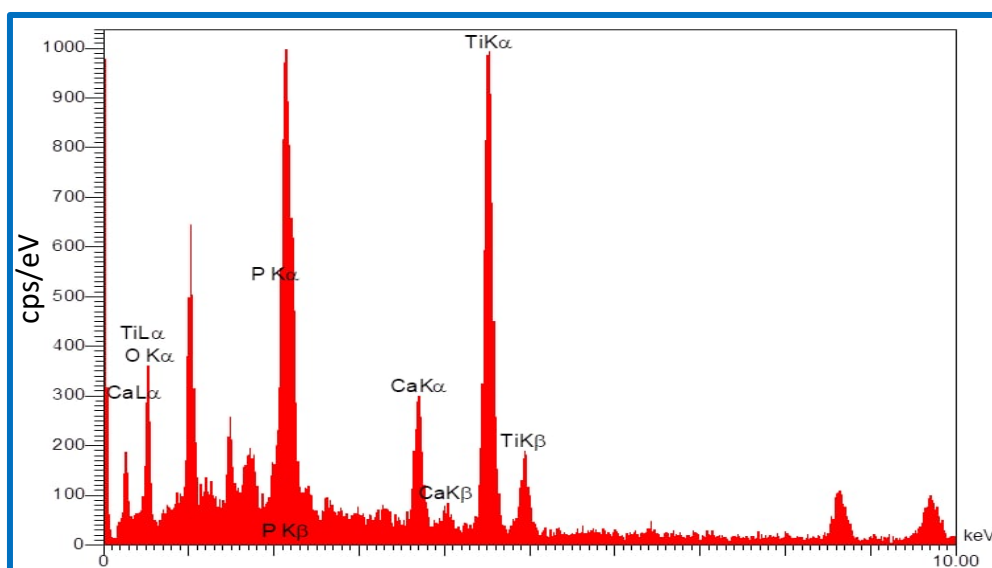
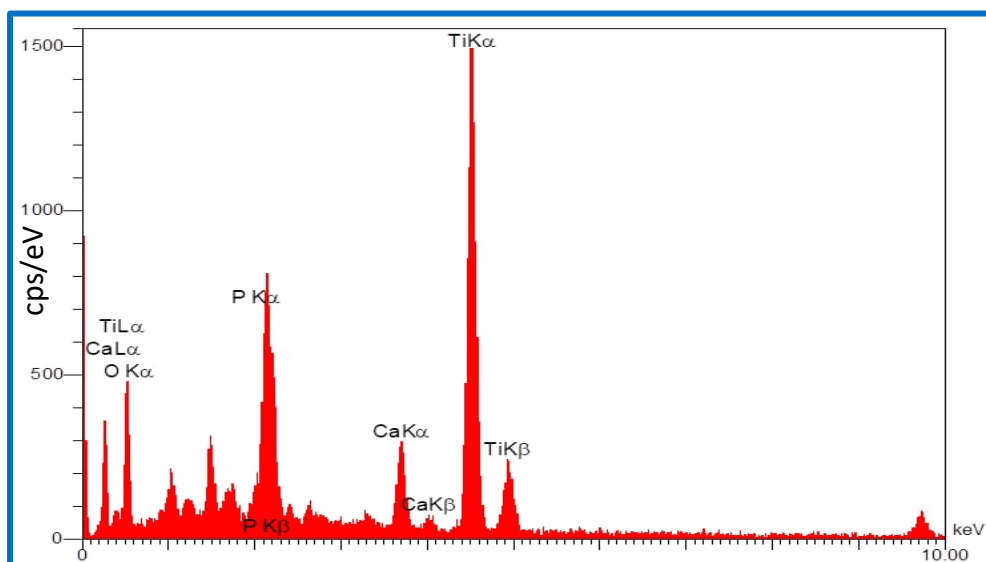
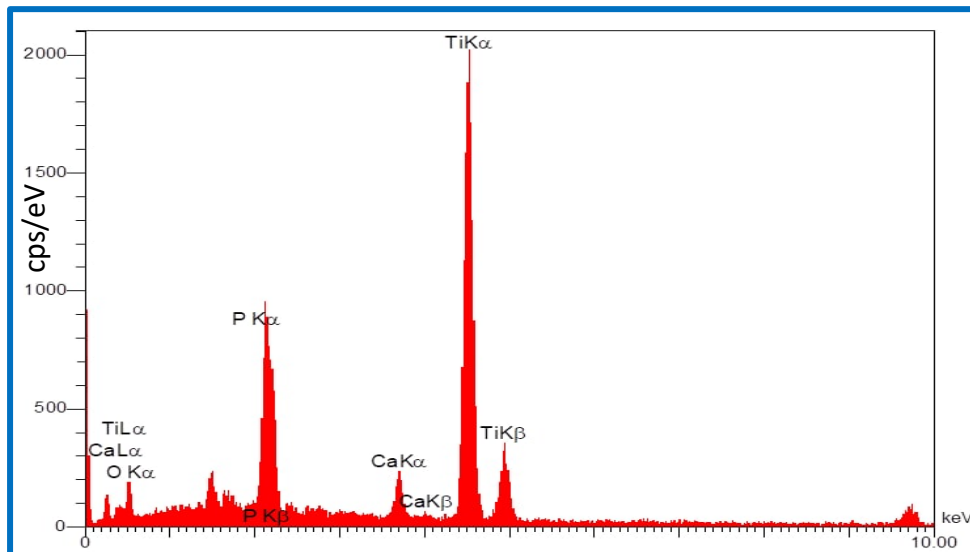


Figure (4.6): EDX analysis of composite biocoatings HA/TiO₂ coatings for different area.

Table (4.1): Quantitative EDX Results for selective area.

Elt	Line	Int	Error	K	Kr	W%	A%	ZAF	Ox%	Cat#
O	Ka	359.2	36.1154	0.0897	0.0486	52.86	65.08	0.1152	0.00	0.00
P	Ka	346.4	232.6824	0.0845	0.0481	6.46	5.19	0.7715	0.00	0.00
Ca	Ka	769.8	6.5952	0.2013	0.1122	11.75	7.01	1.0260	0.00	0.00
Ti	Ka	2326.1	6.5952	0.6246	0.3598	28.93	22.72	0.8604	0.00	0.00
				1.0000	0.5687	100.00	100.0		0.00	0.00

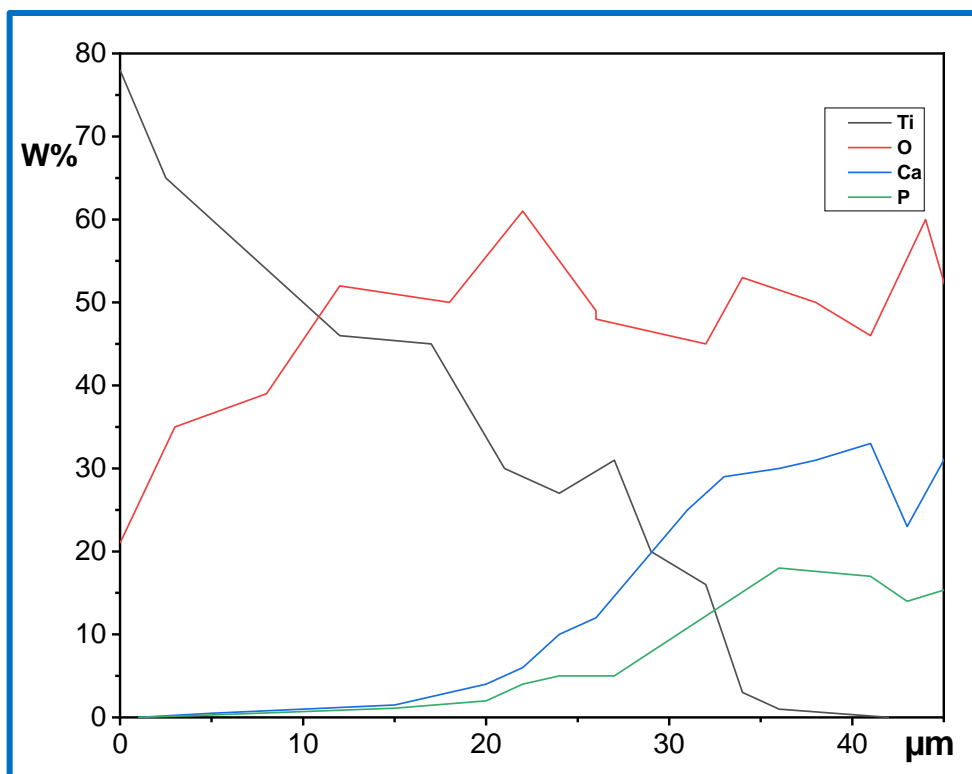


Figure (4.7): The linear EDX analysis of composite biocoatings HA/TiO₂ coatings.

4.4 X-Ray Diffraction Test Result

The phases of the sintered biocoatings were analyzed by Philips analytical X-ray diffractometer. The XRD patterns were compared with the standard JCPDS data and it was found that all the phases could be distinctly identified showing the existence of original component powders in the HA, TiO₂.

Ti-6Al-4V is an $\alpha+\beta$ alloy because α and β microstructural phases coexist at room temperature. The $\alpha+\beta$ alloys are interesting because they combine the strength of α alloys with the ductility of β alloys, and their microstructures and properties can be varied widely by appropriate heat treatments and thermomechanical processing [156].

Identification of phases present in Ti6Al4V substrate before coating are showed in **Figure (4.8)**, where there are two main phases appeared, the (α -HCP) and (β -BCC). These phases are identified with their crystalline planes according to the JCPDS card numbers where the diffraction pattern of the α -Ti phase match with the (JCPDS Card No. 06-0694) peaks and the β -Ti phase match with the (JCPDS Card No. 33- 0397).

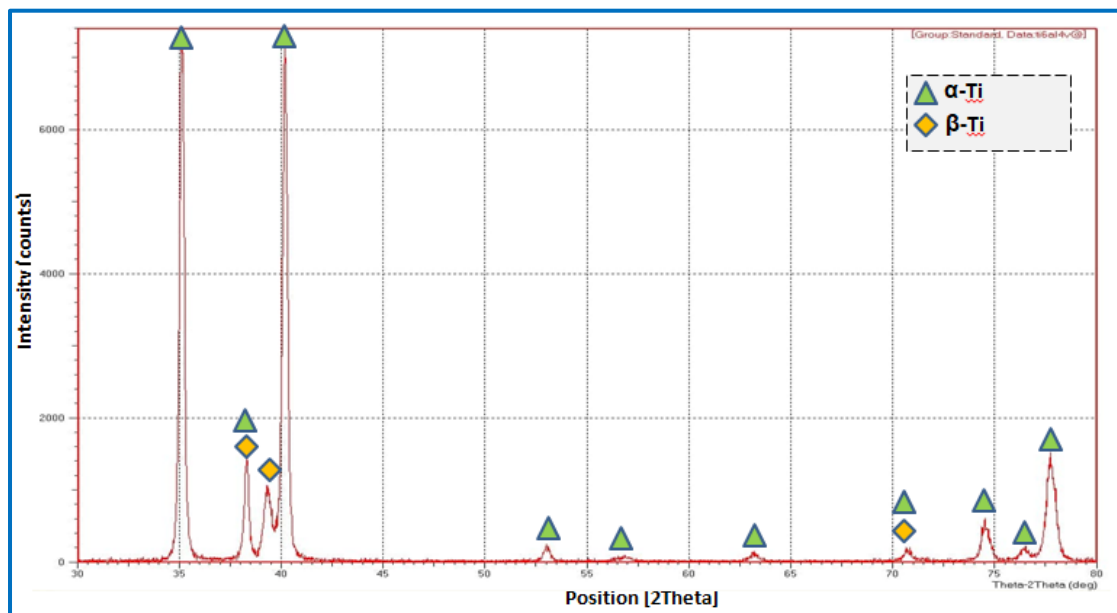


Figure (4.8): XRD pattern for the Ti-6Al-4V sample, indicating $\alpha+\beta$ phases.

The XRD pattern of the sintered TiO_2 coating sample was compared with JCPDS#88-1175 for rutile TiO_2 and JCPDS#84-1286 for anatase TiO_2 phases. **Figure (4.9)** reveals the presence of a large number of peaks corresponding to the anatase phase compared to the rutile phase. The sharp peaks of TiO_2 suggest that its structure is polycrystalline.

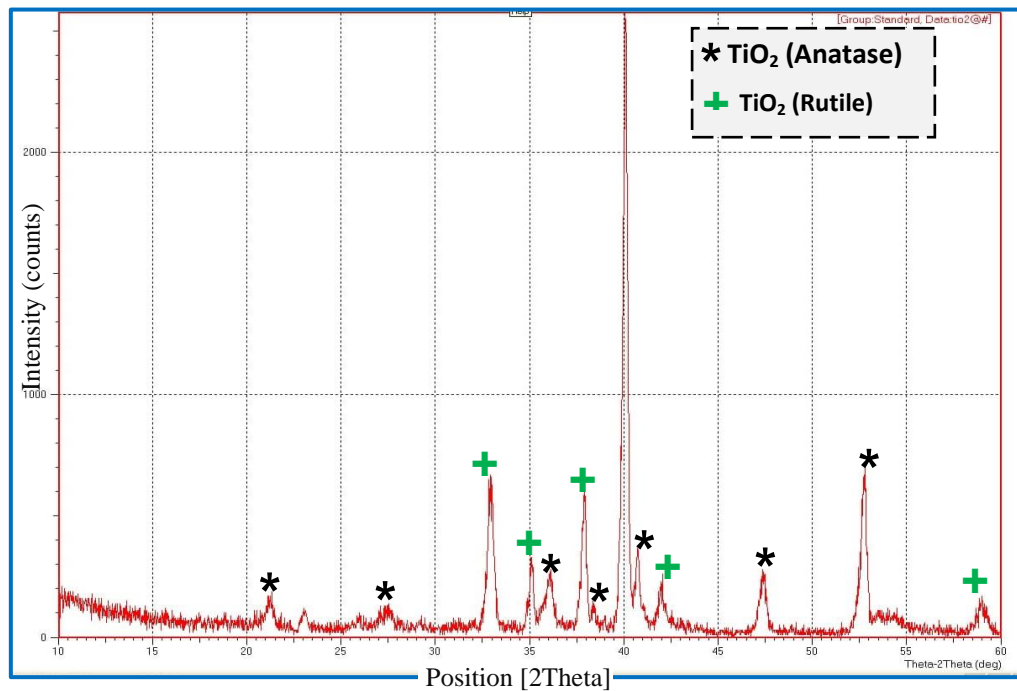


Figure (4.9): XRD pattern for the TiO_2 coated specimen.

Figure (4.10) shows the XRD patterns of HA single layer coating that is sintered in argon condition at 950°C for 1 hr. As seen, two series of peaks are observed in all the patterns, those related to the Hydroxyapatite compound (JCPDS No. 9-0432). In addition, there are some of peaks related to the β -TCP and α - $\text{Ca}_2\text{P}_2\text{O}_7$ in the XRD pattern of the sample which means that HAp decomposition occurs at such temperature and sintering time in argon condition.

The decomposition of HAp phase in contact with substrate which is due to the migration of metallic ions at the interface.

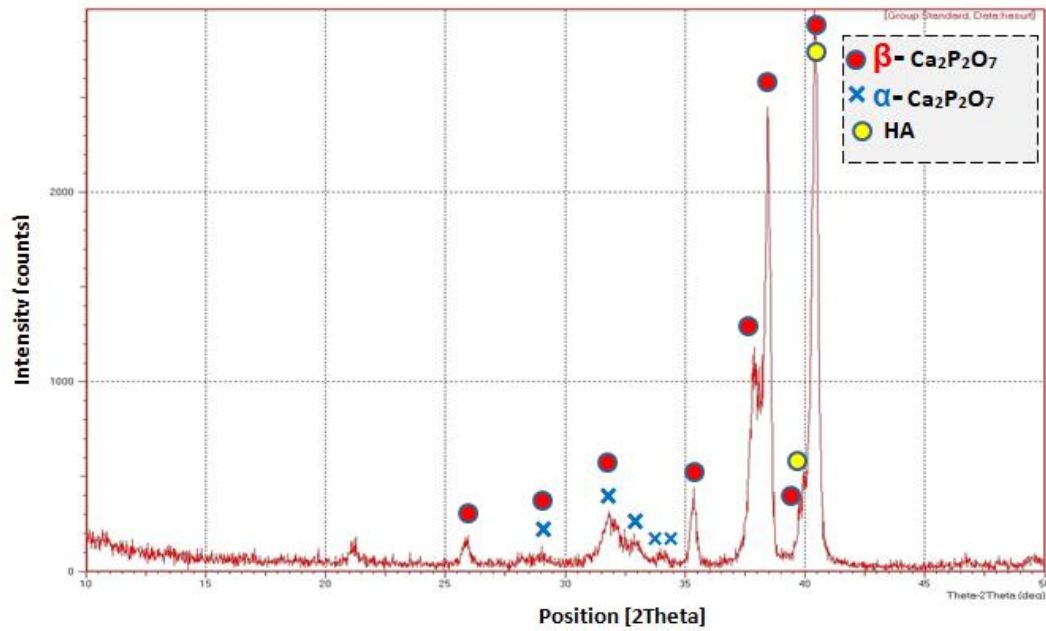


Figure (4.10): XRD pattern for the HAp coated specimen.

The XRD pattern of sintered HAp/TiO₂ composite biocoating in argon condition at temperature of 950 °C for 1 hr is given in **Figure (4.11)**. The pattern prove the presence HAp and rutile/anatase phases of TiO₂ (JCPDS No. 4-0551 and JCPDS No. 21-1272) in the coating. Since the phase transformation of anatase to rutile took place at the temperature range of 400-1000°C (which depends on the microstructure, impurity and particle size of anatase particles), the anatase TiO₂ in the deposited composite biocoating starts to convert to rutile during the sintering process and the corresponding reflections of rutile phase are observed in the XRD patterns obtained after sintering, see **Figure (4.11)**. These results agreed with that obtained by other investigators [54, 58].

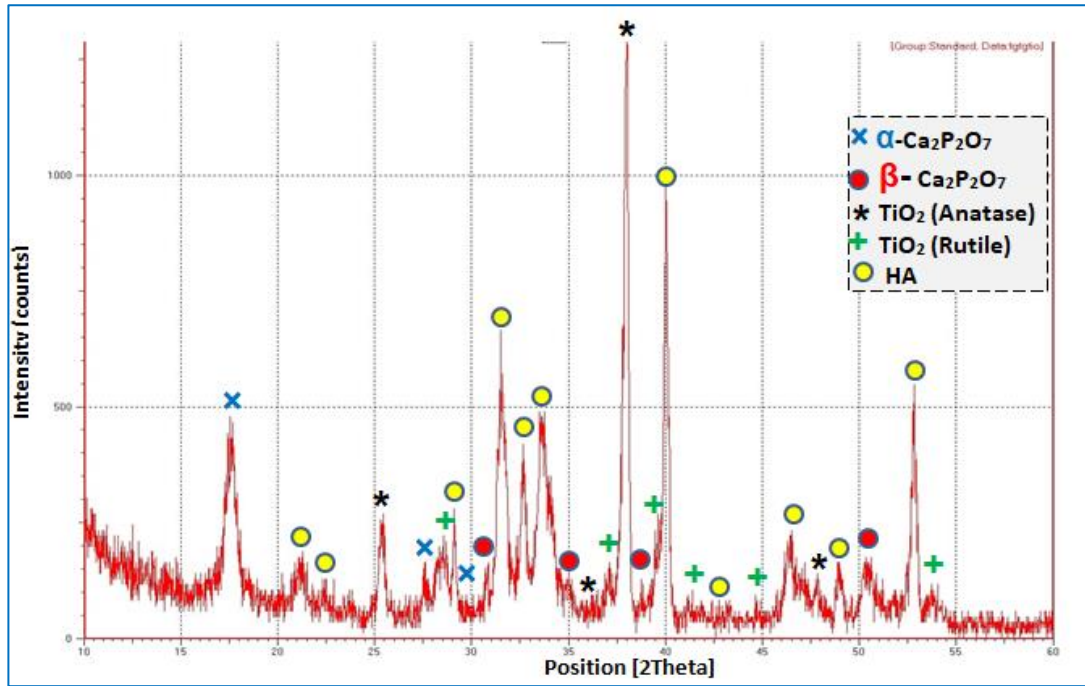


Figure (4.11): XRD pattern for the composite biocoatings HAp/ TiO₂ coating specimen.

Finally, from the XRD patterns in **Figure (4.11)**, it is clear that HAp starts to decompose to β -TCP at 950°C when it is not pure and present in composite biocoatings with TiO₂. Moreover, there is some peaks, related to α -TCP phase in the patterns that means decomposition of HAp to α -TCP, has been occurred during sintering.

The HA phase is most stable phase with the lowest solubility in body fluid. The reduction in peaks intensity of α -TCP and β -TCP unstable phases (high solubility in the body fluids) in composite biocoatings sample denotes that the graded structure of coating acted as a barrier layer against ion diffusion between HAp and substrate, and reduced the decomposition of HA at the surface.

4.5 Micro Hardness

As is well identified, the biomaterial utilized for long-term implants should possess higher mechanical strength and better biological properties owing to the complex nature of human body

environment [157]. Therefore, in this study, the micro-hardness, as one of the mechanical properties required for coated surfaces, is evaluated, and the results of uncoated and coated samples are represented in **Figure (4.12)**. It can be seen from this figure that the hardness of uncoated substrate is 80.91 HV, which is the lowest value compared with that of coated substrates. On the other hand, the average micro-hardness of the HAp/TiO₂ graded coated sample at three different regions is 219.63 HV, which is higher than the uncoated substrate and even higher than the hardness of HAp, TiO₂ alone (197.2) HV, (211) HV respectively .

The values of the Vickers hardness test results are summarized in **Table (4.2)**. From this Table, it can be concluded that the value of hardness HAp coated slightly less than its counterpart TiO₂ coated. While, it is found that there is a maximum value of hardness 219 HV for composite biocoatings. This can be attributed to the fact, that the presence of TiO₂ particles in HAp coating layer will improve the physical reliability between the substrate and coating layer to produce a higher bonding between the particles, and this lead to a marked increase in the hardness of the layer. Furthermore, the coating with coherent layer, significant bonding strength and lower amount of porosity provides higher hardness [58, 114].

Table (4.2): Experimental data of the coated and uncoated samples.

Sample	Load (N)	Dwell Time (sec)	Vickers Hardness (HV)
HAp	25	10	197.2
TiO ₂	25	10	211.5
composite biocoatings	25	10	219.6
Ti6Al4V	100	10	80.91

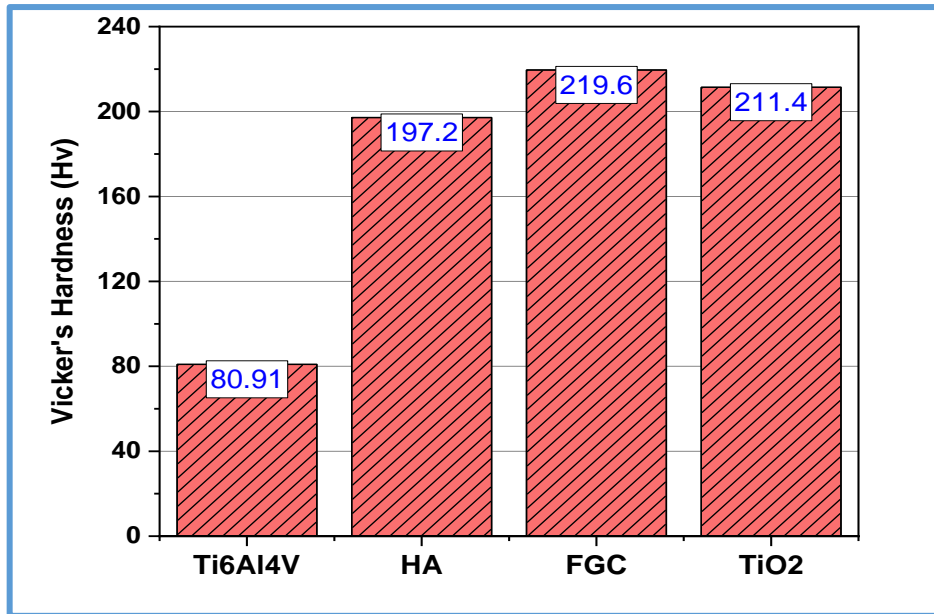


Figure (4.12): Vicker's micro-hardness (HV).

4.6 Surface Roughness

The HAp coating has textured surface with higher roughness among samples, nevertheless, without appropriate mechanical strength, high roughness will be unworthy. This roughness can be attributed to the brittle character of HAp [34, 84]. By surface roughness measurement, the composite biocoatings is the optimal option among others. It was pointed out that the rapid attachment of the osteoblast cells onto the implant surface can be achieved by increasing the surface roughness, which may provide a substantial improving in contact area with the bone. Roughness acts as a driving force for osseointegration due to the high surface energy of the rough surface as well as the improvement of contact between the bone and implant. On the other hand higher surface roughness lead to increase bacteria adhesion.

Adding TiO₂ to the HAp coating reduces the brittleness of the coating and the cracks are almost eliminated, thus showing less roughness for composite biocoatings. TiO₂ has lowest surface roughness than other coatings. Also, the calculated average surface roughness parameters for all

coatings are in the micro-metric range. The surface roughness values are represented by **Figure (4.13)**.

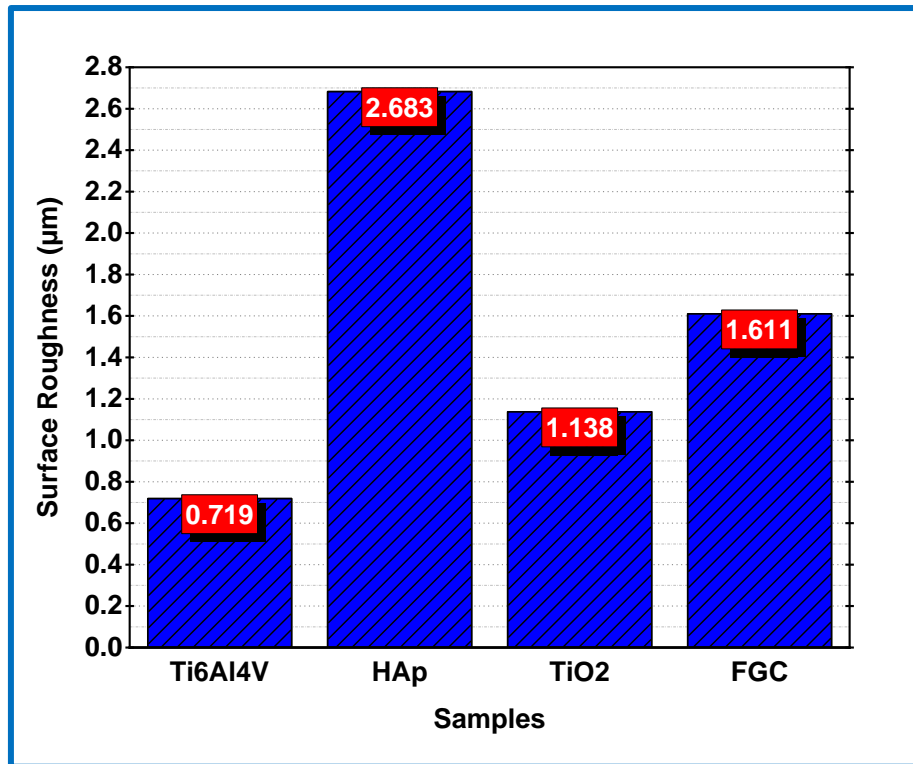


Figure (4.13): Surface roughness values (Ra) μm .

4.7 Wettability

The surface of non-coated titanium sample has a higher aqueous contact angle of 84.48° indicates a less hydrophilic surface compared to the coated samples that presents a water contact angle of test values as illustrated in **Table (4.3)**.

Table (4.3): Contact angle (θ°) of Ti6Al4V and coated samples.

Sample	Ti6Al4V	HAp	TiO ₂	composite biocoatings
Contact angle θ (deg)	84.48°	12.52°	41.6°	13.11°

The reduced contact angle may be attributed to the effect of surface texture (surface roughness) as shown in **Figure (4.14)** and other biocompatible phases (α - $\text{Ca}_3(\text{PO}_4)_2$, β - $\text{Ca}_2\text{P}_2\text{O}_7$ and TiO_2 (rutile and anatase)) formed during sintering because of formation of more bioactive phases (α -TCP and TiO_2 (anatase)) with the phases (β -TCP and TiO_2 (rutile)) in the composite biocoatings as these phases provide synergistic effect to make the surface more hydrophilic. These results agreed with that obtained by other investigators [123, 130]. **Figure (4.15)** reveals surface roughness values of uncoated Ti6Al4V and electrophoreses depositing coatings. The results of previous research indicate that the high surface wettability and surface roughness at the micron scale were for the synergistic effect of reduction on cell adhesion and growth.

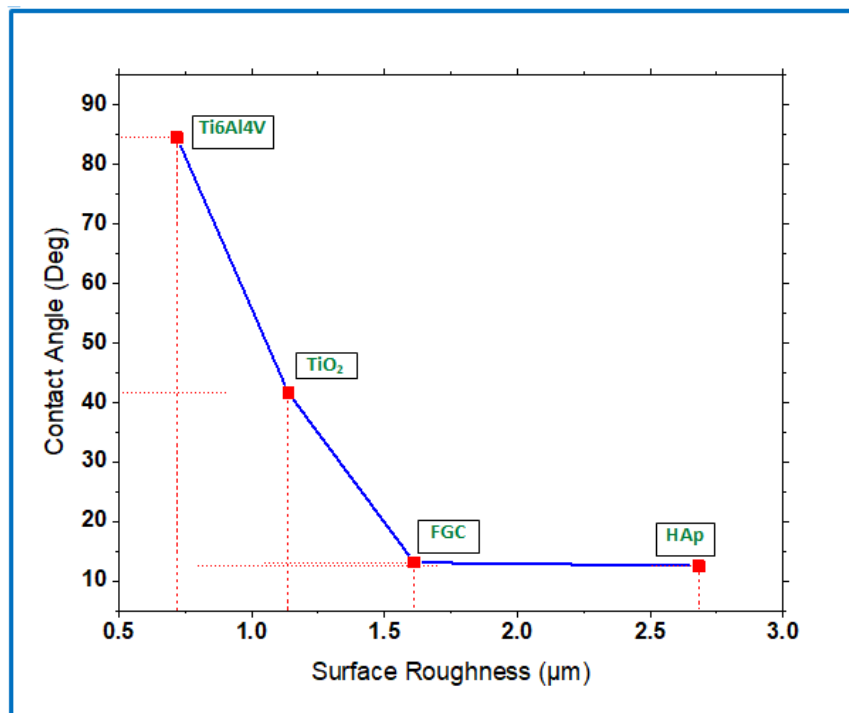


Figure (4.14): Effect of surface roughness on wettability.

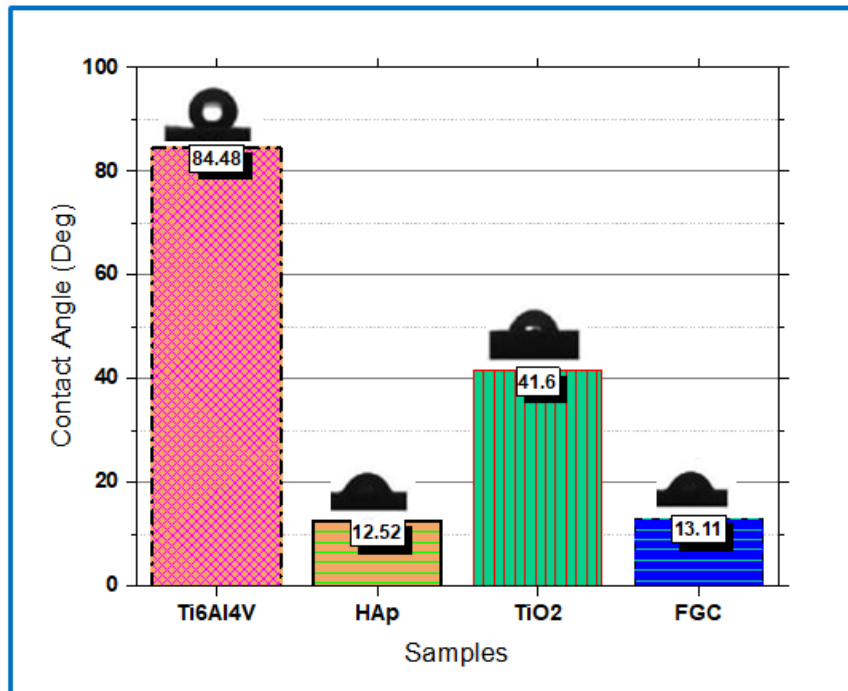


Figure (4.15): Photometric quantification of contact angle θ° bound to the different experimental coating surfaces.

4.8 Electrochemical Corrosion

Titanium and Ti6Al4V have higher breakdown potential and lower passivity current, indicating that these materials have higher corrosion resistance. In the presence of chloride ions, a breakdown potential of several more positive than the free corrosion potential are necessary. localized corrosion is caused by the migration of ions across the passive film. Accumulation of oxychloride at the metal-film interface is responsible for the oxide film rupture as a nucleation event. The potentiodynamic polarization curves of base Ti6Al4V, HAp, TiO₂ and composite biocoatings samples in the SBF solutions are illustrated in **Figures (4.16) to (4.18)** Polarization curves, which are used to report the corrosion properties of a metal, are commonly used in research on electrochemical corrosion. A large free corrosion potential and smaller passivation current yield a better

corrosion resistance. The corrosion parameters, extracted from polarization curves using Tafel least square fitting method, are listed in **Table (4.4)**.

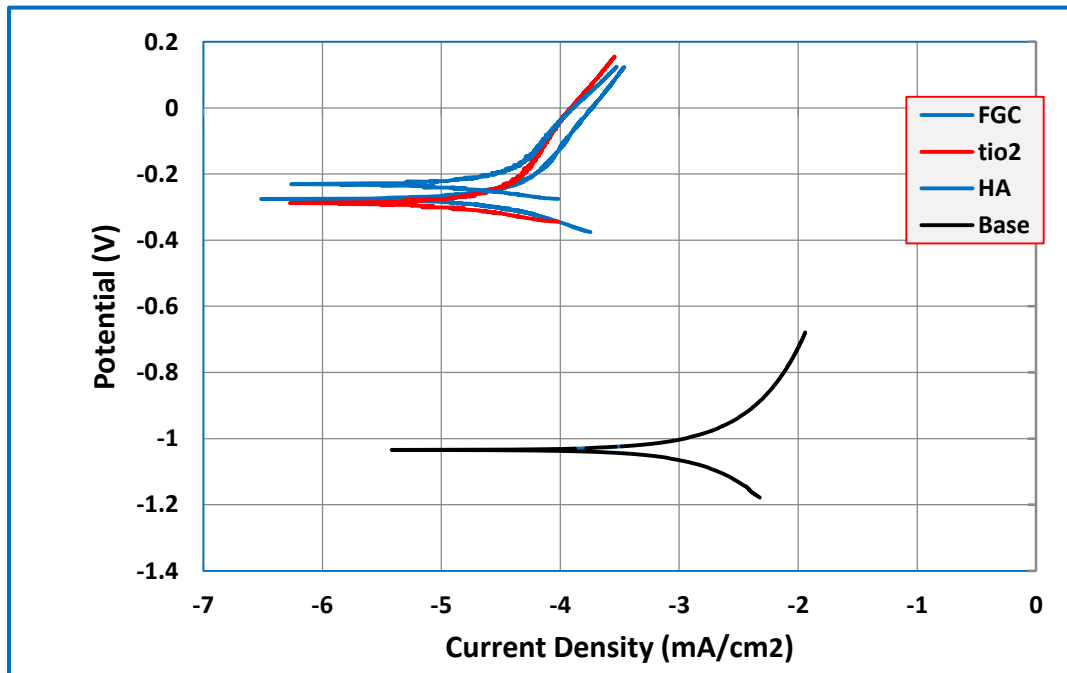


Figure (4.16): Potentiodynamic polarization curves of coated and uncoated samples in Ringer's solution.

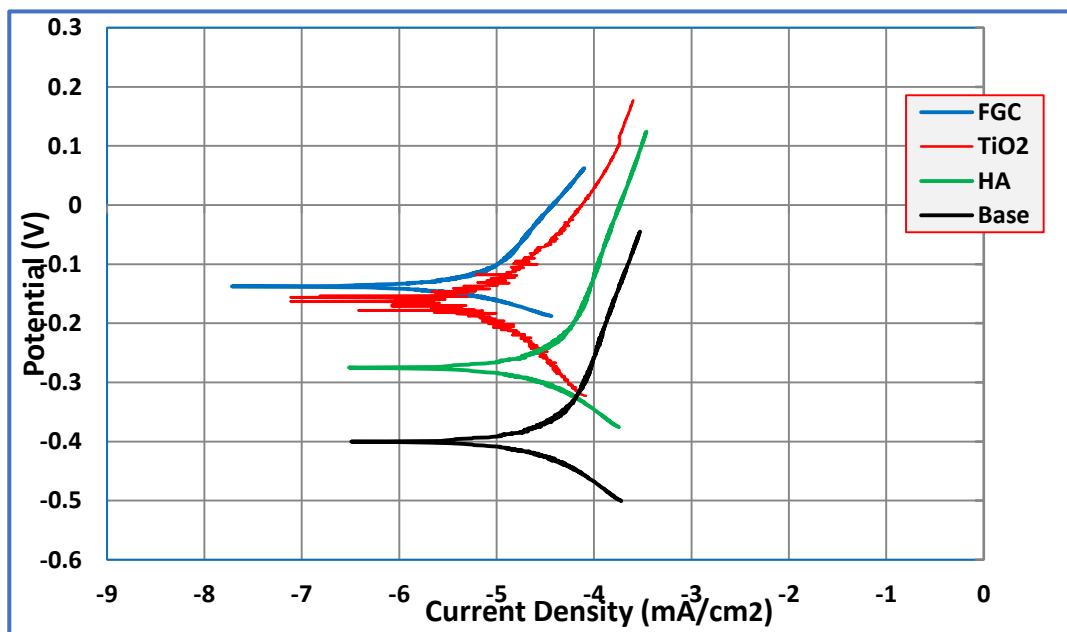


Figure (4.17): Potentiodynamic polarization curves of coated and uncoated samples in NaCl 0.9%.

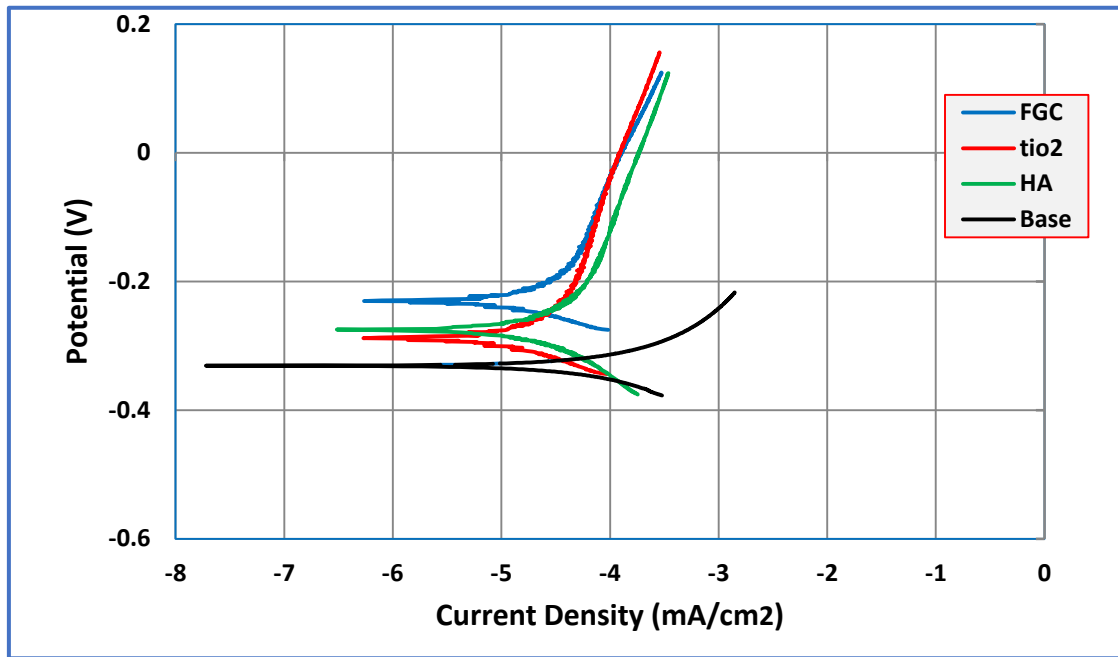


Figure (4.18): Potentiodynamic polarization curves of coated and uncoated samples in artificial saliva.

In all media used in the examination, it can be seen from the results obtained in **Table (4.4)**, the uncoated substrate has higher corrosion current density and thus lowest corrosion resistance because of the occurrence of metal ions dissolution on the surface of the uncoated substrate.

Table (4.4): Electrochemical parameters of Ti6Al4V substrate and coated samples in different media.

Media	Sample	E_{corr} (V)	I_{corr} ($\mu\text{A}/\text{cm}^2$)	CR (mpy)	$R_p \times (10^{-3})$
Ringer's Solution	Base	-0.84	20.09	0.176	1.29
	HA	-0.29	4.00	0.035	6.50
	TiO ₂	-0.26	3.18	0.027	8.17
	Comp.C	-0.23	2.52	0.022	9.90
NaCl 0.9%	Base	-0.42	7.99	0.070	3.25
	HA	-0.31	6.35	0.055	4.09
	TiO ₂	-0.18	1.79	0.014	14.5
	Comp.C	-0.15	1.42	0.012	18.3

Artificial Saliva	Base	-0.235	15.96	0.140	1.62
	HA	-0.18	10.07	0.088	2.58
	TiO ₂	-0.13	6.53	0.057	3.98
	Comp.C	-0.14	2.52	0.022	10.31

By observing the values of the corrosion current for the uncoated samples, we find that the value of the corrosive current density in the Ringer's solution and NaCl 0.9% is higher than the corrosive current value of the uncoated sample in the artificial saliva solution and the reason for this is that the artificial saliva and NaCl 0.9% have a higher pH value than that of Ringer's solution. In the case of coated samples, there are a clear improvement in the polarization behaviour after coating in the values of E_{corr} , I_{corr} and CR. The value of E_{corr} after coating is shifted towards the noble direction of potential. In the case of TiO₂ coated samples, the crystallization of the TiO₂ on Ti6Al4V rendered the layer very stable, showing the most effective corrosion resistance.

The results corresponding to composite biocoatings samples imply a significant decrease in the corrosion current density (I_{corr}) and corrosion rate, and an increase in the corrosion potential (E_{corr}), which means an increasing in the resistance corrosion **Figure (4.19)**. This indicates that composite biocoatings structure of coatings helps to produce a coating with fewer micro-cracks due to the improvement in CTE HA ($\alpha_{HA}=14-16 \times 10^{-6} K^{-1}$) and Ti-6Al-4V ($\alpha_{Ti-6Al-4V}=8.9 \times 10^{-6} K^{-1}$) by incorporating graded coating with TiO₂ ($\alpha_{TiO_2}=10.2 \times 10^{-6} K^{-1}$) mismatch between Ti6Al4V and the coating [133]. When micro-cracks are present in the coatings, conducting paths between the corrosive medium and the Ti6Al4V substrate will eventually be formed. Gradient layer of HAp/TiO₂ improves this consequence by progressing the coating integrity. The

corrosion rate of the base (Ti6Al4V) alloy and different ceramic coatings in different medias as shown in **Figure (4.20)**.

The shift I_{corr} towards the negative direction means improvement in the passivation layer after coating leads to reduce the I_{corr} value. In the other words, the TiO_2 interlayer adheres well to the titanium alloy substrate, and on the other hand, a HAp bioceramic coating can be formed with less porosity and microcracks on Ti6Al4V/ TiO_2 . Therefore, the interlayer reduces the contact between the SBF solution and the substrate, reducing the corrosion current density. These results agreed with that obtained by other investigators [63, 111].

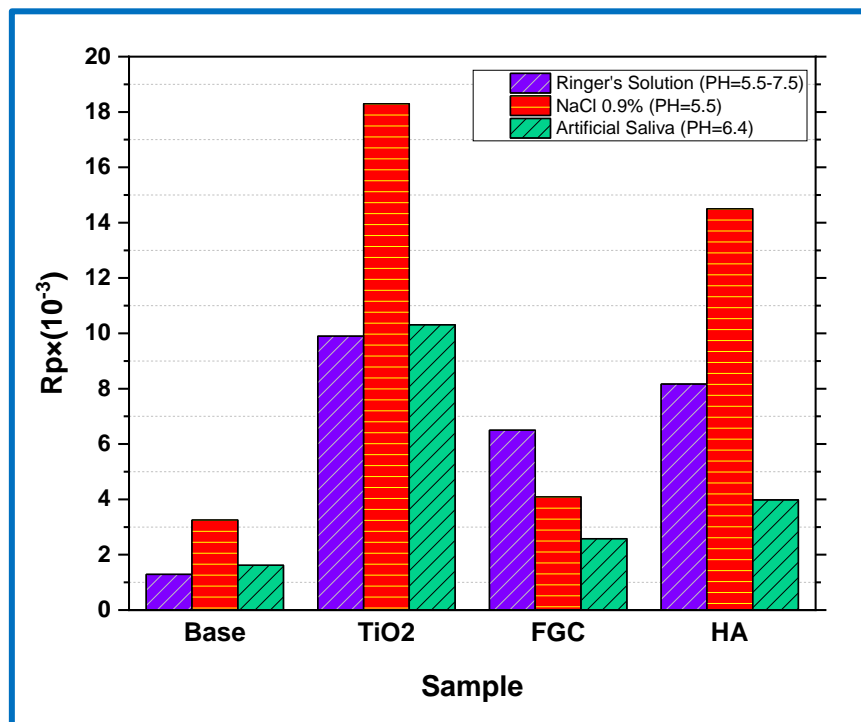


Figure (4.19):Corrosion resistance of experimental samples in different medias.

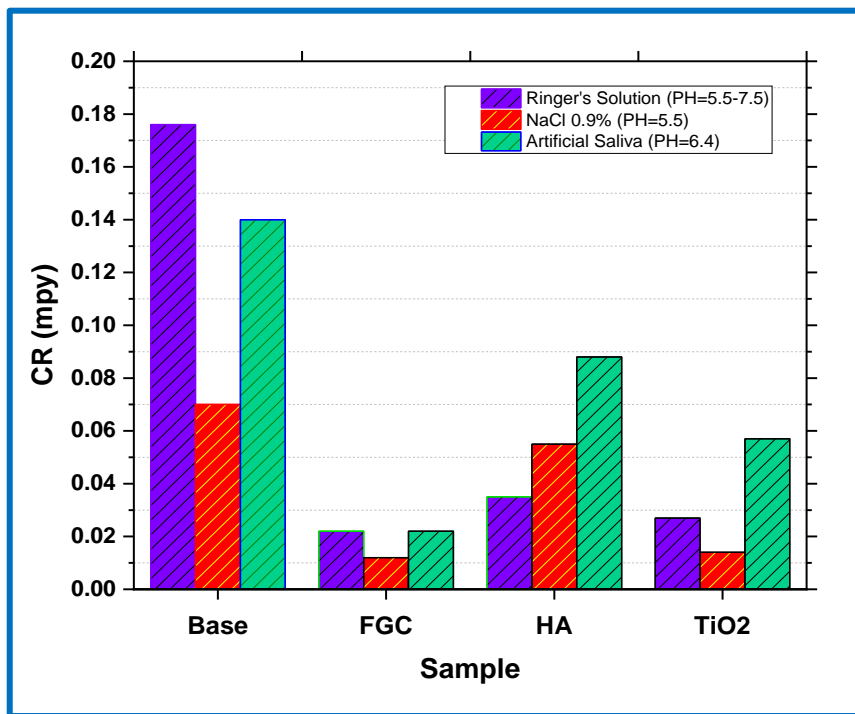


Figure (4.20): Corrosion rate of the base (Ti6Al4V) alloy and different ceramic coatings in different medias.

4.9 Metal Ion Release

Metal ion release test is used to ensure the capability of alloys to be used in human bodies. The uncoated and composite biocoatings samples are immersed in synthetic artificial saliva and Ringer's solutions at 37°C for 21 day. The purpose of this study was to investigate the type and amount of ions released from Ti6Al4V into bio fluids. **Figure (4.21)** shows the effect of different immersion media on the accumulative ions release concentrations (Ug/l) from composite coated/uncoated Ti6Al4V. By observing the practical results of the examination listed in **Table (4.5)**. From previous Table and Figure, it can be observed that the concentration of ions released from the uncoated sample is greater than the concentration of ions released from the gradient coating sample, and the reason for this is due to alloying titanium as Ti-6Al-4V reduces the electrochemical

stability induced by passivity, and the alloy shows some breakdown events in Ringer's solution. We may take into account the effect of the pH value of the Ringer's solution is less than that of artificial saliva.

In the case of the coated samples, the composite biocoatings samples exhibit a minor decrease in ion release rate. However, the reduction range in ion release were (21-38 %) noted with the coated sample. This reduction in metal ion release is attributed to a dense, stable and crack free graded HAp/TiO₂ coating, which act as a barrier that prevents the release of ions from the implant surface.

Table (4.5): Results of atomic adsorption spectroscopy test for base (Ti6Al4V) and composite biocoatings.

Samples		Ion Release (Ug/l)		
		Al	Ti	V
Ringer	base	3.12	2.53	1.61
	Comp.C	2.21	1.98	1.21
Saliva	base	2.42	2.10	1.43
	Comp.C	1.74	1.65	0.88

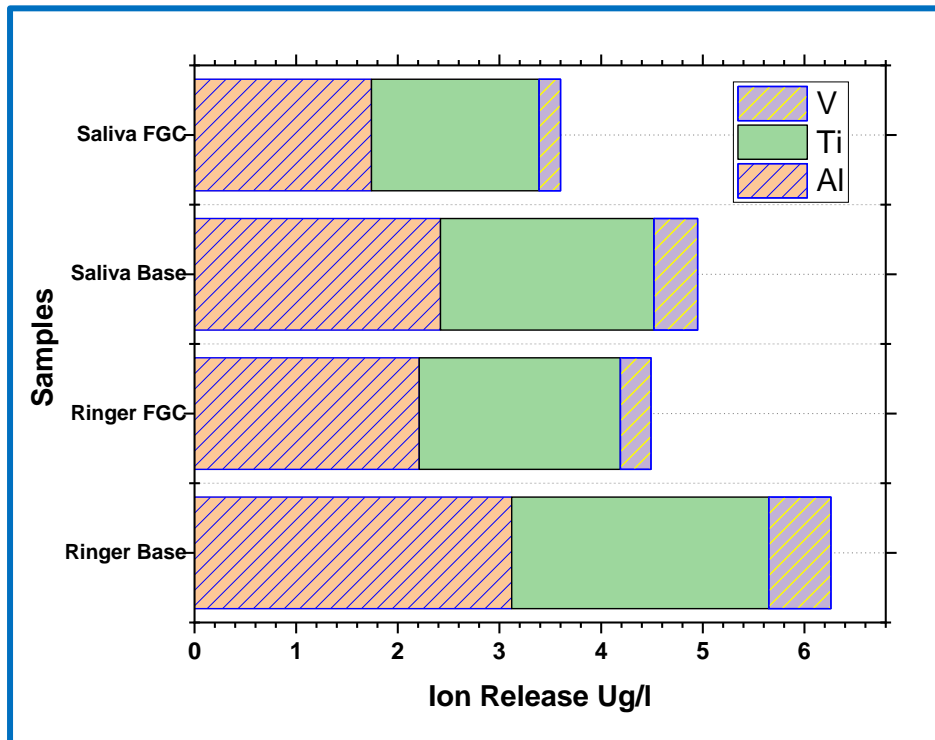


Figure (4.21): The effect of different immersion media on the accumulative ions release concentrations (Ug/l) from composite coated/uncoated Ti6Al4V.

4.10 Antibacterial Study

The antibacterial effect of composite biocoatings HAp/TiO₂ and uncoated specimens are investigated against *E. coli* culture as shown in **Figure (4.22)**. The formation of clear region around the disc refers to the bacterial inhibition zone. It can be observed that the case exhibited a good antibacterial effect after 24hrs. of incubation period, but the uncoated specimen © and pure HAp sample have a small inhibition zone as compared with the HAp/TiO₂ one. This is because of that the anatase TiO₂ itself is antibacterial [161] and therefore a strong antibacterial effect of the HAp/TiO₂ (1, 2, 3 and 4) particles is obtained. Therefore, the presence of TiO₂ particles in the HAp coatings is effective in preventing the bacterial adhesion on the

surface and in turn, preventing bacteria growth that would improve the antibacterial activity.

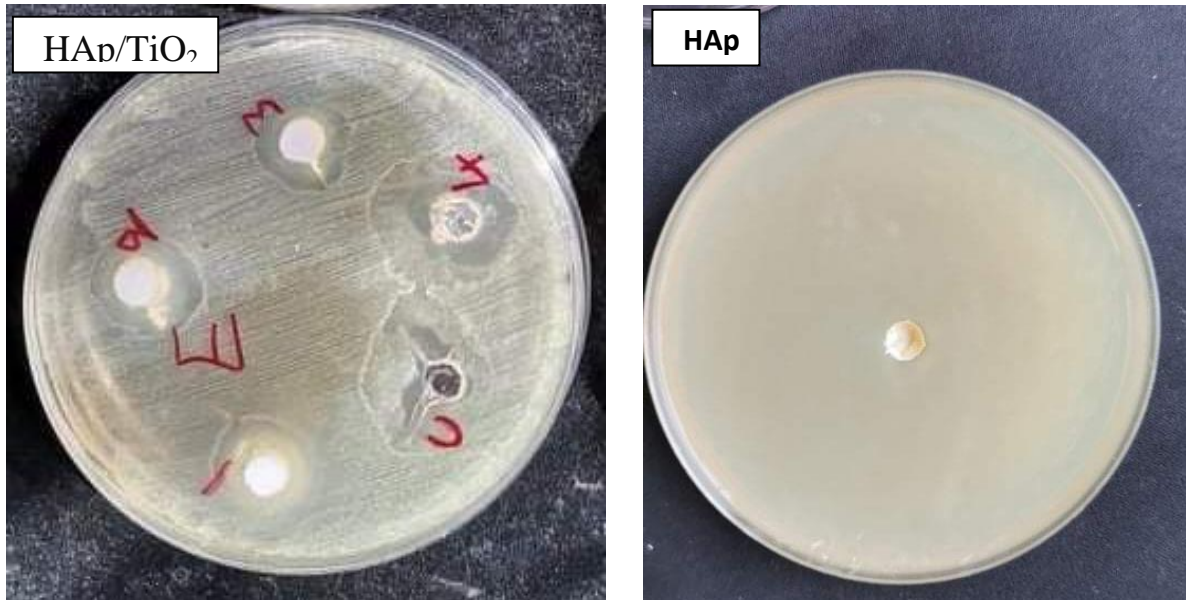


Figure (4.22): Images of the antibacterial tests of HAp and HAp/TiO₂ against *E. coli*.

Conclusions and Recommendations

5.1 Key Findings

In the current study, the HAp/TiO₂ composite biocoatings has been deposited on the surface of medical Ti6Al4V alloy successfully by using EPD process for biomedical applications. The effect of gradient layer on mechanical and chemical properties of composite biocoatings HAp/TiO₂ coating was investigated in comparison with single-layer HAp / TiO₂ coatings. In view of the test results, the following conclusions can be presented.

1. The composite biocoatings HAp/TiO₂ coatings were successfully fabricated on Ti6Al4V substrates by electrophoretic deposition after choosing the optimal conditions for coating by trial and error method.
2. Addition of Polyethyleneimine PEI to the HAp/TiO₂ EPD bath resulted in more stable suspensions and deposition of uniform crack free coatings.
3. The XRD, analysis results showed desired phases (hydroxyapatite and TiO₂ (rutile and anatase)) acquired in the coatings by utilizing prepared suspension and heat treatment at 950°C. In addition to some

bio-phases resulting from the decomposition of hydroxyapatite at sintering temperature.

4. Based on the electrochemical corrosion behavior of samples in SBF solution at 37°C, the corrosion current density and corrosion rate significantly decreased by implementation of TiO₂ and graded structure of coating while corrosion potential and linear polarization resistance increased.

5. The morphology of composite biocoatings was homogenous and crack-free when coating with the optimum condition at 20 V for 1 min.

6. Gradient layer of HAp/TiO₂ improved the average surface micro-hardness by progressing the coating integrity.

7. EDS results showed that the coated sample at (20V-1min) has 1.81 Ca/P ratio, which is corresponding to the theoretical ratio of HAp, while the amount of TiO₂ (50 wt.%) present in the coating at this condition agreed with the theoretical value of titania added in the total suspensions of EPD.

8. The incorporation of titanium within the HAp deposited provides excellent adhesion to the substrates and may prevent implant loosening, which are highly desirable traits for bio implants, and the results of the examination of the released metal ions proved this.

9. HAp/TiO₂ composite biocoatings offer a protective effect and can prevent the release of toxic metallic ions from Ti6Al4V alloy in a physiological environment. The levels of released ions increased with decreasing the pH value of the solution.

10. The obtained coatings thus can be successfully used to change the surface of Ti6Al4V implants to improve their biological properties and antibacterial performance.

5.2 Recommendations for Further Research

1. Studying experimentally and numerically the corrosion behavior of composite biocoatings HAp/TiO₂ on Ti6Al4V implant, but in vivo.
2. The tribo-corrosion behavior of Ti6Al4V coated with HAp/TiO₂ by EPD technique must be further pondered scientifically and experimentally.
3. The effect of laser surface treatment on the morphology and corrosion resistance of the composite biocoatings HAp/TiO₂ coating layer should be scrutinized.
4. Experimental study of the corrosion behavior of composite biocoatings HAp/TiO₂ in human body fluid by using TiAlNb, and Ni-Cr alloy need to be carried out.

References

1. T Albrektsson, P.I. Brånemark, Hans-Arne Hansson and Lindström JJ Osseointegrated titanium implants. Requirements for ensuring a long-lasting direct bone-to-implant anchorage in man. 1981. 52(2): p. 155-170.
2. Tsou, H.K. and P.Y.J.A.o.T.D. Hsieh, Anticorrosive, antimicrobial and bioactive Titanium Dioxide coating for surface-modified purpose on biomedical material. 2017: p. 103-22.
3. Paul S Nnamchi, Camillus Obayi, I. Todd, and M.W. Rainforth, Mechanical and electrochemical characterisation of new Ti–Mo–Nb–Zr alloys for biomedical applications. International Journal of Oral Implantology and Clinical Research, 2016. 60: p. 68-77.
4. K Prem Ananth, A Joseph Nathanael, Sujin P Jose, Tae Hwan Oh, and D Mangalaraj, A novel silica nanotube reinforced ionic incorporated hydroxyapatite composite coating on polypyrrole coated 316L SS for implant application. 2016. 59: p. 1110-1124.
5. Dehghanghadikolaei, A. and B.J.M. Fotovvati, Coating techniques for functional enhancement of metal implants for bone replacement: Journal National Library of Medicine : a review. 2019. 12(11): p. 1795.
6. Heness, G. and B. Ben-Nissan, Innovative bioceramics. in Materials forum, 2004, VOL. (27) 104 – 11,.
7. Osman, R.B. and M.V.J.M. Swain, A critical review of dental implant materials with an emphasis on titanium versus zirconia. Journal Materials (Basel), 2015. 8(3): p. 932-958.
8. Muddugangadhar, B., et al., Biomaterials for dental implants: An overview. International Journal of Oral Implantology and Clinical Research, 2011. 2(1): p. 13-24.

9. Manivasagam, G., D. Dhinasekaran, and A.J.R.p.o.c.s. Rajamanickam, Biomedical implants: corrosion and its prevention-a review. *Materials Science*, 2010.
10. Bedi, R.S., et al., Biocompatibility of corrosion-resistant zeolite coatings for titanium alloy biomedical implants. *Acta Biomaterialia*, 2009. 5(8): p. 3265-3271.
11. Hornberger, H., S. Virtanen, and A.R.J.A.b. Boccaccini, Biomedical coatings on magnesium alloys—a review. *Acta Biomaterialia*, 2012. 8(7): p. 2442-2455.
12. Chen, Q., Electrophoretic Deposition of Composite Coatings with Bioactive Character and Drug Delivery Capability. Thesis for: Doctoral, 2015, 167 pages.
13. Sumitomo, N., et al., Experiment study on fracture fixation with low rigidity titanium alloy. *Journal of Materials Science: Materials in Medicine*, 2008. 19(4): p. 1581-158
14. Niinomi, M.J.M. and m.t. A, Recent metallic materials for biomedical applications. *Metallurgical and Materials Transactions A* :(3)33 .2002 ,p. 477-486.
15. Niinomi, M.J.M.S. and E. A, Mechanical properties of biomedical titanium alloys. *Journal Materials Science and Engineering*, 1998. 243(1-2): p. 231-236.
1. Sumner, D.J.J.o.B., Long-term implant fixation and stress-shielding in total hip replacement. *Journal of biomechanics* 2015. 48(5): p. 797-800.
2. Engh Jr, C.A., Clinical consequences of stress shielding after porous-coated total hip arthroplasty. *Clinical Orthopedics and Related Research* 2003. 417: p. 157-163.

3. M.I.Z. Ridzwan, Solehuddin Shuib, A.Y. Hassan, A.A. Shokri and M.N. Mohamad Ibrahim, Problem of Stress Shielding and Improvement to the Hip Implat Designs: A Review. *Journal of Medical Sciences*, 2007. 7(3): p. 460-467.
4. Eliaz, N. and U.J.C.R. Kamachi Mudali, Special Issue: Biomaterials Corrosion. 2003. 2: p. 2-3.
5. Mudali, U.K. and B. Rai, Corrosion science and technology: mechanism, mitigation and monitoring. Narosa Publishing House: New Delhi, India, 2008.
6. Kubie, L.S. and G.M.J.T.J.o.e.m. Shults, Studies on the relationship of the chemical constituents of blood and cerebrospinal fluid. *J Exp Med* 1925. :(4)42p. 565.
7. Hongping Duan, Keqin Du, Chuanwei Yan and Fuhui Wang, Electrochemical corrosion behavior of composite coatings of sealed MAO film on magnesium alloy AZ91D. *Electrochimica Acta*, 2006. 51(14): p. 2898-2908.
8. Yongjun Zhang, Chuanwei Yan, Fuhui Wang and Wenfang Li, Electrochemical behavior of anodized Mg alloy AZ91D in chloride containing aqueous solution. *Corrosion Science*, 2005. 47(11): p. 2816-2831.
9. Amogh Tathe, Mangesh Ghodke and Anna Pratima G. Nikalje, A brief review: biomaterials and their application. *Int J Pharm Pharm Sci* 2010. 2(4): p. 19-23.
10. Raghavendra, G.M., K. Varaprasad, and T. Jayaramudu, Biomaterials: design, development and biomedical applications, in *Nanotechnology applications for tissue engineering*. 2015, Elsevier. p. 21-44.

11. Isa, Z. and J.J.A.o.D.U.o.M. Hobkirk, Dental Implants: Biomaterial, Biomechanical And Biological Considerations. *Annals of Dentistry University of Malaya*, 2000. 7(1): p. 27-35.
12. Anselme, K.J.B., Osteoblast adhesion on biomaterials. *Biomaterials*, 2000. 21(7): p. 667-6.81
13. Mehdizadeh, M. and J.J.M.b. Yang, Design strategies and applications of tissue bioadhesives. *Macromol Bioscience* 2013. 13(3): p. 271-288.
14. Yoruc, ABH, Sener, BC. Biomaterials. In: Prof. Kara S, editor. *A roadmap of biomedical engineers and milestones*; 2012, ISBN: 978-953-51-0609-8.
15. Vallet-Regí, M.J.J.o.t.C.S., Dalton Transactions, Ceramics for medical applications. *Journal of the Chemical Society, Dalton Transactions*, 2001(2): p. 97-108.
16. Overgaard S, Lind M, Glerup H, Grundvig S, Bunger C, Soballe K. *Clinical Orthopaedics and Related Research*. 1997:286.
17. Suchanek, W. and M.J.J.o.M.R. Yoshimura, Processing and properties of hydroxyapatite-based biomaterials for use as hard tissue replacement implants. *Journal of Materials Research*, 1998. 13(1): p. 9.117-4.
18. Moroni A, Toksvig-Larsen S, Maltarello MC, Orienti L, Stea S, Giannini S. *Journal of Bone and Joint Surgery-American Volume*. 1998;80A:547.
19. Jordan DR, Munro SM, Brownstein S, Gilberg SM, Grahovac SZ. A synthetic hydroxyapatite implant: the so-called counterfeit implant. *Ophthalmic Plast Rec* 1998;14(4):244 9.
20. Orlovskii, V., V. Komlev, and S.J.I.m. Barinov, Hydroxyapatite and hydroxyapatite-based ceramics. *Inorganic Materials*, 2002. 38(10): p. 973-984.

21. Bermejo R, Danzer R. High failure resistance layered ceramics using crack bifurcation and interface delamination as reinforcement mechanisms. *Eng Fract Mech* 2010;77(11):2126-35.
22. L. Pawlowski; "Thick Laser coatings: a review"; *Journal of Biomaterials* Vol.5, No.8, P. 279-295(1999).
23. Karin Eufinger; "Effect of deposition conditions and doping on the structure, optical properties and photocatalytic activity of d.c. magnetron sputtered TiO₂ thin films"; Ph.D. thesis University of Wetenschappen: Natuurkunde, (2007).
24. Priyadarshini, B., Bioactive coating as a surface modification technique for biocompatible metallic implants: a review. *Journal of Asian Ceramic Societies*, 2019. 7(4): p. 397-406.
25. Lorenzetti, M., The influence of surface modification on bacterial adhesion to titanium-based substrates. *ACS Applied Materials & Interfaces*, 2015. 7 (3) p. 1644-1651.
26. Niinomi M. Recent metallic materials for biomedical applications. *Metal Mater Trans A* 2002;33 (3):477-86.
27. Silver, F.H. and D.L. Christiansen, Introduction to biomaterials science and biocompatibility, in *Biomaterials science and biocompatibility*. 1999, Springer. p. 1-26.
28. Iftekhar, A.J.S.h.o.b.e. and N.Y. design. McGraw-Hill, *Biomedical composites*. 2004.
29. Y. Miyamoto, W. A. Kaysser, B. H. Rabin, A. Kawasaki, and R. G. Ford. *Functionally Graded Materials. Design, Processing and Applications*, Kluwer Academic Publishers, Dordrecht, 1999.

30. K. A. Khor, Y. W. Gu, C. H. Quek, and P. Cheang, "Plasma Spraying of Functionally Graded Hydroxyapatite/Ti-6Al-4V Coatings," *Surf. Coat. Technol.*, 168 195–201 (2003).
31. Radhi N.S., Preparation, Characterization, and Modeling Functionally Graded Materials in Bio-application. . PhD thesis. University of Technology. Iraq, 2015.
32. Sola, A., D. Bellucci, and V.J.B.a. Cannillo, Functionally graded materials for orthopedic applications—an update on design and manufacturing. 2016. 34(5): p. 504-531.
33. Nabaa S. Radhi , A Review for Functionally Gradient Materials Processes and Useful Application.(2018).
34. Sebbowa, T.M., Surface Modification of a Titanium Alloy via Electro spraying for Biomedical Engineering Applications. 2013, UCL (University College London).
35. A. Gupta and M. Talha, "Recent development in modelling and analysis of functionally graded materials and structures", *Progress in Aerospace Sciences*, vol. 79, pp. 1–14, 2015.
36. Marin, L., Numerical solution of the Cauchy problem for steady-state heat transfer in two-dimensional functionally graded materials. *International Journal of Solids and Structures*, 42(15), pp.4338-4351, 2005.
37. MÜLLER E., DRAŠAR C., SCHILZ J., KAYSSER W.A., Functionally graded materials for sensor and energy applications, *Materials Science and Engineering A: Structural Materials: Properties, Microstructure and Processing* A362(1-2), 2003, pp. 17–39.
38. Lu, L., Chekroun, M., Abraham, O., Maupin, V. and Villain, G., Mechanical properties estimation of functionally graded materials using surface waves recorded with a laser interferometer. *NDT & E International*, 44(2), pp.169-177, 2011.
39. Weikai Li and Baohong Han, Research and Application of Functionally Gradient Materials, *Materials Science and Engineering* ,(2018).

40. Craveiro, F., de Matos, J.M., Bártolo, H. and Bártolo, P., An innovation system for building manufacturing. In ASME 2012 11th Biennial Conference on Engineering Systems Design and Analysis (pp. 175-179). American Society of Mechanical Engineers, 2012 July.
41. Lütjering, G., u. JC Williams: Titanium. 2003, Springer, Berlin.
42. Donachie, M.J., Titanium: a technical guide. 2000: ASM international.
43. I.J. Polmear. Light alloys: Metallurgy of the light metals. 3rd Edition. London: Arnold, 1995.
44. Leyens, C. and M. Peters, Titanium and titanium alloys: fundamentals and applications. 2006: Wiley Online Library.
45. E.W. Collings. Materials properties handbook: Titanium alloys. Materials Park, Ohio: ASM International, 1994.
46. Joshi, V.A., Titanium alloys: an atlas of structures and fracture features. 2006: Crc Press.
47. Radecka, A., Ordering and the deformation mechanisms of Ti-Al alloys. 2015.
48. I. Weiss and S.L. Semiatin. Thermomechanical processing of alpha titanium alloys; An overview. Materials Science and Engineering A, 263(2):243–256, 1999.
49. Boyer, R.J.J., Attributes, characteristics, and applications of titanium and its alloys. JOM, 2010. 62(5): p. 21-24.
50. Boyer, R.J.A.P.M., Titanium for aerospace: Rationale and applications. Advanced Performance Materials volume 199 :(4)2 .5p. 349-368.
51. C.N. Elias, J.H.C. Lima, R. Valiev, and M.A. Meyers. Biomedical applications of titanium and its alloys. JOM, 60(3):46–49, 2008.
52. J.P. Immarigeon, R.T. Holt, A.K. Koul, L. Zhao, W. Wallace, and J.C. Beddoes. Lightweight materials for aircraft applications. Materials Characterization, 35(1):41–67, 1995.
53. Thair L.Al- Zubaydi;" Studies on thermo mechanically processed and nitrogen ion implanted Ti-6Al-7Nb Biomedical alloy"; Ph.D thesis, University of Anna (2002).

54. Satendra Kumar, T.S.N. Sankara Narayanan and S. Ganesh Sundara Raman; "Thermal oxidation of Ti6Al4V alloy : Microstructural and electrochemical characterization"; *Material Chemistry and Physics* Vol. 119, P.337-346(2010).
55. Peckner, D., I.M. Bernstein, and D. Peckner, *Handbook of stainless steels*. 1977: McGraw-Hill New York.
56. Eliaz, N.J.M., *Corrosion of metallic biomaterials: a review*. 2019. 12(3): p. 407.
57. D. Mareci, R. Chelariu, D.M. Gordin, G. Ungureanu, T. Gloriant, *Comparative corrosion study of Ti-Ta alloys for dental applications*, *Acta Biomaterialia* 5/9 (2009) 3625-3639.
58. K.J. Qiu, Y. Liu, F.Y. Zhou, B.L. Wang, L. Li, Y.F. Zheng, Y.H. Liu, *Microstructure, mechanical properties, castability and in vitro biocompatibility of Ti-Bi alloys developed for dental applications*, *Acta Biomaterialia* 15 (2015) 254-265.
59. Blackwood, D.J.C.r., *Biomaterials: past successes and future problems*. 2003. 21(2-3): p. 97-124.
60. Loch, J., et al., *Corrosion resistance of titanium alloys in the artificial saliva solution*. 2016. 74(1): p. 29-36.
61. Oskouei, R.H.; Barati, M.R.; Farhoudi, H.; Taylor, M.; Solomon, L.B. *A new finding on the in-vivo crevice corrosion damage in a CoCrMo hip implant*. *Mater. Sci. Eng. C* 2017, 79, 390–398.
62. N.A. Al-Mobarak, A.M. Al-Mayouf, A.A. Al-Swayih, *The effect of hydrogen peroxide on the electrochemical behavior of Ti and some of its alloys for dental applications*, *Materials Chemistry and Physics* 99/2-3 (2006) 333-340.
63. Huang, G.Y.; Jiang, H.B.; Cha, J.Y.; Kim, K.M.; Hwang, C.J. *The effect of fluoride-containing oral rinses on the corrosion resistance of titanium alloy (Ti-6Al-4V)*. *Korean J. Orthod.* 2017, 47, 306–312.
64. Hussenbocus, S.; Kosuge, D.; Solomon, L.B.; Howie, D.W.; Oskouei, R.H. *Head-neck taper corrosion in hip arthroplasty*. *Biomed Res. Int.* 2015, 2015, 758123.
65. Milimonfared, R.; Oskouei, R.H.; Taylor, M.; Solomon, L.B. *An intelligent system for image-based rating of corrosion severity at*

- stem taper of retrieved hip replacement implants. *Med. Eng. Phys.* 2018, 61, 13–24.
66. Kamachimudali, U., T. Sridhar, and B.J.S. Raj, Corrosion of bio implants. 2003. 28(3): p. 601-637.
67. Balamurugan, A., et al., Corrosion aspects of metallic implants—An overview. 2008. 59(11): p. 855-869.
68. Hanawa, T.J.M.S. and E. C, Metal ion release from metal implants. 2004. 24(6-8): p. 745-752.
69. Cristiano C Gomes 1, Leonardo M Moreira, Vanessa J S V Santos, Alfeu S Ramos, Juliana P Lyon, Cristina P Soares, Fabio V Santos, Assessment of the genetic risks of a metallic alloy used in medical implants. *Genetics and Molecular Biology*, 2011. 34: p. 116-121.
70. Hallab, N.J.; Anderson, S.; Staord, T.; Glant, T.; Jacobs, J.J. Lymphocyte responses in patients with total hip arthroplasty. *J. Orthop. Res.* 2005, 23, 384–391.
71. Bhat, S.V. *Biomaterials*; Narosa Publishing House: New Delhi, India, 2002; pp. 36–38.
72. Mohanty, M., S. Baby, and K.J.J.o.b.a. Menon, Spinal fixation device: A 6-year postimplantation study. *Journal of Biomaterials Applications*, 2003. 18(2): p. 109-121.
73. Schutz, R.W. *Corrosion of titanium and titanium alloys, corrosion: materials*. Materials Park, Ohio, US: ASM International; 2005.
74. U KAMACHI MUDALI, T M SRIDHAR and BALDEV RAJ, Corrosion of bio implants, *Metallurgy and Materials Group, Indira Gandhi Centre for Atomic Research, Vol. 28, Parts 3 & 4, June/August 2003*, pp. 601–637.
75. Gilbert, J.L., C.A. Buckley, and J.J.J.J.o.b.m.r. Jacobs, In vivo corrosion of modular hip prosthesis components in mixed and similar metal combinations. The effect of crevice, stress, motion, and alloy coupling. 1993. 27(12): p. 1533-1544.
76. Roberge, P.R., *Corrosion engineering*. 2008: McGraw-Hill Education.
77. Eliaz, N. and E. Giladi, *Physical Electrochemistry: Fundamentals, Techniques, and Applications*. 2019: John Wiley & Sons.

- 78.J.L. Gilbert, "Method of Preparing Biomedical Surface," U.S. Patent, September 6, 2011.
- 79.Gilbert, J.L., In vivo oxide-induced stress corrosion cracking of Ti-6Al-4V in a neck-stem modular taper: Emergent behavior in a new mechanism of in vivo corrosion. 2012. 100(2): p. 584-594.
- 80.Jeremy L. Gilbert Corrosion in the Human Body: Metallic Implants in the Complex Body Environment, 2017, NACE International.
- 81.Henk J Busscher, Margareta Rinastiti, Widowati Siswomihardjo and Henny C. van der Mei, Biofilm formation on dental restorative and implant materials. J Dent Res, 2010. 89(7): p. 657-665.
- 82.Abrahamsson, L., T. Berglundh, and J.J.C.o.i.r. Lindhe, Soft tissue response to plaque formation at different implant systems. A comparative study in the dog. Clin Oral Implants Res, 1998. 9(2): p. 73-79.
- 83.van Brakel, R., Early bacterial colonization and soft tissue health around zirconia and titanium abutments: an in vivo study in man. Clin Oral Implants Res, 2011. 22(6): p. 571-577.
- 84.Anders Palmquist , Omar M Omar, Marco Esposito, Jukka Lausmaa, and Peter Thomsen, Titanium oral implants: surface characteristics, interface biology and clinical outcome. J R Soc Interface, 2010. 7(suppl_5): p. S515-S527.
- 85.O'gorman, J. and H.J.J.o.H.I. Humphreys, Application of copper to prevent and control infection. Where are we now? 2012. 81(4): p. 217-223.
- 86.BOCCACCINI, A.R., The electrophoretic deposition of inorganic nanoscaled materials-a review. 2006. 114(1325): p. 1-14.
- 87.Chen, Q., Electrophoretic Deposition of Composite Coatings with Bioactive Character and Drug Delivery Capability. 2015.
- 88.Gibson, I.R. and W.J.J.o.M.S.M.i.M. Bonfield, Preparation and characterization of magnesium/carbonate co-substituted hydroxyapatites. 2002. 13(7): p. 685-693.
- 89.Hamaker, H.J.T.o.t.F.S., Formation of a deposit by electrophoresis. 1940 :35 .p. 279-287.

90. Avgustinik, A., V. Vigdergauz, and G.J.J.A.C.U. Zhuravlev, Electrophoretic deposition of ceramic masses from suspensions and calculation of deposit yields. 1962. 35(10): p. 2175-80.
91. Biesheuvel, P.M. and H.J.J.o.t.A.C.S. Verweij, Theory of cast formation in electrophoretic deposition. 1999. 82(6): p.1455-1451 .
92. Sarkar, P. and P.S.J.J.o.t.A.C.S. Nicholson, Electrophoretic deposition (EPD): mechanisms, kinetics, and application to ceramics. 1996. 79(8):(p. 1987-2002.
93. Besra, L. and M.J.P.i.m.s. Liu, A review on fundamentals and applications of electrophoretic deposition (EPD). 2007. 52(1): p. 1-61.
94. Van der Biest, O.O. and L.J.J.A.R.o.M.S. Vandeperre, Electrophoretic deposition of materials. 1999. 29(1): p. 327-352.
95. Dickerson, J.H.J.E.d.o.n., Electrophoretic deposition of nanocrystals in non-polar solvents. 2012: p.155-131 .
96. Heavens, S.J.N.P., Advanced Ceramic Processing and Technology., Electrophoretic deposition as a processing route for ceramics. 1990. 1: p. 255-283.
97. Pouya Amrollahi, Jerzy S. Krasinski, Ranji Vaidyanathan, Lobat Tayebi and Daryoosh Vashae,” Electrophoretic Deposition (EPD): Fundamentals and Applications from Nano- to Micro-Scale Structures”, Handbook of Nanoelectrochemistry, Springer, (2015).
98. Krüger, H. G., Knote, A., Schindler, U. ,Kern, H. and Boccaccini, A. R., Composite ceramic-metal coatings by means of combined electrophoretic deposition and galvanic methods. 2004. 39(3): p. 839-844.
99. Isyraf Aznam, Joelle C.W. Mah, Andanastuti Muchtar and Mariyam Jameelah Ghazali, A review of key parameters for effective electrophoretic deposition in the fabrication of solid oxide fuel cells. 2018. 19(11): p. 811-823.
100. Vandeperre L, Van Der Biest O, Clegg WJ. Silicon carbide laminates with carbon interlayers by electrophoretic deposition. Journal of Key Engineering Materials, (Pt. 1, Ceramic and Metal Matrix Composites) 1997;127–131: 567–73.

101. Basu, R.N., C.A. Randall, and M.J.J.J.o.t.A.C.S. Mayo, Fabrication of dense zirconia electrolyte films for tubular solid oxide fuel cells by electrophoretic deposition. *Journal of the American Ceramic Society*, 2001. 84(1): p. 33-40.
102. Wang, Y.C., I.C. Leu, and M.H.J.J.o.t.A.C.S. Hon, Kinetics of electrophoretic deposition for nanocrystalline zinc oxide coatings. *Journal of the American Ceramic Society*, 2004. 87(1): p. 84-88.
103. Zhitomirsky, I. and L.J.J.o.M.S.M.i.M. Gal-Or, Electrophoretic deposition of hydroxyapatite. *Journal Mater Sci Mater Med*, 1997. 8(4): p. 213-219.
104. Mendoza Gallego, Carlos, González, Zoilo, Castro, Yolanda, Gordo, Elena and Ferrari, Begoña, Improvement of TiN nanoparticles EPD inducing steric stabilization in non-aqueous suspensions. 2016. 36(2): p. 307-317.
105. Zarbov, M., I. Schuster, and L.J.J.o.m.s. Gal-Or 'Methodology for selection of charging agents for electrophoretic deposition of ceramic particles. *Journal of Materials Science*, 2004. 39(3): p. 813-817.
106. Yao, H., Characterization and Microstructure of Titanium Dioxide Prepared by Radio Frequency Magnetron Sputtering. *Journal of Electrochemical Society Active Member*, 2011, Vol. (158), 5.
107. Zhao, X., In vitro bioactivity of plasma-sprayed TiO₂ coating after sodium hydroxide treatment. *Journal of Surface and Coating Technology*, 2006. 200(18-19): p. 5487-5492.
108. Maria C. Advincula, Firoz G. Rahemtulla, Rigoberto C, Earl T. Ada, Jack E. Lemons and Susan L Bellis; " Osteoblast adhesion and matrix mineralization on sol-gel-derived titanium oxide"; *Journal of Biomaterials* Vol.27, P.2201-2212(2006).
109. Xu, S., et al., RF plasma sputtering deposition of hydroxyapatite bioceramics: synthesis, performance, and biocompatibility. *Journal of Plasma Process*, 2005. 2(5): p. 373-390.
110. Chen, C.-C. and S.-J.J.M.t. Ding, Effect of heat treatment on characteristics of plasma sprayed hydroxyapatite coatings. *Materials Transactions* 2006. 47(3): p. 935-940.
111. Paulo G Coelho, Sérgio Luiz de Assis, Isolda Costa, and Van P Thompson, Corrosion resistance evaluation of a Ca-and P-based

- bioceramic thin coating in Ti-6Al-4V. *Journal of Mater Sci*, 2009. 20(1): p. 215-222.
112. Azari, R., H. Rezaie, and A.J.C.I. Khavandi, Investigation of functionally graded HA-TiO₂ coating on Ti-6Al-4V substrate fabricated by sol-gel method. *Ceramics International*, 2019. 45(14): p. 17545-17555.
113. Deligianni DD, Katsala ND, Koutsoukos PG, Missirlis YF. *Biomaterials*. 2001;22:87.
114. Mohamed Shatta, Magdy Badawy, and Diab Haddad, 'Surface Hardness Evaluation of A Thermoplastic Nylon Denture Base Material', *Al-Azhar Journal of Dental Science*, Vol. 23- No. 4- 343:346- October 2020.
115. ASTM G44-99, 'Standard Practice for Exposure of Metals and Alloys by Alternate Immersion in Neutral 3.5 % Sodium Chloride Solution, January 2000.
116. J. Lee, C. H. Jeong, M. H. Lee, E. G. Jeong, Y. J. Kim, S. I. Kim and Y. R. Kim, Emphysematous osteomyelitis due to *Escherichia coli*, *Infection & Chemotherapy*, Vol. 49, No. 2, 2017, pp. 151-154.
117. A. Hamzaoui, R. Salem, M. Koubaa, M. Zrig, H. Mnif, A. Abid, M. Golli and S. Mahjoub, *Escherichia coli* osteomyelitis of the ischium in an adult. *Orthopaedics & Traumatology: Surgery & Research*, Vol. 95, 2009, pp. 636-638.
118. Hanawa, T. (2004) 'Metal ion release from metal implants', *Materials Science and Engineering: C*, Vol. 24, No. 6-8, pp.745-752.
119. S.K. Kar, Modeling of mechanical properties in alpha/beta-titanium alloys, 2005.
120. V. Khalili, J. Khalil-Allafi and H. Maleki Ghaleh; "Titanium oxide coating on NiTi shape memory substrate using electrophoretic deposition process"; *International Journal of Engineering* Vol.26, Vol.7, P.707-712(2013).
121. Rajan Anand; " Electrophoretic Deposition of Hydroxyapatite on Ti6Al4V"; B.Sc. thesis, National Institute of Technology, Rourkela (2012).
122. Michal Bartmanski ,Bartłomiej Cieslik, Joanna Glodowska, Pamela Kalka, Lukasz Pawlowski, Maja Pieper, Andrzej Zielinski;

- Electrophoretic deposition (EPD) of Nano hydroxyapatite – nanosilver coatings on Ti13Zr13Nb alloy.(2017).
123. Kumar, R.R. and M.J.M.L. Wang, Functionally graded bioactive coatings of hydroxyapatite/titanium oxide composite system. *Journal of Biomaterials Applications*, 2002. 55(3): p. 133-137.
 124. L. Mohan, D. Durgalakshmi, M. Geetha, T.S.N. Sankara Narayanan, R. Asokamani, Electrophoretic deposition of nanocomposite (HAp+ TiO₂) on titanium alloy for biomedical applications. *Ceramics International* :(4)38 .2012 p. 3435-3443.
 125. Sorkhi, L., M. Farrokhi-Rad, and T.J.S. Shahrabi, Electrophoretic deposition of hydroxyapatite–chitosan–titania on stainless steel 316 L. 2019. 2(3): p. 458-467.
 126. In vitro study: Evaluation of mechanical behavior, corrosion resistance, antibacterial properties and biocompatibility of HAp/TiO₂/Ag coating on Ti6Al4V/TiO₂ substrate.
 127. G. Pezzotti, *Advanced materials for joint implants*, CRC Press, 2013.
 128. B. Dikici, M. Niinomi, M. Topuz, Y. Say, B. Aksakal, H. Yilmazer and M. Nakai, Synthesis and characterization of hydroxyapatite/TiO₂ coatings on the β -type titanium alloys with different sintering parameters using sol-gel method, *Protection of Metals and Physical Chemistry of Surfaces*, Vol. 54, No. 3, 2018, pp. 457-462.
 129. Rasmi Ranjan Behera, Abshar Hasanb, Mameilla Ravi Sankara, Lalit Mohan Pandeyb, Laser cladding with HA and functionally graded TiO₂-HA precursors on Ti–6Al–4V alloy for enhancing bioactivity and cyto-compatibility.
 130. A. Kocijan, M. Conradi and M. Hocevar, The influence of surface wettability and topography on the bioactivity of TiO₂/Epoxy coatings on AISI 316L stainless steel, *Materials*, Vol. 12, No. 11, 2019.

أظهرت النتائج أيضًا أن العينة المطلية عند ظروف طلاء (20V, 1.0min) كانت نسبة الكالسيوم الى الفوسفات مساوية الى 1.81 وهي مقاربة للنسبة الموجودة في عظم الكائن الحي. كما بينت نتائج فحص قابلية التبلل ان زاوية التماس للطلاء المترسب هي 13.11 درجة وهذه النتيجة الايجابية مفيدة للتطبيقات الحياتية وبرهنت بان الطلاء محب للماء.

الخلاصة

في هذه الدراسة، تم ترسيب الطلاءات ذات الطبقة الواحدة والمتدرجة وظيفياً من دقائق هيدروكسي اباتايت / ثاني أكسيد التيتانيوم عن طريق الترسيب الكهربائي على سبيكة التيتانيوم نوع Ti-6Al-4V. نتيجة للحوادث والأمراض وغيرها من الأسباب ، تستمر الجهود والابحاث للوصول إلى النتائج الأقرب الى الواقع. الأضرار التي تحدث بعض منها في جسم الكائن الحي بشكل عام، والإنسان بشكل خاص. يمكن التغلب على ذلك من خلال الزرعات المعدنية الطبية وأربطة العظام والأسنان والأجزاء الأخرى التي يمكن تعويضها. من خلال العلم ، تم توفير الفرص والتجارب للحصول على نتائج مرضية من حيث التوافق الحيوي لغرسات التيتانيوم وسبائكها ، والتي تصنف على أنها واحدة من أفضل المواد المتوافقة حيوياً داخل الأنسجة الحية.

تهدف هذه الدراسة إلى زيادة التقابلية الحيوية للسبائك التي اساسها التيتانيوم، لتحسين خصائصها المضادة للتآكل والنمو البكتيري عن طريق طلاء السطح بمساحيق من السيراميك الحيوي (هيدروكسي اباتايت/ثنائي اوكسيد التيتانيوم). تم ترسيب طبقة منفردة من كل من هيدروكسي اباتايت / ثاني أكسيد التيتانيوم النقيان وطبقة مركبة من من المساحيق اعلاه على سبيكة Ti-6Al-4V باستخدام تقنية الترسيب الكهربائي (EPD)، والجسيمات المشحونة المعقدة في الإيثانول بتركيز 50 جم / لتر ، لكل مسحوق، مع اضافة 6 جم / لتر على شكل مادة رابطة PEI في درجة حرارة الغرفة ، مع ظروف مثالية تبلغ 20 فولت ووقت ترسيب 1 دقيقة ، وتم إجراء معالجة حرارية للعينات المطلية في جو خامل من الأرجون عند 950 درجة مئوية لمدة ساعة واحدة لتحسين الالتصاق.

تم تقييم ومقارنة الخصائص السطحية للركائز المطلية، مثل السمك وخصائص السطح والتحويلات الطورية وسلوك التآكل والصلادة الدقيقة وخشونة السطح وقابلية البلل والاختبار المضاد للبكتيريا. أظهرت النتائج أن EPD هي تقنية واعدة لإنشاء طلاء حيوي متدرج وظيفياً على سطح Ti-6Al-4V بهيكل متميز وخصائص للتطبيقات الطبية الحيوية.



إلى

أئمة الهدى وأعلام التقى
آل بيت النبي (ع)

إلى

الشمعتين اللتين احترقتا لتضيئاً طريق حياتي
أمي وأبي

إلى

ذخري وسندي في الحياة
زوجي الغالي... ابني وبناتي
أخوتي وأختي

وإلى

كل من يحبون لي الخير

إليهم جميعاً ، أهدي ثمرة ما وفقني الله إليه





جمهورية العراق
وزارة التعليم العالي والبحث العلمي
جامعة بابل
كلية هندسة المواد
قسم هندسة المعادن

دراسة التركيب والخواص لمواد طلاء مركبة على سطح Ti-6Al-4V باستخدام تقنية الايكتروفوريتيك للتطبيقات الطبية

رسالة

مقدمه إلى كلية هندسة المواد / جامعة بابل
وهي جزء من متطلبات نيل شهادة الماجستير في هندسة المواد/المعادن

من قبل

سرى بهاء محمد

بكالوريوس هندسة مواد (2008)

إشراف

أ. د عبد الرحيم كاظم عبد علي